CORONAL HOLES AND THE HIGH-SPEED SOLAR WIND

STEVEN R. CRANMER
Harvard-Smithsonian Center for Astrophysics, Cambridge, MA 02138, USA

Abstract. Coronal holes are the lowest density plasma components of the Sun's outer atmosphere, and are associated with rapidly expanding magnetic fields and the acceleration of the high-speed solar wind. Spectroscopic and polarimetric observations of the extended corona, coupled with interplanetary particle and radio sounding measurements going back several decades, have put strong constraints on possible explanations for how the plasma in coronal holes receives its extreme kinetic properties. The Ultraviolet Coronagraph Spectrometer (UVCS) aboard the Solar and Heliospheric Observatory (SOHO) spacecraft has revealed surprisingly large temperatures, outflow speeds, and velocity distribution anisotropies for positive ions in coronal holes. We review recent observations, modeling techniques, and proposed heating and acceleration processes for protons, electrons, and heavy ions. We emphasize that an understanding of the acceleration region of the wind (in the nearly collisionless extended corona) is indispensable for building a complete picture of the physics of coronal holes.

Table of Contents

Space Science Reviews **101:** 229–294, 2002.

1. Introduction

This paper surveys the current state of understanding about how the high-speed component of the solar wind is heated and accelerated. It is based on talks and workshop discussions at the UVCS/*SOHO* Science Meeting held on 24–28 September 2000 in Northeast Harbor, Maine. The primary goal of this review is to provide a new perspective on the physics of coronal holes and the fast solar wind, though it is also important to present a convenient set of pathways into the primary research literature, which is rapidly growing in traditional journals, conference proceedings, new monographs, and the Internet. Thus, this paper attempts to provide a broad reconnaissance of the present state of the field and a selective review of its history. Some background is included where necessary, though unfortunately not all pertinent references can be listed.

The *Solar and Heliospheric Observatory* (*SOHO*) spacecraft, launched in December 1995, has led to a dramatic increase in our understanding of the physics of the solar interior, atmosphere, corona, and heliosphere (e.g., Domingo *et al.* 1995; Fleck and Svestka 1997). Specifically, the Ultraviolet Coronagraph Spectrometer (UVCS) instrument has been able to measure for the first time the detailed kinetic properties of charged particles in the acceleration region of the solar wind (Kohl *et al.* 1995, 1997). The 2000 UVCS/*SOHO* Science Meeting was a heterogeneous gathering of approximately 70 observers, *in situ* space physicists, and theorists. A major goal of this meeting was to put UVCS observations into the larger context of building a comprehensive picture of the physics of the extended corona and the solar wind. The theoretical explanation of UVCS empirical properties of coronal holes was a substantial part of the meeting discussions, but equally important was the growing observational rapprochement between remote-sensing and *in situ* approaches to plasma diagnostics of the solar wind (see, e.g., Huber 1981).

The history of space physics and the solar wind traditionally begins at the dawn of the space age in the late 1950s, but the field has a fascinating "pre-history," from Aristarchus of Samos to Hannes Alfvén, that has been reviewed by Dessler (1967), Stern (1989), Hufbauer (1991), Holzer and Leer (1997), and Parker (1999, 2001). General reviews of contemporary ideas about the solar wind have been presented by Parker (1963, 1965, 1997a), Hundhausen (1972), Leer *et al.* (1982), Isenberg (1991), Barnes (1992), Golub and Pasachoff (1997), Jokipii, Sonett, and Giampapa (1997), Axford *et al.* (1999), and Marsch (1999). Perceptive overviews of the physical processes underlying modern conceptions of the solar corona and wind have been given by, e.g., Pneuman (1986), Gómez (1990), Parker (1991), Cargill (1994), Leer *et al.* (1998), Meyer-Vernet (1999), Velli (2001), and Hollweg and Isenberg (2001). Finally, no survey of progress in this field of study can neglect the impact of the nine (so far) international Solar Wind Conferences, which have been unifying, inclusive, and strongly influential on the evolution of solar wind research (see, for example, Habbal *et al.* 1999).

This paper is organized as follows. An overview of *in situ* and remote-sensing measurements of the properties of coronal holes and the high-speed solar wind is presented in § 2. The evolution of our theoretical understanding is reviewed both from the standpoint of how the primary proton/electron plasma is modeled (§ 3) and what are its most plausible heating and acceleration mechanisms (§ 4). The energization of heavy, minor ions is discussed separately in § 5 because of their potential importance in the determination of the dominant physical processes. Finally, some subjective philosophical conclusions are offered with a grain of salt in § 6.

2. Observations

In order to understand how the solar corona and the solar wind (i.e., the steady supersonic outflow of ionized gas from the corona) are produced and maintained, one must have detailed empirical knowledge about the properties of the plasma. This section reviews the results of direct measurements of atoms, ions, and electrons in the solar wind from *in situ* spacecraft detection (§ 2.1), spectroscopy and polarimetry (§ 2.2), and radio sounding (§ 2.3). The importance of determining plasma parameters in the primary acceleration region of the particles—typically between 1.5 and 10 solar radii ($R_\odot$) from Sun center—is emphasized as the most direct means of identifying the processes responsible for this acceleration.

2.1. Spacecraft Particle Diagnostics

The first direct detection of particles in the solar wind was accomplished by a series of Russian *Lunik* and *Venera* deep space probes between 1959 and 1961 (Gringauz *et al.* 1961). Also in 1961 the American satellite *Explorer 10* measured solar wind velocities and densities in the vicinity of the Earth's variable magnetopause. The continuous nature of the solar wind was determined by *Mariner 2,* sent to Venus in 1962, which observed alternating dense, low-speed (300–500 km s^{-1}) streams and tenuous, high-speed (500–800 km s^{-1}) streams (Snyder and Neugebauer 1964; see also Neugebauer 1997 for a first-hand account of the discovery). Enormous progress has been made in the detection of solar wind particles and fields since *Mariner 2* (e.g., Neugebauer 1975, 1982; Dobrowolny and Moreno 1977; Smith and Wolfe 1979; Goldstein *et al.* 1996; Ogilvie and Desch 1997; Richardson *et al.* 1999; Ness and Burlaga 2001). The remainder of this section will focus on the high-speed component of the wind, which is believed to be the simplest, most "ambient" state of the plasma.

The fundamental nature of the high-speed solar wind was not recognized for at least a decade after its initial detection in 1962. Uncertainty arose because of the limited perspective of spacecraft that remained in or near the ecliptic plane and only detected high-speed streams intermittently. Also, the earliest solar wind

models seemed to be able to explain 200–400 km s^{-1} outflows, but not the rarer values in excess of 500 km s^{-1}. Even with these biases it soon became apparent that the high-speed component represents a relatively structureless and ambient state of the plasma (e.g., Feldman *et al.* 1976; Axford 1977), whereas the slow-speed component is intrinsically more variable and filamentary. The high-speed wind emerges primarily from coronal holes on the Sun and often expands to fill the majority of the volume of the heliosphere. The slow wind is associated with coronal streamers and active regions on the Sun, and may have components arising from boundary flow along current sheets and the magnetic reconnection of closed-field loops. At solar minimum, the high-speed wind dominates at high latitudes (greater than $\pm$20–30°) and the low-speed wind coexists at lower latitudes with occasional high-speed streams. The *Ulysses* spacecraft, launched in 1992, passed over both solar poles and confirmed this basic picture (Gosling 1996; Woch *et al.* 1997; Marsden 2001).

The primary observable quantities by spacecraft in the solar wind are the velocity distribution functions of electrons, protons, and other ions, as well as electric and magnetic fields. Velocity distributions contain information about the macroscopic plasma properties (density, flow velocity, temperature, heat flux), but they also provide clues about the physics on microscopic scales. Because of the rarity of Coulomb collisions in most of the extended corona and solar wind, the distributions depart from equilibrium Maxwell-Boltzmann distributions. These departures seem to be strongest at small heliocentric distances, as observed by the two *Helios* spacecraft in the near-ecliptic high-speed wind between 0.29 and 1 AU (Marsch 1991; Feldman and Marsch 1997). It is hoped that this "inner frontier" will be extended in about a decade by the *Solar Probe* mission, which is expected to fly through the corona with a perihelion of only 4 $R_\odot$ (see, e.g., Möbius *et al.* 2000).

In the high-speed solar wind, the following kinetic properties highlight the main constraints on theoretical explanations of how the high-speed wind is heated and accelerated.

1. *Electron* distributions generally have three distinct components: an isotropic, nearly Maxwellian "core" (trapped particles in an electrostatic potential well), a higher-energy "halo" (with electrons fast enough to escape frequent collisions but still affected by the other components), and a narrow, forwardly beamed "strahl" component (believed to be a collisionless remnant of the hot coronal electron distribution). The *Wind* spacecraft detected an isotropic, but variable strength "super-halo" of solar wind electrons reaching 100 keV energies (Lin *et al.* 1997). The main halo component contains only about 4% of the total electron number density, though it carries the majority of the heat flux (e.g., Scime *et al.* 1994; Gary *et al.* 1999). The radial dependence of the core and halo temperatures varies between isothermal and adiabatic (Phillips *et al.* 1995), suggesting extended heating.

2. *Proton* distributions have anisotropic cores that are well represented by bi-Maxwellian distributions aligned to the local magnetic field, with $T_\perp > T_\parallel$. The

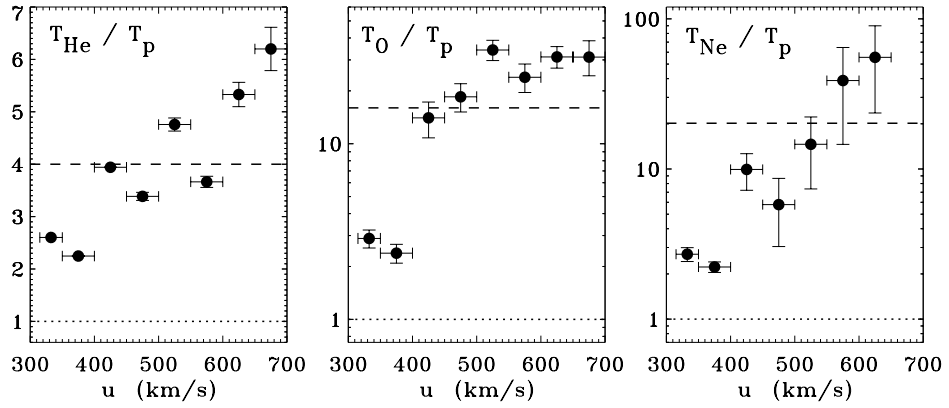

Figure 1. Ion temperature ratios at 1 AU for varying solar wind speed (Collier *et al.* 1996). The proton temperatures were computed from the empirical relation $T_p = -0.240u^2 + 836u - 213000$, where T_p is in K and u is in km s^{-1}. This is a fit to data presented by Ogilvie *et al.* (1980), for low speeds, and Goldstein *et al.* (1996), for high speeds. Dotted lines denote equal ion and proton temperatures, and dashed lines denote mass-proportional temperatures. Small differences between the proton and helium speeds (the latter used by Collier *et al.* 1996) are neglected in this plot.

magnitude of the core anisotropy ratio $T_\perp/T_\parallel$ decreases from 2–4 at 0.3 AU to unity at 1 AU (Marsch *et al.* 1982c). The protons also exhibit an additional field-aligned "beam" component that flows ahead of the core by about the local Alfvén speed V_A (see Hammond *et al.* 1995 for an example of the beam's velocity changing simultaneously with V_A). *Helios* measurements in the inner solar system found that the proton magnetic moment—proportional to the ratio between $T_\perp$ and the magnetic field strength B—rises with distance between 0.3 and 1 AU and thus is not conserved (Schwartz and Marsch 1983). Average core proton temperatures around 1 AU ($T_p \sim 3 \times 10^5$ K) are typically about two times larger than characteristic core electron temperatures (e.g., Schwenn and Marsch 1990).

3. *Heavy ion* distributions have been measured mainly for He^{2+}, but also for ions of C, O, Ne, Mg, Si, and Fe. The ionization fractions of individual species are strong constraints on models of the coronal electron velocity distribution, which controls the ionization and recombination rates (see § 5 for more details). Most, though not all, ion species appear to flow faster than the protons by about V_A, and this velocity difference decreases with increasing radius and decreasing proton flow velocity (Ogilvie *et al.* 1980; Marsch *et al.* 1982b; Hefti *et al.* 1998; Reisenfeld *et al.* 2001). The temperatures of heavy ions are significantly larger than proton and electron core temperatures. In the highest-speed wind, ion temperatures exceed simple mass proportionality (i.e., heavier ions have larger most-probable speeds), with $(T_i/T_j) \gtrsim (m_i/m_j)$, for $m_i > m_j$. Figure 1 shows He, O, and Ne temperatures at 1 AU from *Wind* data (Collier *et al.* 1996), divided by empirical proton temperatures. Temperature anisotropies are difficult to measure for heavy ions,

though for He^{2+}, Marsch *et al.* (1982b) found $T_{\parallel}$ greater than $T_{\perp}$ by about 10 to 30% in the highest speed flows.

4. *Fluctuations* in magnetic field strength, velocity, and density have been measured on time scales ranging from 0.1 second to months and years (see extensive reviews by Goldstein *et al.* 1995; Tu and Marsch 1995). Both propagating waves (probably Alfvénic in nature; Belcher and Davis 1971) and nonpropagating/pressure-balance structures advecting with the wind are observed. Nonlinear interactions between different oscillation modes create strong turbulent mixing, and Fourier spectra of the fluctuations show clear power-law behavior—indicative of inertial and dissipation ranges—in agreement with many predictions for fully developed magnetohydrodynamic (MHD) turbulence (Coleman 1968; Barnes 1979; Matthaeus *et al.* 1994; Horbury 1999; Velli 1999; Goldstein 2001). Spacecraft instruments have also detected many small-scale nonlinear features, such as tangential and rotational discontinuities, collisionless shocks, and "magnetic holes" (e.g., Dobrowolny and Moreno 1977; Moses and Kennel 1991; Winterhalter *et al.* 1994; Tsurutani *et al.* 1996) that indicate departures from ideal MHD and that probe plasma kinetic effects in parameter regimes inaccessible to laboratories.

2.2. Coronal Spectroscopy and Polarimetry

Until the 20th century, total solar eclipses were the only means of observing the solar corona. However, with the invention of the coronagraph by Lyot in the 1930s (see, e.g., Billings 1966; Koutchmy 1988) and the development of ultraviolet coronagraph spectrometers in the 1970s (Kohl *et al.* 1978; Withbroe *et al.* 1982), a continuous and detailed exploration of coronal plasma physics became possible. The existence of 10^6 K gas in the corona was established in 1939 when Grotrian and Edlén showed that several previously unexplained emission lines are produced by high ionization stages of iron, calcium, and nickel. Coronagraphs allow the large-scale magnetic geometry of the solar atmosphere to be observed, and Waldmeier (1957) discovered the long-lived dark regions known as *coronal holes,* now known to be associated with high-speed wind flow from open magnetic fields (see also Wilcox 1968; Krieger *et al.* 1973; Zirker 1977; Withbroe and Noyes 1977; Wang and Sheeley 1990; Esser and Habbal 1997; Roberts and Goldstein 1998). Figure 2 shows a composite image of the representative solar minimum corona, overplotted with empirically derived field lines to indicate the large-scale magnetic geometry.

The following sections describe different types of spectroscopic and polarimetric observations of the corona. In § 2.2.1 we briefly summarize on-disk and white-light coronagraphic observations of coronal holes. The review of UVCS/*SOHO* observations of coronal holes is divided into a discussion of polar coronal holes at solar minimum (§ 2.2.2) and coronal hole structure and variability throughout the solar cycle (§ 2.2.3). The high-speed wind has also been probed with remote sensing measurements of backscattered solar radiation by interstellar atoms (Fahr 1974; Bertaux *et al.* 1996) and via the wind's interaction with comets (e.g., Brandt

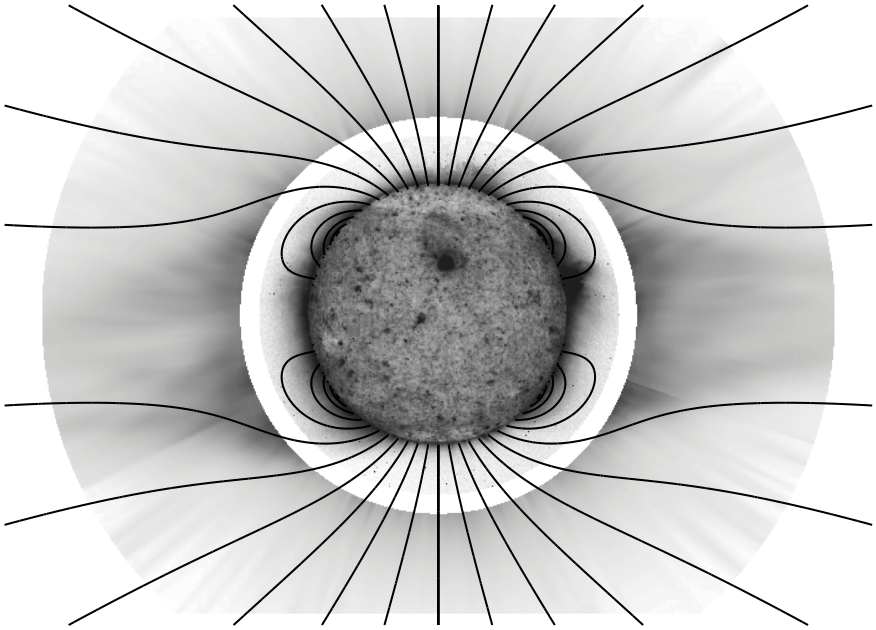

Figure 2. The solar corona on 17 August 1996 (near solar minimum), with bright regions plotted as dark. The inner image is the solar disk in Fe XII 195 Å emission, from the EIT instrument on *SOHO*. The outer image is the extended corona in O VI 1032 Å emission, from the UVCS instrument on *SOHO*. The axisymmetric field lines are from the model of Banaszkiewicz *et al.* (1998).

et al. 1972; Ip and Axford 1982; Raymond *et al.* 1998; Uzzo *et al.* 2001), but a more complete review of these observations is beyond the scope of this paper.

2.2.1. *Disk and White Light Observations*

Recent spaceborne observations of the solar corona fall into two broad classes: (1) direct imaging and spectroscopy of the solar disk and inner corona, typically out to 0.2–0.4 $R_\odot$ above the limb, and (2) coronagraphic imaging and spectroscopy of the outer "extended corona," out to as far as 30 $R_\odot$.* The first type of observation often allows simultaneous probing of the chromosphere, transition region, and innermost corona, with emphasis usually placed on bright closed-field loops, active regions, and flares. Instruments aboard the *Yohkoh, TRACE* (*Transition Region And Coronal Explorer*), and *SOHO* (*Solar and Heliospheric Observatory*) spacecraft—especially EIT, CDS, and MDI on the latter—have revealed strong variability and complexity on the smallest observable scales (100–1000 km; see § 4.1). The SUMER (Solar Ultraviolet Measurements of Emitted Radiation) instrument on *SOHO* has investigated the origins of the high-speed solar wind in

* Some descriptive terms, such as "coronal holes" and "quiet regions," are used in different ways when applied to on-disk and off-limb structures, and care must be taken that the interpretation of data is not clouded by assumptions imported from other uses of the terms.

the chromospheric network by mapping out blueshifts in coronal emission lines (Hassler *et al.* 1999; Peter and Judge 1999; see also Rottman *et al.* 1982; Dupree *et al.* 1996). The topologically complex nature of the transition region, probably made up of loops and open "funnels" with varying spatial scales, is being further elucidated by this instrument (Peter 2000, 2001; Hackenberg *et al.* 2000). SUMER measurements have also shown that ion temperatures exceed electron temperatures at very low heights (Seely *et al.* 1997; Tu *et al.* 1998) and that plasma conditions in dense polar plumes differ significantly from those in interplume regions (Wilhelm *et al.* 1998, 2000; Banerjee *et al.* 2000). Spectroscopic evidence is also mounting for the presence of waves propagating upwards through the chromosphere and transition region (Curdt and Heinzel 1998; Erdelyi *et al.* 1998) and into the corona (Doyle *et al.* 1998).

Measurements of plasma properties in the extended corona, where the main solar wind acceleration occurs, require the bright solar disk to be occulted. White light coronagraphs combine stray light rejection with linear polarimetry to measure the Thomson scattered continuum polarization brightness (pB) in the corona. Because the coronal plasma is optically thin to these photons, pB is proportional to the line-of-sight integral of the electron density n_e (multiplied by a known scattering function). Thus, van de Hulst (1950), Altschuler and Perry (1972), Munro and Jackson (1977), and Guhathakurta and Holzer (1994), among many others, have inverted this integral to derive n_e as a function of position in various coronal structures. For coronal holes, the LASCO (Large Angle and Spectrometric Coronagraph) instrument on *SOHO* has also been used to probe the superradial expansion of open magnetic flux tubes (DeForest *et al.* 1997, 2001a, 2001b; see, however, Woo *et al.* 1999, 2000) and the evolution of transient polar jets (Wang *et al.* 1998a; Wood *et al.* 1999). The White Light Coronagraphs on *Spartan 201* (Fisher and Guhathakurta 1995) and on the UVCS (Ultraviolet Coronagraph Spectrometer) instrument aboard *SOHO* (see, e.g., Romoli *et al.* 1997) have provided electron densities between 1.5 and 5 $R_\odot$ in coronal holes. However, these values are slightly higher than expected from extrapolating chromospheric and transition region densities to larger heights (Esser and Sasselov 1999); more work must be done to resolve these differences.

2.2.2. *UVCS Observations of Polar Coronal Holes*

Spectroscopy of the extended corona allows a detailed study of the kinetic properties of atoms, ions, and electrons (e.g., Withbroe *et al.* 1982). The shapes of emission lines formed by resonance scattering and collisional excitation are direct probes of the line-of-sight (LOS) distributions of electron, atom, and ion velocities. Doppler shifts of these lines reveal bulk flows along the LOS. Integrated intensities of resonantly scattered lines can be used to constrain the solar wind velocity and other details about the velocity distribution in the radial direction (see below). Intensities of collisionally dominated lines—especially when combined into an emission measure distribution—can constrain electron temperatures, densities, and

elemental abundances in the coronal plasma. Departures from Maxwellian and bi-Maxwellian velocity distributions are detectable with spectroscopic measurements having sufficient sensitivity and spectral resolution.

The *Spartan 201* spacecraft and the UVCS instrument on *SOHO* contain sophisticated ultraviolet coronagraph spectrometers that measure emission line profiles and intensities in the extended corona (see Kohl *et al.* 1978; 1994, 1995). Initial results from the first flight of *Spartan 201* indicated hydrogen kinetic temperatures possibly as large as 4 to 6 million K (Kohl *et al.* 1996). UVCS/*SOHO* measurements have allowed more details about the velocity distributions of H^0, O^{5+}, and Mg^{9+} in polar coronal holes to be derived. H^0 atoms are closely coupled to the protons by charge transfer below about 3 $R_\odot$ (e.g., Olsen *et al.* 1994; Allen *et al.* 1998, 2000), and H I Lyα observations have indicated the possibility of a mild proton temperature anisotropy (with $T_\perp \gtrsim T_\parallel$) above heights of 2–3 $R_\odot$. The O^{5+} ions, however, are strongly anisotropic at these heights, with perpendicular kinetic temperatures exceeding 2×10^8 K at 3 $R_\odot$ and $T_\perp / T_\parallel \approx$ 10–100 (Kohl *et al.* 1997, 1998). The measured kinetic temperatures of O^{5+} and Mg^{9+} are significantly greater than mass-proportional when compared with H^0 (i.e., $T_i / T_H > m_i / m_H$; see also Kohl *et al.* 1999). The surprisingly extreme properties of heavy ions in the extended corona have given rise to a resurgence of interest in theories of ion cyclotron resonance as a heating and acceleration mechanism for the solar wind (see §§ 4–5).

Doppler dimmed line intensities from UVCS are consistent with the outflow velocity for O^{5+} being larger than the outflow velocity for H^0 by as much as a factor of two (Kohl *et al.* 1998; Cranmer *et al.* 1999b; see also Li *et al.* 1998; Antonucci *et al.* 2000). The Doppler dimming technique provides a diagnostic of bulk outflow velocity when the local coronal scattering profile is substantially Doppler shifted away from the stationary profile of "source" solar-disk photons. There also exists "Doppler pumping" when the coronal scattering profile is shifted onto neighboring solar-disk emission lines which act as additional sources of photons. The general idea of Doppler dimming and pumping was suggested originally by Swings (1941) for the analysis of cometary spectra, and it was developed further for the solar atmosphere by Hyder and Lites (1970), Beckers and Chipman (1974), Kohl and Withbroe (1982), Noci *et al.* (1987), Strachan *et al.* (1993, 2000), Cranmer (1998), and Noci and Maccari (1999). Particular care must be taken in the analysis of the highly anisotropic O^{5+} distributions (Li *et al.* 1998) because the LOS passes through a large range of different most-probable speeds.

Figure 3 shows a summary of temperature and velocity measurements gathered remotely (between 1 and 5 $R_\odot$) and *in situ* (greater than 60 $R_\odot$, or 0.3 AU) in the high-speed wind. The latter values were assembled from *Helios, IMP, Ulysses,* and *Voyager* particle data, and double sets of curves denote rough lower and upper bounds on representative fast-wind values. The electron temperature T_e in coronal holes is known to rise to about 800,000 K by 1.1 $R_\odot$, though above that height

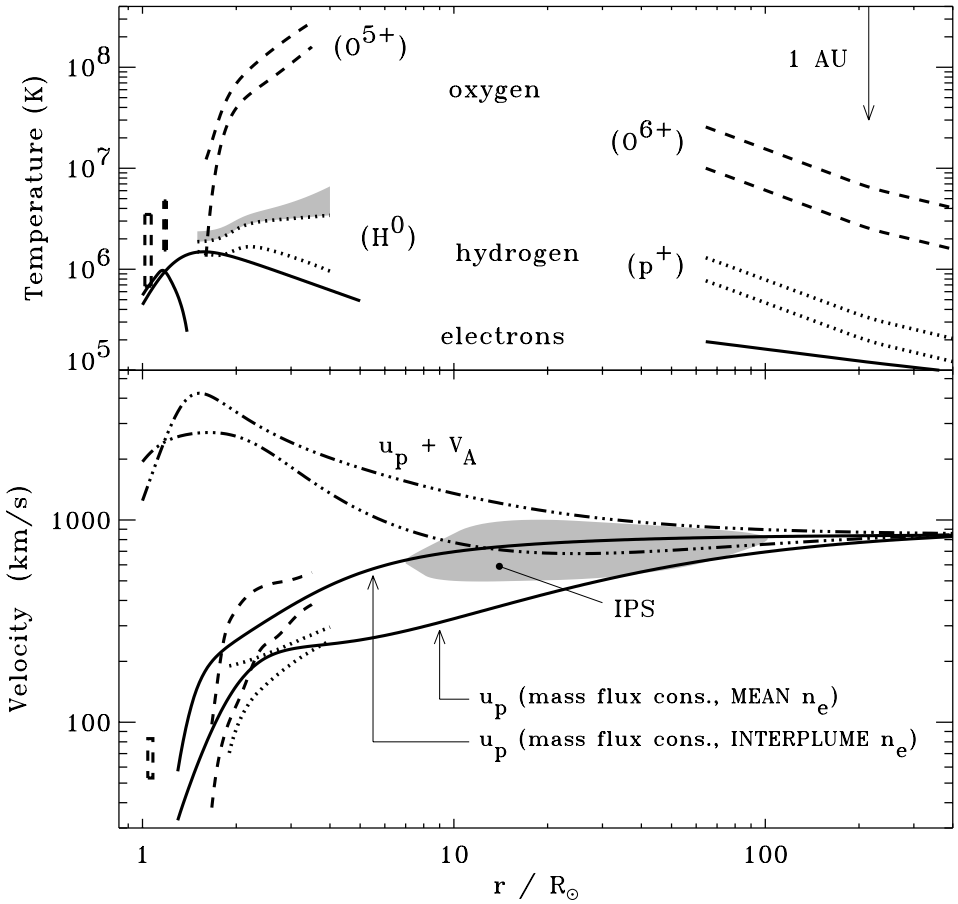

Figure 3. Summary plot of empirically derived temperatures and wind velocities. *Upper panel:* electron (solid), hydrogen (dotted), and oxygen (dashed) temperatures, with neutral hydrogen and O^{5+} in the corona, and protons and O^{6+} in the far solar wind. *Lower panel:* proton velocities u_p derived from mass flux conservation (solid lines), Doppler dimming velocities for hydrogen (dotted) and oxygen (dashed), and the summed $(u_p + V_A)$ "surfing" speeds (dash-triple-dot). The gray region denotes the range of polar IPS speeds reported by Grall *et al.* (1996).

there is some controversy (see Esser and Edgar 2000). CDS and SUMER line ratios suggest T_e rapidly decreases to about 300,000 K by 1.3–1.4 $R_\odot$ (David *et al.* 1998), or at least remains at about 800,000 K at these heights (e.g., Wilhelm *et al.* 1998; Doschek *et al.* 2001). However, models of the freezing in of *in situ* ionization states suggest that T_e continues to increase to about 1.5×10^6 K by 1.5 $R_\odot$ before beginning to decrease (e.g., Ko *et al.* 1997). The analysis of *Yohkoh* X-ray filter ratios yields similar values in excess of 1.3×10^6 K (Aschwanden and Acton 2001). A more direct method of measuring the electron temperature in the corona—thus possibly able to clear up the above discrepancies (see also § 5.1)—would be to detect light that is Thomson scattered (and substantially Doppler broadened) by

coronal electrons. Methods of precisely measuring the electron-scattered component of the H I Lyα resonance line (Fineschi *et al.* 1998) and spectral features in the visible K-corona (e.g., Reginald and Davila 2000) are being developed with the goal of determining T_e in coronal holes.

The hydrogen and oxygen temperatures $T_{\perp\mathrm{eff}}$ plotted in Figure 3 are derived from UVCS (1.5–4 $R_\odot$) and SUMER (1–1.2 $R_\odot$) line widths, which are expressed as

$$V_{1/e} = \left(\frac{2k_\mathrm{B} T_{\perp\mathrm{eff}}}{m_i} + \xi^2 \right)^{1/2} \tag{1}$$

where $V_{1/e}$ is the $1/e$ half-width of the emission line profile in Doppler velocity units, $T_{\perp\mathrm{eff}}$ reflects the random component of the ion velocity distribution along the coronal line of sight (typically perpendicular to the near-radial magnetic field), k_B is Boltzmann's constant, and ξ is a nonthermal component that can be attributed to unresolved MHD wave motions along the line of sight. The nonresonant wave broadening velocity ξ should not depend on ion mass or charge (e.g., Withbroe *et al.* 1982; Esser 1990). The UVCS values of $T_{\perp\mathrm{eff}}$ are derived from an "empirical model" that takes line-of-sight and other radiative transfer effects into account (Cranmer *et al.* 1999b). The upper limits for the derived coronal temperatures assume $\xi = 0$ and the lower limits assume a base value of $\xi = 30$ km s^{-1}, with wave action conservation determining its radial dependence (Esser *et al.* 1999). Note the additional uncertainty in the upper limit of the hydrogen temperature (gray region) which reflects possible differences between plumes and interplume regions and solar cycle variations.

The high-speed wind velocities u_p plotted with solid lines in Figure 3 were derived by using time-steady mass flux conservation for protons,

$$\frac{1}{A} \frac{d}{dr} \left(n_p u_p A \right) = 0 \ , \tag{2}$$

where n_p is the proton number density computed from two different measurements of the electron density n_e. Also, A is the cross-sectional area of a polar plasma flow tube in the magnetic field model of Banaszkiewicz *et al.* (1998). The required normalizing constant is specified at 1 AU by *Ulysses* observations of $n_p u_p \approx 2 \times 10^8$ cm^{-2} s^{-1} (Goldstein *et al.* 1996). The two adopted sets of electron densities come from Guhathakurta and Holzer (1994) and Fisher and Guhathakurta (1995), where the former provided *mean* coronal-hole values, averaged between plumes and interplume regions, and the latter provided *minimum*—presumably all interplume—densities. The empirical and theoretical outflow speeds of McKenzie *et al.* (1997) and Sittler and Guhathakurta (1999, 2002) are in good agreement with the "interplume" u_p curve in Figure 3, but the UVCS Doppler dimming velocity for hydrogen is in better agreement with the "mean" u_p curve. This latter agreement makes sense because the UVCS observations were similarly averaged over plumes

and interplume regions. It is still not known, though, whether the bulk of the high-speed wind comes from plumes, interplume regions, or a mixture of the two (see also § 2.2.3).

Plotted for comparison in Figure 3 are UVCS H^0 and O^{5+} Doppler dimming velocities (Kohl *et al.* 1998; Cranmer *et al.* 1999b) and a SUMER O^{5+} Doppler dimming measurement at 1.05 $R_\odot$ (Patsourakos and Vial 2000). The UVCS measurements were averaged over several arcminutes in polar coronal holes, so these velocities represent an average over both plumes and interplume regions. Also shown are radio interplanetary scintillation (IPS) measurements of speeds approaching 1000 km s^{-1} at 7–10 $R_\odot$ over the solar poles (Grall *et al.* 1996; Esser *et al.* 1997). It is unclear whether the IPS data represent bulk plasma speeds or the phase or group speeds of fluctuations propagating in the wind. The phase speed of Alfvén waves in the high-speed wind can be estimated by computing the sum of u_p and the local Alfvén speed,

$$V_A = B \left(4\pi \sum_{\text{ions}} m_i n_i \right)^{-1/2} , \tag{3}$$

and this sum is also shown in Figure 3 for the two above sets of density measurements, with the magnetic field strength $B \propto A^{-1}$. *In situ* measurements between 0.3 and 1 AU indicate that heavy ions tend to "surf" ahead of the protons and electrons at approximately this phase speed, though it is not known how close to the Sun these differential speeds are maintained.

2.2.3. *Coronal Hole Structure and Variability over the Solar Cycle*

A major emphasis of the 2000 UVCS/*SOHO* Science Meeting was the discussion of observations that shed light on how coronal holes vary over the 11-year solar cycle and how the plasma properties vary *within* coronal holes. The large polar coronal holes that dominate the extended corona at solar minimum are not homogeneous, and their latitudinal extent is a strong function of solar activity. Smaller and more transient coronal holes appear at low latitudes at times other than solar minimum. Figure 4 shows a summary of UVCS synoptic observations at 2.25 $R_\odot$ over the rising phase of solar cycle 23 (Miralles *et al.* 2000). The most noticeable change is the shrinking and disappearance of the polar coronal holes; the sporadic appearance of smaller equatorial holes is not apparent because the image samples the corona only once per rotation. It was fortunate that *SOHO* began its comprehensive observations when the corona exhibited a simple, nearly axisymmetric geometry. More recent analysis of the topologically complex solar maximum corona has benefited from the diagnostic insights gained from the 1996–1997 solar minimum.

During times of low solar activity, large polar coronal holes are observed to contain bright raylike *polar plumes* that appear to follow open magnetic field lines (see, e.g., Newkirk and Harvey 1968; Ahmad and Withbroe 1977; Koutchmy and

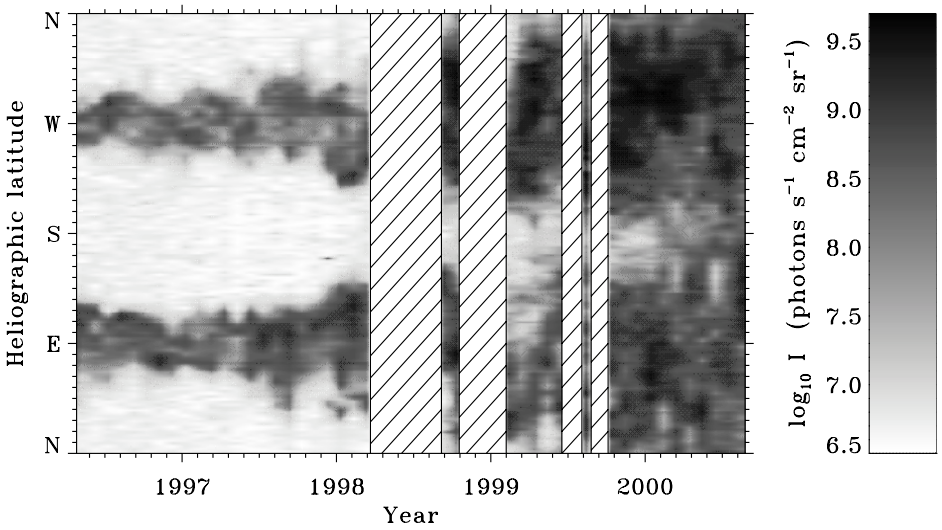

Figure 4. Profile-integrated intensity of the O VI 1032 Å line measured by UVCS, sampled once per rotation (27.3 days) from August 1996 to August 2000, and interpolated to a common height of 2.25 $R_\odot$. The lightest shades denote coronal holes, and the darkest shades denote streamers. Periods when no *SOHO* data exist are indicated by hatched rectangles.

Bocchialini 1998). These dense inhomogeneities often stand out strongly from the surrounding low-density interplume corona, though it is not clear if observations of the extended corona can ever isolate "pure" plume or interplume material (i.e., without line-of-sight contamination from the other component). In any case, UVCS observations above 1.5 $R_\odot$ have found that the densest concentrations of polar plumes along the line of sight exhibit lower ion kinetic temperatures (Noci *et al.* 1997; Corti *et al.* 1997; Giordano *et al.* 1997; Kohl *et al.* 1997, 1999) and have lower outflow speeds (e.g., Giordano *et al.* 2000) compared to low density—presumably interplume—lines of sight. The SUMER instrument aboard *SOHO* has also detected similar general properties between the solar limb and 1.5 $R_\odot$ (see § 2.2.1). The observed characteristics are roughly consistent with Wang's (1994) model of plume formation by intense basal heating (on spatial scales of $\sim$0.01 $R_\odot$), which counterintuitively results in a lower temperature above 1.2 $R_\odot$—because the extended heating per particle decreases when the density increases—and smaller gas pressure gradients in the accelerating wind.

Although polar plumes can be readily identified in the extended corona (see also Walker *et al.* 1993; Corti *et al.* 1997; Cranmer *et al.* 1999b; DeForest *et al.* 2001a), somewhere between about 30 and 100 $R_\odot$ they seem to blend in with the interplume medium. *In situ* measurements outside 0.3 AU have not identified any density, temperature, or velocity fluctuations that can be definitively correlated with plumes. Reisenfeld *et al.* (1999) reported *Ulysses* measurements between 1.5 and 4 AU which point to a significant correlation between helium abundance enhance-

ments and regions of high plasma β (the ratio of gas pressure to magnetic pressure). These fluctuations are of the right spatial scale to be the last remnants of polar plume flux tubes (see also Thieme *et al.* 1990). Del Zanna *et al.* (1998) explained the smoothing out of the plume/interplume density contrast as an eventual transverse pressure balance in the high-β interplanetary medium. However, the strong differences in coronal outflow speed between the two regions seems to demand additional "momentum mixing" above $\sim$30 $R_\odot$. A likely physical process that can lead to substantial mixing (but without magnetic reconnection, which would disrupt the *in situ* abundance correlations) is a growing MHD shear instability. Both the nonresonant Kelvin-Helmholtz instability (Parhi *et al.* 1999; Parhi and Suess 2000) and the resonant coupling instability between trapped Alfvén waves and the plume/interplume velocity shear (Andries *et al.* 2000) have been explored.

Polar plumes and other inhomogeneities in coronal holes exhibit significant time variability. Plumes are not always "filled" with dense plasma, though their magnetic flux tubes have been seen to retain their identity over several solar rotations (e.g., Lamy *et al.* 1997). Compressive MHD waves, observed as propagating intensity fluctuations, seem to be channeled in polar plumes (DeForest and Gurman 1998; Ofman *et al.* 1999, 2000), and if the oscillations are slow magnetosonic waves they should steepen into shocks at relatively low coronal heights (Cuntz and Suess 2001). High-latitude extensions of coronal streamers are often observed in projection against coronal holes, but these so-called "polar rays" often are clearly distinguishable from true coronal hole structure (Li *et al.* 2000).

At the short-time end of the coronal hole variability spectrum are impulsive *polar jets* that have been traced from the solar limb out to the LASCO C2 coronagraph's field of view in the extended corona (Wang *et al.* 1998a; Wood *et al.* 1999). Dobrzycka *et al.* (2000, 2002) reported observations of polar jets with UVCS/*SOHO* in 1996 and 1997. The brief intensity enhancements in H I Lyα and O VI 1032, 1037 Å were accompanied by significant narrowing of the emission lines, indicating cool plasma possibly similar to that of longer-lived polar plumes. However, extended heating of the same order as that of the background coronal hole is needed to combat the strong adiabatic cooling that affects jets more strongly than the surrounding steady-state plasma (i.e., because jets expand *along* the flux tube in addition to transversely with the superradial divergence). Studying the expansion and entrainment of polar jets into the ambient solar wind may yield insights into how plumes are eventually mixed with interplume plasma.

At times other than solar minimum, coronal holes of various sizes and shapes can appear at all latitudes and last for several solar rotations. When polar coronal holes are present, transient holes at lower latitudes have been seen to form by stretching out from the edges of the polar holes—e.g., the "boot of Italy" (Timothy *et al.* 1975) and the "elephant's trunk" (Bromage *et al.* 2000). The *in situ* wind speeds correlated with low-latitude coronal holes are roughly proportional to their areas on the solar disk (Nolte *et al.* 1976; Neugebauer *et al.* 1998), and the largest

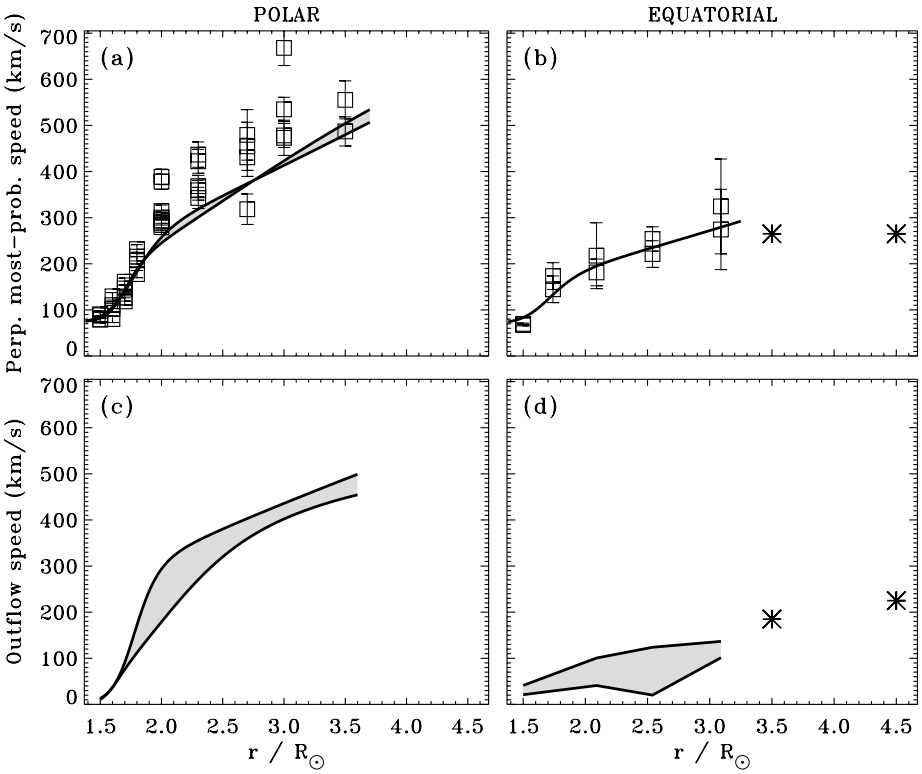

Figure 5. O^{5+} plasma properties in coronal holes derived from UVCS measurements: (a,b) perpendicular most-probable speeds $w_\perp$, and (c,d) outflow speeds u. Panels (a) and (c) plot line widths (squares) and derived plasma properties (lines) for polar coronal holes in 1996–1997. Panels (b) and (d) plot line widths (squares: 1999 data from Miralles *et al.* 2001a; asterisks: 1998 data from Poletto *et al.* 2002) and derived plasma properties (lines; asterisks in [d]) for equatorial coronal holes.

holes exhibit fast-wind speeds comparable to those from polar coronal holes. The high-speed solar wind connected to coronal holes is also characterized by low values of the *in situ* O^{7+}/O^{6+} ionization fraction and the Mg/O abundance ratio (Zurbuchen *et al.* 1999); indeed, these properties help strengthen the identification of coronal-hole-associated plasma in interplanetary space.

UVCS has measured the properties of several equatorial coronal holes from 1998 to 2000. Figure 5 displays the derived O^{5+} most-probable speeds $w_\perp$ (perpendicular to the near-radial magnetic field) and outflow speeds u. Miralles *et al.* (2001a) found that both $w_\perp$ and u in an equatorial hole on 12 November 1999 were approximately three times lower, at similar heights, than in the polar coronal hole in 1996–1997. These empirical properties are consistent with SUMER measurements of the same equatorial hole (on the solar disk) that indicate blueshifts about three times smaller in magnitude than for a solar-minimum polar hole (Buchlin and Hassler 2000). The UVCS O^{5+} properties for an equatorial coronal hole on 2 De-

cember 1998 were derived by Poletto *et al.* (2002) at the time the *Ulysses* spacecraft was in quadrature with the Sun-*SOHO* line of sight. These independently derived properties, also plotted in Figure 5, are consistent with those of the 1999 equatorial hole.

The equatorial coronal holes discussed above exhibited approximately three times lower O^{5+} outflow speeds than the polar coronal holes in 1996–1997 at heights between 2 and 3 $R_\odot$. However, *in situ* measurements with the *ACE* spacecraft indicate the high-speed stream associated with this equatorial hole had an asymptotic wind speed of 600–700 km s^{-1}, or only about 15% lower than the asymptotic wind speeds measured by *Ulysses* at solar minimum over the poles. Thus the bulk of the solar wind acceleration must occur *above* 3 $R_\odot$ for the equatorial coronal hole. Ongoing analysis of UVCS white-light pB data also seems to indicate that the electron density in the equatorial hole is several times larger than in a polar, solar-minimum hole at corresponding heights (Romoli *et al.* 2002). Coulomb collisions are more efficient in the equatorial hole (compared to the polar hole) at equilibriating temperatures and outflow speeds of different particle species. Collisions could thus be responsible for the lower values of oxygen $w_\perp$ and u there. It is also possible that the equatorial coronal holes exhibit an intrinsically lower rate of ion heating and acceleration than the polar coronal holes at solar minimum. Hollweg (1999b) suggested that coronal holes with different cross-sectional flux-tube areas are probably "fed" by different levels of wave power, which would modulate the extended energy and momentum deposition accordingly.

Since the 2000 UVCS/*SOHO* Science Meeting, there have been several new observations of coronal holes at solar maximum. Miralles *et al.* (2001b) reported the resurgence of very broad O VI profiles in a high-latitude coronal hole that was observed nearly simultaneously with the large-scale magnetic polarity reversal of solar cycle 23. The reappearance of extreme "solar-minimum-like" ion conditions at a time when the new polar coronal holes were only beginning to manifest was a surprising and interesting development. Miralles *et al.* (2001c) observed several other coronal holes over multiple rotations and found a continuum of examples between the two extreme cases of the 1996–1997 polar holes and the 1999 equatorial hole. Broad [narrow] O VI profiles tend to imply fast [slow] outflow speeds (as evidenced by the O VI 1032 Å to 1037 Å intensity ratio), and low [high] electron densities. There may be just one parameter—possibly the flux tube expansion rate or the wave power injected from the coronal base—that determines where along this continuum a given coronal hole is positioned. This represents a strong constraint on possible theoretical explanations for the ion heating and acceleration.

2.3. Radio Sounding of the Solar Corona

An additional useful probe of plasma conditions in the solar corona is the analysis of the scattering of radio waves. Radio sources can be either spacecraft beacons or cosmic sources such as pulsars or radio galaxies. As the radio waves propagate

through the corona on their way from the radio source to the Earth, they are modified by the coronal plasma. We can measure these modifications and distortions and use them to infer properties of the coronal plasma and its turbulence (see reviews by Coles 1978; Bird and Edenhofer 1990; Mullan and Yakovlev 1995; Yakovlev and Mullan 1996; Bastian 2001). These studies should be distinguished from the direct radio and microwave detection of magnetic structures in the low corona (Dulk 1985; White and Kundu 1997; Nindos *et al.* 2000), which will not be discussed here.

The physics of radio remote sensing of the corona is conveyed by the expression for the refractive index n of radio waves in a plasma (Nicholson 1983)

$$n^2 = \frac{c^2}{V_{\rm ph}^2} = 1 - \frac{\omega_p^2}{\omega(\omega \pm \Omega_e)} \tag{4}$$

where ω is the radio wave frequency, $\omega_p = (4\pi e^2 n_e/m_e)^{1/2}$ is the plasma frequency, $\Omega_e = eB/m_e c$ is the electron gyrofrequency, and $V_{\rm ph}$ is the wave phase speed. The frequencies typically utilized in such measurements are 300 to 5000 MHz. In the limit $\omega \gg \Omega_e$,

$$n^2 = 1 - \frac{\omega_p^2}{\omega^2}\left(1 \mp \frac{\Omega_e}{\omega}\right) \quad . \tag{5}$$

For the corona at a heliocentric distance of approximately 5 $R_\odot$, the dimensionless ratios ω_p^2/ω^2 and Ω_e/ω are approximately 2.5×10^{-6} and 3×10^{-4}, respectively. This means that, in the corona, radio propagation effects are (to first order) diagnostics of density and (to second order) diagnostics of the magnetic field. The first and second order effects are the basis of two methods of probing coronal turbulence, discussed below.

In a plasma containing turbulence or a field of waves, the magnetic field and density will vary spatially and temporally. Equations (4) and (5) then indicate that the refractive index will vary similarly, so radio waves will undergo random phase shifts and changes in propagation direction and Poynting flux. The theory of inverting this problem, i.e., determining statistical properties of the plasma fluctuations from the statistical properties of fluctuations in the radio observables, is by now well developed and has in some cases been corroborated by "ground truth" measurements. Such measurements can be an important complement to the information gained by coronal spectroscopy.

There are in the literature a number of investigations of turbulence in the corona, with the goal of determining if the turbulence is in quantitative agreement with the requirements of wave-driven models of coronal heating and solar wind acceleration (see § 4.2). The approaches listed below measure either the first order, density dependent contribution to the refractive index indicated in equation (5), or the second order, magnetic field dependent term.

2.3.1. *Density Fluctuations*

The first order term in equation (5) produces significant variations in the coronal radio wave properties. The effects of this density-only term are large, easily observed, and are the subject of an extensive literature on interplanetary scintillations (IPS). For example, scintillation phenomena resulting from the first order term have allowed us to determine the form of the density power spectrum on spatial scales from a few kilometers to several thousand kilometers, and for heliocentric distances ranging between a few solar radii to several tenths of an astronomical unit (e.g., Coles and Harmon 1989). Intensity scintillations probe inhomogeneities on the Fresnel scale (typically tens of km) and VLBI (Very Long Baseline Interferometry) phase scintillations probe inhomogeneities on the length scale of the multiple-telescope baseline (up to the Earth's diameter). Mutual interference of the scattered radio waves produces diffraction patterns that allow the drift speed of the density inhomogeneities to be deduced (Coles 1978; Kojima and Kakinuma 1990; Grall *et al.* 1996; Spangler *et al.* 2002). Delays in arrival times of pulsed radio sources have been used to derive the absolute electron density in the corona (see Mullan and Yakovlev 1995).

The relatively small role these observations have hitherto played in discussions of coronal plasma physics is due to the problematic status of density as a diagnostic for plasma waves and turbulence. Alfvén waves and parallel-propagating fast-mode MHD waves have no density fluctuations in the linear MHD limit, even though they can have substantial energy density. Evaluating the compressibility of realistic wave fields and general turbulence remains a basic problem in plasma physics. While there exist excellent data on the properties of density fluctuations in the corona and inner solar wind, it is difficult to use these observations as diagnostics of the fluctuations which possess the bulk of the energy density, i.e., magnetic field and velocity fluctuations.

However, in a recent paper Hollweg (2000a) utilized these abundant data in a test of one class of models in which coronal heating is due to high frequency waves (see § 4.2). Hollweg noted that the high frequency theories posit a large energy density of waves with wavelengths on the spatial scales probed by IPS measurements. Furthermore, there are theoretical arguments that MHD waves will become more compressive as the wave frequency approaches the gyrofrequency (Harmon 1989). Thus, Hollweg points out that we would expect large amplitude density fluctuations on the size scales probed by IPS. Hollweg (2000a) shows, in Figure 4 of his paper, that a plausible model of the sort put forward by Tu and Marsch (1997) would predict density fluctuations larger than those observed. Hollweg also points out that this result is not yet definitive, in that there are classes of models in which the waves could produce the requisite ion heating, but still be consistent with the radio observations. Nonetheless, Hollweg has emphasized that theories of coronal heating by wave damping must contend with the substantial body of radio IPS data.

2.3.2. *Faraday Rotation Measurements*

The second order term in equation (5) describes the phenomenon of Faraday rotation, in which the plane of polarization of a radio wave is rotated by propagation through a plasma. The appeal of this approach is that the measurements are more directly comparable to the parameters in heating and acceleration theories. If the waves causing the ion heating are electromagnetic (becoming familiar MHD waves if the frequency is sufficiently low), it makes sense to look for a spatially or temporally fluctuating magnetic field.

A number of such investigations have been carried out, such as Hollweg *et al.* (1982), Bird (1982), Pätzold *et al.* (1987), Efimov *et al.* (1993), Sakurai and Spangler (1994), Andreev *et al.* (1997), and Mancuso and Spangler (1999, 2000). All of these investigations have reported a time-varying component of Faraday rotation through the corona. The time variations probably represent spatial variations in magnetic field which then propagate past the line of sight. Most of the observations refer to the corona at heliocentric distances of 5 to 10 $R_\odot$.

At this time, it still remains to be demonstrated that all of the projects are in adequate agreement as regards the amplitude and time scale of the fluctuations, and that observations of extended radio sources such as radio galaxies give equivalent results as those derived from the monochromatic point sources provided by spacecraft transmitters. Nonetheless, all of these investigations find variations of the order of a few tenths of a radian m^{-2} to a few radians m^{-2} on time scales of an hour to a few hours. Efimov *et al.* (1993) and Andreev *et al.* (1997) published power spectra of Faraday rotation fluctuations which show variability on time scales down to several minutes.

There are at least two problems in associating these fluctuations with the waves or turbulence responsible for heating the corona and accelerating the solar wind. The first has to do with their energy density, or as more commonly expressed, the wave flux emerging from the coronal base into the corona. Wave-driven models require this base flux to be in the range of 2×10^5 to 5×10^5 erg cm^{-2} s^{-1} (see, e.g., Hollweg 1986b; Roberts 1989). Those who have analyzed these sorts of observations differ on whether the observed flux is entirely consistent with the theoretical requirements (Hollweg *et al.* 1982), or below the required level by an amount which may be as large as an order of magnitude (Sakurai and Spangler 1994; Mancuso and Spangler 1999). In support of the former conclusion, it can be argued that, given the uncertainties of using a measurement at 5 to 10 $R_\odot$ (in itself not an unambiguous measure of the root-mean-square magnetic field fluctuation) to infer the wave flux at the coronal base, it is amazing that the observational values are so close to the theoretically-stipulated numbers. At any rate, the present observations are not in major discord with the theoretical requirements for the wave flux in the corona.

However, the second problem appears to be more fundamental. Cyclotron resonance heating requires the wave power to be on the scale of an ion Larmor radius, or

more exactly the wave must satisfy the gyroresonance condition, which generally occurs for wavelengths the size of the gyroradius. These sizes will be of the order of kilometers at a heliocentric distance of 5 $R_\odot$. In contrast, the waves revealed in the aforementioned observational programs have much larger wavelengths. To give a specific example, Mancuso and Spangler (1999) found that the correlation length, or typical scale of the waves causing the Faraday rotation fluctuations, is at the very least 0.15 $R_\odot$ (i.e., 10^5 km), and is probably larger by a factor of up to an order of magnitude. There is thus a vast mismatch between the scale at which there is observational evidence for magnetic field fluctuations, and the scale which would permit efficient dissipative coupling to the kinetic energy of ions. See § 4.2.2 for further discussion of specific wave dissipation mechanisms and the heating of the extended corona.

As pointed out above, the high-frequency waves that have been suggested by, e.g., McKenzie *et al.* (1995, 1997) and Tu and Marsch (1997) for heating the extended corona may have nothing to do with the lower-frequency waves responsible for Faraday rotation variations on time scales of an hour or so. A potential problem for the existence of a substantial population of high-frequency waves was pointed out by Spangler and Mancuso (2000). These authors noted that a high level of short-wavelength electromagnetic plasma waves in the corona could make the coronal Faraday rotation fine-grained on a scale smaller than commonly used radio telescope beams. These waves could then cause a phenomenon called *Faraday screen depolarization,* which is a reduction of the degree of polarization for a linearly polarized radio source viewed through a medium such as the corona. Spangler and Mancuso (2000) showed that for the sort of wave and coronal properties which were being discussed in these models, there could be measurable depolarization, while existing observations (which were not extensive and were not carried out with this measurement in mind) showed no depolarization. This paper did not constitute a severe observational counterargument to the idea of base-generated cyclotron waves, since there are families of turbulence models which would accomplish the heating and not produce measurable depolarization.

It must further be noted that the existing radio measurements have been made at heliocentric distances in excess of 5 $R_\odot$. There are technical radioastronomical problems in making such observations lower in the corona. Since most wave heating models require the region of most intense energization to be between 1 and 5 $R_\odot$, the existing radio observations constrain only the "residue" of the undamped wave power. It is possible that the wave dissipation is extremely efficient at heliocentric distances of 2–3 $R_\odot$, so that the observationally-accessible residue at 5–10 $R_\odot$ is a poor indicator of the wave flux deeper in the corona. In any case, it is important to utilize the constraints provided by radio remote sensing observations, along with those from spectroscopy and *in situ* particle and field measurements, when testing theoretical models of extended coronal heating and wind acceleration.

3. Solar Wind Models: Historical Developments

The idea of a continuous outflow of charged particles from the Sun developed gradually in the first half of the 20th century and gained acceptance in the late 1950s and early 1960s. The history of the observational and theoretical work that led up to Parker's (1958a) initial steady-state fluid model is reviewed by, e.g., Hundhausen (1972), Holzer and Leer (1997), and Parker (1997b, 2001). Parker's key insight was that high temperatures in the corona can provide enough energy per particle to produce a natural transition from a subsonic (bound, negative total energy) state near the Sun to a supersonic (outflowing, positive total energy) state in interplanetary space. Most of the theoretical work in the 1960s and 1970s was devoted to explaining the properties of the low-speed solar wind, but since the 1980s, steady-state models have focused mainly on the high-speed component of the wind.

Theoretical descriptions of solar wind plasma have fallen into two main categories: fluid or MHD models, which assume a specific particle velocity distribution and solve for its moments (§ 3.1), and kinetic models, which solve directly for the velocity distribution function itself (§ 3.2). Fluid models have the advantage of being easier to compute and to extend to multiple dimensions or time-dependent flow, and the disadvantage of an unphysical "rigidity" when the velocity distributions would naturally want to depart from the parameterized functional form. Kinetic models are a more self-consistent description of the plasma, but they are considerably more difficult to implement. One reason why fluid models have outnumbered kinetic models is that it is straightforward to include an arbitrary deposition of heat or momentum (from an unspecified source) into the moment equations. The Boltzmann equation for kinetic models, however, allows only specific types of modifications, each of which is usually tied to a specific physical process.

In both fluid and kinetic models, the dominant outward force on particles comes from the thermal pressure gradient in the hot corona. It is worthwhile to note that this force is a completely *collisionless* phenomenon. The concept of pressure is often depicted as the force per unit area of particles striking the "wall" of an idealized "box," but the actual presence of the wall is unnecessary. Consider the case of two volumes of gas—one with a higher density or temperature than the other—that are brought into contact. Purely random motions of the particles will result in more particles going from the denser/hotter volume into the other volume than go in the opposite direction. This net motion is the manifestation of the pressure gradient force, which required no collisions to occur.

The following two subsections outline the basic properties of fluid and kinetic models that have been constructed since Parker's initial single-fluid model. It is assumed that all models, unless otherwise noted, are one-dimensional descriptions of the solar wind along a given radius or magnetic field line. This restriction does not necessarily require spherical symmetry along the specified magnetic flux tube (Kopp and Holzer 1976; Banaszkiewicz *et al.* 1998), or even that the tube is ori-

ented radially (e.g., Owocki 1982). Proposed sources of heat and momentum for these models are described separately in § 4.

3.1. Fluid and MHD Models

Parker's first model of the solar wind was isothermal, though it was quickly discovered that transsonic outflow could also exist if the single-fluid temperature decreases with increasing distance (Parker 1963; Noble and Scarf 1963; Whang and Chang 1965). Two-fluid models having $T_e \neq T_p$ (but $u_e = u_p$) were developed by Sturrock and Hartle (1966) and Hartle and Sturrock (1968) because Coulomb collisions are expected to be too infrequent to maintain energy equipartition in interplanetary space. These models solved internal energy moment equations containing adiabatic expansion effects, classical heat conductivity (Chapman 1954, 1957), and collisional energy exchange. However, conductivity and collisions were not strong enough to combat adiabatic cooling for protons at large distances ($T_p \propto r^{-4/3}$) and the resulting proton temperatures at 1 AU were too small by orders of magnitude. Holzer and Axford (1970) found that a *perfectly* adiabatic corona (with polytropic index $\gamma = 5/3$) cannot even produce a time-steady supersonic solar wind. The conclusion at this time was that some as-yet-unknown energy source was required to heat the corona and maintain a high gas pressure beyond the point where conduction and collisions are important (see also Parker 1965; Hartle and Barnes 1970; Hollweg 1973).

Useful extensions to the basic two-fluid solar wind idea included the addition of viscosity (Whang *et al.* 1966; Axford and Newman 1967) and collisionless modifications to the heat conductivity (Wolff *et al.* 1971; Cuperman *et al.* 1972). Continuing insight into the complexities of transport phenomena in coronal and solar wind plasma can be found in, e.g., Hollweg (1986a), Cowley (1990), Montgomery (1992), Williams (1997), and Narayan and Medvedev (2001). Another important early modification to the basic fluid wind scenario was the inclusion of magnetic $\mathbf{J} \times \mathbf{B}$ forces in the momentum equations (Weber and Davis 1967). Transsonic MHD equilibrium solutions have been put on a more rigorous mathematical footing by the models of, e.g., Sakurai (1985), Tsinganos and Sauty (1992), and Lifschitz and Goedbloed (1997). None of these effects, though, have altered the above basic conclusions about the necessity of an external heat source.

In the presence of a magnetic field, the stress tensor of a plasma is generally anisotropic (Chew, Goldberger, and Low 1956; Spitzer 1962). This allows the pressures—and thus temperatures—parallel and perpendicular to the magnetic field direction to be unequal (see Figure 6a). Hydrodynamic models assuming such a bi-Maxwellian or "double adiabatic" velocity distribution were first applied to the solar wind by Hollweg (1971b), Toichi (1971), Leer and Axford (1972), Whang (1972), and Fahr *et al.* (1977). This type of distribution has been used extensively over the last several decades. In the absence of external heating, the magnetic moment, proportional to $T_\perp / B$, is conserved and the anisotropy ratio $T_\perp / T_\parallel$ naturally

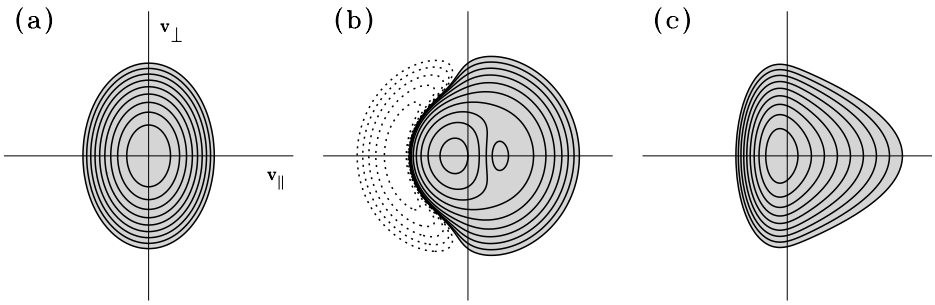

Figure 6. Contour plots of various analytic velocity distribution functions, where the positive $v_\parallel$ axis of symmetry points to the right and the peaks of the distributions are normalized to unity. The three panels show (a) a bi-Maxwellian distribution with $T_\perp = 2T_\parallel$, (b) an 8-moment perturbation about a Maxwellian with parallel heat flux variations, and (c) an example of the Whealton and Woo (1971) skewed distribution. Contours are plotted three per decade between -1 and -0.001 (*dotted*), and between +0.001 and +1 (*solid*).

decreases to values much less than one by 1 AU. The momentum equation for a time-steady, two-fluid plasma (with a bi-Maxwellian proton distribution) can be written

$$\left(u - \frac{a_\parallel^2}{u}\right)\frac{du}{dr} = -\frac{da_\parallel^2}{dr} + \frac{a_\perp^2}{A}\frac{dA}{dr} - \frac{GM_\odot}{r^2} \tag{6}$$

where the squared (parallel and perpendicular) effective one-fluid most-probable speeds are $a_\parallel^2 = k_B(T_{\parallel p} + T_e)/m_p$ and $a_\perp^2 = k_B(T_{\perp p} + T_e)/m_p$, and collisions and external sources of momentum are neglected. Note that the parallel pressure gradient force (first term on right) is augmented by an effective magnetic mirror force (second term on right) proportional to the perpendicular pressure and the relative flux tube expansion rate. The treatment of Coulomb collisions for a bi-Maxwellian plasma is reviewed by Barakat and Schunk (1982).

More complicated sets of transport equations can be obtained by taking higher moments of the Boltzmann equation and "closing" the system by assuming a specific parameterized form for the velocity distribution function (see Chapman and Cowling 1964; Whang 1971; Schunk 1977; Cuperman *et al.* 1987). These descriptions have the advantage of self-consistently specifying the heat flux densities and temperatures in regions of both collision-dominated and collisionless plasma. Models based on first order polynomial expansions about Maxwellians ("8 moment") and bi-Maxwellians ("16 moment") have only been explored relatively recently in a solar wind context because of difficulties in numerical implementation (e.g., Demars and Schunk 1990, 1991; Olsen and Leer 1996a, 1996b, 1999; Li 1999). As expected, the resulting heat fluxes are smaller than classical Spitzer and Härm (1953) values, but they still play an important role in determining temperatures. Also, Li (1999) found that added proton heating [cooling] in the direction perpendicular [parallel] to the magnetic field is required to reproduce realistic *in*

situ solar wind conditions. These models achieve conservation of mass, momentum, and energy at the price of introducing a small population of "antiparticles" (i.e., negative values of the velocity distribution; see Figure 6b). However, there exist well-defined mathematical means of determining the overall physical validity of the expansions (see, e.g., Gombosi and Rasmussen 1991; Cordier and Girard 1996) and the existence of negative regions in velocity space may not invalidate the models.

Additional generalized transport models have been constructed that do not exhibit negative values of the velocity distribution. An analytic solution to a simplified form of the Boltzmann equation was found by Whealton and Woo (1971), and an example is plotted in Figure 6c (see also Kinzelin and Hubert 1992, for a similar solution applied to the Earth's ionosphere). The analytic distribution contains only one more descriptive parameter (proportional to the parallel skewness) than an *ad hoc* bi-Maxwellian function. Despite its usefulness in modeling "beamed" distributions, this formalism results in considerably more complicated moment equations when compared with the simpler expansions discussed above (Leblanc and Hubert 1997; Leblanc *et al.* 2000). An alternate approach was taken by Benz and Gold (1977), who modeled the proton distribution as the sum of a collision-dominated (nearly Maxwellian) population and an escaping high-velocity tail. The standard fluid equations for the collisional protons were modified by including appropriate mass, momentum, and energy "sink" terms to account for acceleration into the escaping population.

Multidimensional and time-dependent fluid models of the solar wind have been computed for many sets of assumptions and boundary conditions, and it is impossible to do more than reference a small fraction of this work here (e.g., Pneuman and Kopp 1971; Steinolfson *et al.* 1982; Low 1990; Wang *et al.* 1993; Cuperman *et al.* 1995; Stewart and Bravo 1997; Ofman and Davila 1998; Guo and Wu 1998; Suess *et al.* 1999; Sittler and Guhathakurta 1999, 2002; Linker *et al.* 1999; Keppens and Goedbloed 1999; Groth *et al.* 1999; Usmanov *et al.* 2000). The idea that even the "mean" wind is intrinsically structured on small scales has been explored by, e.g., Parker (1964), Mullan (1990), and Feldman *et al.* (1974, 1993, 1997); see also § 4.3 for discussion of momentum deposition by "plasmoids." Most of the work referenced in this paragraph assumed Maxwellian velocity distributions and simple parameterized heating functions, but ongoing efforts are steadily incorporating the results of more detailed one-dimensional studies. One practical goal of modeling the variable three-dimensional structure of the solar wind is the ability to predict geoeffective disturbances and space weather in the Earth's local plasma environment (see Tsurutani *et al.* 1990; Balasubramaniam *et al.* 1996; Sibeck and Richardson 1997; Baker 1998).

3.2. KINETIC MODELS

In a nonrelativistic plasma containing a sufficiently large number of particles that it can be treated as a statistical continuum, the velocity distribution function $f_i(\mathbf{v}, \mathbf{r}, t)$ of particle species i is determined by the Boltzmann equation:

$$\frac{\partial f_i}{\partial t} + \mathbf{v} \cdot \frac{\partial f_i}{\partial \mathbf{r}} + \left[\mathbf{g} + \frac{q_i}{m_i} \left(\mathbf{E} + \frac{\mathbf{v}}{c} \times \mathbf{B} \right) \right] \cdot \frac{\partial f_i}{\partial \mathbf{v}} = \left(\frac{\partial f_i}{\partial t} \right)_{\text{coll}} , \tag{7}$$

where $\mathbf{g}$ is the gravitational acceleration, q_i and m_i are the charge and mass of species i, and $\mathbf{E}$ and $\mathbf{B}$ are the electric and magnetic fields (see, e.g., Stix 1962; Montgomery and Tidman 1964; Krall and Trivelpiece 1973; Galeev and Sudan 1983). The $\partial f_i / \partial \mathbf{r}$ term above corresponds to the advection and parallel pressure gradient terms in the fluid momentum equation, and the zero-order Lorentz term in square brackets gives rise to magnetic mirror acceleration. Wavelike fluctuations in the fields and in f_i can also result in a nonvanishing component of the Lorentz term when it is averaged over the fluctuation time scale. Coulomb collisions (term on right hand side) are often expressed in the Fokker-Planck formalism (e.g., Hinton 1983), which assumes that collisions produce a Markov-like diffusion in velocity space (see, however, Shoub 1988).

A kinetic approach to the solar wind was considered even before the term "solar wind" was coined. When the existence of 10^6 K plasma in the corona was discovered, it became apparent that almost 50% of the electrons at that temperature would exceed the outward escape speed at the solar surface, but $\ll 1\%$ of the protons would do so. The question of whether the corona would build up a large net positive charge—or if it would relax to a zero current equilibrium via a parallel electric field (Pannekoek 1922; Rosseland 1924)—was addressed by Pikel'ner (1950) and van de Hulst (1953). The net evaporation of protons from this ionized "exosphere" was modeled by Chamberlain (1960, 1961), though the controversy at that time regarding subsonic versus supersonic flow clouded the usefulness of Chamberlain's kinetic treatment (see also reviews by Lemaire and Scherer 1973; Fahr and Shizgal 1983; Lemaire and Pierrard 2001).

Chamberlain (1961) compared his subsonic kinetic results to nearly adiabatic hydrodynamic models, which similarly do not produce a fast wind (see Holzer and Axford 1970). It was thus suspected for a time that evaporative models may not be applicable to the supersonic portions of the corona. However, Jensen (1963) and Brandt and Cassinelli (1966) succeeded in producing outflows of the order 200 to 300 km s^{-1} by using kinetic approaches that incorporated Coulomb collisions and a Pannekoek-Rosseland electric field. Subsequent efforts that modeled the corona as collisionless above a specified "baropause" or "exobase" found better agreement with fluid models by using a more self-consistent electric field (Sen 1969; Jockers 1970; Lemaire and Scherer 1971; Hollweg 1971b).* It thus has become clear that

* Parallel work in the modeling of the *polar wind* of the Earth's ionosphere has contributed greatly to the understanding of solar wind plasma kinetics (see, e.g., Axford 1968; Banks and Holzer

hydrodynamic and kinetic formulations are complementary means of studying the physics of a supersonic solar wind (see also Holzer *et al.* 1971; Demars and Schunk 1992; Pantellini and Landi 2001).

Several recent kinetic models have been inspired by Scudder's (1992a, 1992b) suggestion that suprathermal tails in chromospheric velocity distributions may contribute to coronal heating (see also § 4.1). Lie-Svendsen *et al.* (1997, 2000) and Pierrard *et al.* (1999) solved the Fokker-Planck form of the Boltzmann equation for test-particle populations of electrons. The results from these analyses are still being digested, and it is not yet clear whether suprathermal electrons in the corona are required to reproduce observed *in situ* core, halo, and strahl distributions. Maksimovic *et al.* (1997) and Meyer-Vernet and Issautier (1998) modeled the solar wind as collisionless above a suprathermal exobase and derived realistic high-speed wind velocities and electron temperature profiles. These flows are driven mainly by the assumed population of high-energy electrons, and the models do not generally predict accurate proton or ion properties.

A major problem of purely collisionless kinetic models is that the conservation of magnetic moment results in strong pitch-angle transport in velocity space, creating strong temperature anisotropies (with $T_\parallel \gg T_\perp$) at large heliocentric distances. Measured proton distributions, though, are either close to isotropic (at 1 AU and beyond) or anisotropic in the opposite sense as predicted ($T_\perp > T_\parallel$, between 0.3 and 1 AU). The unrealistic parallel anisotropies that result from simple moment conservation can be reduced significantly by introducing even a small number of Coulomb collisions per AU (Griffel and Davis 1969; Lemons and Feldman 1983; Phillips and Gosling 1990). The combined effect of velocity-dependent Coulomb "runaway" (Dreicer 1959) and the mirror force is able to produce a fast, field-aligned beam component of proton distributions (Livi and Marsch 1987), although there is still considerable disagreement about the origin of the observed proton beams.

Plasma instabilities are also thought to be important as a source of particle isotropization in the solar wind (e.g., Parker 1958c; Perkins 1973; Gary 1993). Electrostatic turbulence can produce a type of stochastic diffusion that isotropizes distribution functions in a similar manner as collisions (Jokipii 1966; Dum 1983; Meister 1992; Kellogg 2000; Kellogg *et al.* 2001). It is evident, however, that for positive ions in the extended corona and wind, isotropization is not enough; the distributions must have $T_\perp > T_\parallel$ as well as greater than mass-proportional temperatures (see § 5).

1968; Lemaire 1972; Gombosi and Schunk 1988; Crew *et al.* 1990; Lie-Svendsen and Rees 1996; Barghouthi *et al.* 1998).

4. Coronal Heating and Acceleration Mechanisms

In the 1970s and 1980s it became clear that even the most sophisticated solar wind models could not produce a fast wind ($u \gtrsim 600$ km s^{-1}) without the direct addition of heat or momentum in some form (e.g., Holzer and Leer 1980). Further, it was found that energy needs to be deposited both close to the solar surface (to produce the sharp transition region) and at a large range of distances in the extended corona into interplanetary space (to accelerate high-speed streams, to prevent pitch-angle beaming to $T_\parallel \gg T_\perp$, and to account for observed superadiabatic temperature gradients). The physical processes responsible for this energy deposition have not yet been identified with certainty.

Parker (1991) discussed the separation of heating mechanisms between the coronal base ($r \approx 1$–$1.5\ R_\odot$) and "extended radial distances beyond the sonic point" ($r \gtrsim 2$–$5\ R_\odot$). This heuristic division into *creating* the lower corona versus *maintaining* and *evolving* the extended corona is supported by the drastic differences in Coulomb collision rates at the base (where all species seem to be collisionally coupled) and in the supersonic wind (which is nearly collisionless). The strong collisions below $\sim 1.5\ R_\odot$ lead to significant downward heat conduction and to the establishment of the sharp transition region. The two regimes are also differentiated by the complexity and topology of the magnetic field: the continually replenished "junkyard" of closed loops and open funnels at the coronal base (e.g., Dowdy *et al.* 1986; Spruit *et al.* 1991) evolves into a relatively uniform flux expansion in the extended corona. Both the plasma density and the volumetric heating rates decrease rapidly with distance from the photosphere, but the heating rates *per particle* are of the same order both at the base and in the wind acceleration region. This implies that both regions are of comparable importance in influencing coronal particle velocity distributions, but because of their drastically different properties, it seems appropriate to consider these environments separately (§§ 4.1–4.2) unless convincing evidence for a unified theoretical explanation arises. Most theories deal only with heating, but some processes have been suggested to also provide direct momentum deposition to the solar wind (§ 4.3).

In the discussions of various heating mechanisms below, it will be useful to define the plasma heating rate Q as the power dissipated per unit volume as thermal energy,

$$Q = |\nabla \cdot \mathbf{F}| \approx \rho \frac{\partial w^2}{\partial t} \approx nuk_B \frac{\partial T}{\partial r} \ , \tag{8}$$

where $\mathbf{F}$ is the heat flux density, typically given in the solar literature in units of erg cm^{-2} s^{-1}, ρ and n are the mass and number densities of the particles being heated, and w is a representative most-probable speed. Multiplicative factors of order 4/3 and 3/2 have been neglected for simplicity, and "sinks" of thermal energy such as radiative cooling and adiabatic expansion are not shown. The last approximate

equality in equation (8) assumes steady-state radial flow, but contains no assumptions concerning superradial flux-tube expansion. In a homogeneous medium, the damping length ℓ of a specific wave mode is given roughly by $|\mathbf{F}|/Q$, and thus it relates to the local damping rate γ (i.e., the imaginary part of the frequency) by $\gamma\ell = V_{\rm gr}$, the latter being the group velocity of the waves. These quantities remain useful as scaling relations for the inhomogeneous corona.

4.1. Heating the Coronal Base

The heat flux that needs to be deposited near the chromosphere-corona transition is thought to be about 5×10^5 erg cm^{-2} s^{-1} (see reviews by Vaiana and Rosner 1978; Kuperus *et al.* 1981; Narain and Ulmschneider 1990, 1996; Browning 1991; Zirker 1993; Jordan 2000). The majority of this energy is deposited over a relatively small range of heights ($\ell \approx 0.01$–$0.1\ R_\odot$), resulting in a local energy gain per proton (i.e., Q/n) of order 0.01 to 1 eV s^{-1}. However, this amount of energy is small compared with either the total radiative output of the Sun or the mechanical energy generated by the subphotospheric convection. The true "base coronal heating problem," then, is to determine the exact manner in which some fraction of the available energy is transferred into microscopic random motions. The main reason this is still not well understood is that the fundamental energy conversion events seem to take place on extremely small scales (1–100 km), previously unresolvable telescopically (see also Athay 2002). Note, though, that it is not necessary for all types of structures in the lower corona to be heated by the same physical process (e.g., Priest 1994), nor is it necessary for only one of the many suggested processes to dominate all others.

The *mass flux* of the solar wind is thought to be determined at or below the coronal base. Truly self-consistent models of the formation of the corona and solar wind must treat the chromosphere, transition region, and corona as a unified system (Hammer 1982; Hansteen and Leer 1995; Hackenberg *et al.* 2000). The dominant physical mechanisms that set the mass flux, however, are not yet known with certainty. Leer and Marsch (1999) contrasted two proposed scenarios: (1) that because the wind is driven by the energy deposition in the low corona, the mass flux should be proportional to this mechanical energy flux, and (2) that the supply of plasma into open "funnels" is constrained and determined by rapid ionization processes. These concepts may be related to one another and it is not yet apparent to what extent each process contributes (see also Sandbæk *et al.* 1994; Axford and McKenzie 1997; Peter and Marsch 1997; Chashei 1997). A more controversial—but persistently recurring—idea is that stellar mass loss rates are determined below the photosphere by nonthermal or entropy-minimizing processes (e.g., Cannon and Thomas 1977; Andriesse 1979, 2000).

Although many different mechanisms for base coronal heating have been proposed, the following general scenario is common to almost all of them. (1) The churning of the Sun's convective motions transports energy into photospheric magnetic flux tubes. (2) This stored energy becomes organized into small-scale struc-

tures, probably with a complex topology and stochastic dynamics. (3) Steep gradients at small scales are efficiently smeared out by Coulomb collisions or wave-particle interactions. (4) The dissipated (kinetic or magnetic) energy becomes randomized, resulting in net particle heating. Traditionally, the suggested physical processes have been divided into two broad groups: AC (wave dissipation) and DC (current-driven reconnection). These are discussed briefly in the following paragraphs, together with a third process (velocity filtration of suprathermal velocity distributions) that, ultimately, may not be so different from the AC models.

Wave dissipation (AC) mechanisms presume that the characteristic time scales of the upward-driven convective motions are short when compared with representative transit times across coronal structures. Under the right conditions, the resulting wavelike oscillations damp out on their way into the corona and provide the required heating. The ultimate damping mechanisms are either collisional (i.e., viscosity, thermal conductivity, ion-neutral friction, and electrical resistivity; see Alfvén 1947; Osterbrock 1961; Whang 1997) or kinetic wave-particle interactions (see Barnes 1968; Habbal, Holzer, and Leer 1979; Øien and Alendal 1993; Viñas *et al.* 2000). Acoustic and slow magnetosonic waves seem to damp out too easily in the upper photosphere and chromosphere to be of much importance in the corona* (e.g., Athay and White 1978). Alfvén and fast magnetosonic waves may survive into the corona, though they may not damp strongly enough to generate substantial amounts of heat. Thus many investigators have focused on how the damping of Alfvén waves in an *inhomogeneous* corona can be enhanced, either by corrugational phase mixing along transverse gradients (Heyvaerts and Priest 1983; Hood *et al.* 1997), by absorption of surface waves along loops acting as resonant cavities (Ionson 1978; Hollweg 1987; Grossmann and Smith 1988; Poedts *et al.* 1990), or by reflection or mode conversion (into more easily damped magnetosonic waves) via weak nonlinearities and large-scale bends in the magnetic field (Uchida and Kaburaki 1974; Wentzel 1976; Moore *et al.* 1991, 1992; Matthaeus *et al.* 1999).

Recent spectroscopic observations from *Spartan 201* and UVCS have led to a renewal of interest in coronal heating models involving extremely high-frequency (10 to 10,000 Hz) MHD waves. Although many models assume these waves are generated in the extended corona and solar wind (see § 4.2), they have also been proposed as a source of *base* coronal heating by, e.g., Axford and McKenzie (1992, 1997), McKenzie *et al.* (1995), Malara *et al.* (1996), Champeaux *et al.* (1997), and Ruzmaikin and Berger (1998). The high-frequency waves are suggested to be emitted during energetic reconnection events ("microflares") in the strong-field supergranular network. Longcope and Sudan (1992) and Shibata (1996, 1997) modeled reconnection events on various scales and found conditions reminiscent

* See, however, Ofman *et al.* (1999, 2000) and Tarbell *et al.* (1999) for discussion of acoustic and slow-mode MHD waves that may be excited in various kinds of open flux tubes. In addition, these waves may be important in heating the coronae of other stars (e.g., Schrijver 1987; Mullan and Cheng 1994).

of observed microflares, X-ray and EUV jets, and spicules. Nonlinear waves (e.g., Kudoh and Shibata 1997) and propagating shocks (Lee *et al.* 1996) are natural by-products of these violent events.

Current-driven reconnection (DC) mechanisms are dominant when the driving time scale is longer than the representative (e.g., acoustic or Alfvénic) transit time across a coronal structure. In this case, the field lines are continuously adapting to the convective driving motions and evolving between near-magnetostatic equilibrium states. The field lines become twisted and braided in response to the continual upward advection of magnetic flux from below the photosphere. Thin current sheets are generated in this unstable medium and magnetic reconnection occurs stochastically to relax the system to a lower-energy configuration. The plasma is thus heated resistively in small bursts at "nanoflare" ($\sim 10^{24}$ erg) to "microflare" ($\sim 10^{27}$ erg) energies (see, e.g., Gold 1964; Parker 1981, 1988, 1994; Priest 1996; Krucker and Benz 1998, 2000; Sturrock *et al.* 1999; Klimchuk and Cargill 2001). The large-scale stationary state of the plasma has also been described in terms of MHD turbulence, in which coronal loops are disrupted into increasingly smaller fragments by the underlying field-line motions (van Ballegooijen 1986; Heyvaerts and Priest 1992; Milano *et al.* 1997). Although it is not yet known whether nanoflare-scale events are responsible for the majority of the base coronal heating, observations have shown that sufficient magnetic flux does emerge within supergranules for the above mechanisms to be energetically important (Schrijver *et al.* 1998; Fisk *et al.* 1999; Simon *et al.* 2001).

The velocity filtration (VF) mechanism was suggested by Scudder (1992a, 1992b, 1994, 1996) as an alternative to theories that demand explicit energy deposition in the low corona (see also Parker 1958b; Levine 1974). A velocity distribution having a suprathermal tail will become increasingly dominated by its high-energy particles at larger distances from the solar gravity well. Thus an effective "heating" occurs as a result of particle-by-particle conservation of (potential + kinetic) energy. The major unresolved issue is whether suprathermal tails of the required strength can be produced and maintained in the upper chromosphere and transition region—where Coulomb collisions are traditionally believed to be strong enough to rapidly drive velocity distributions toward Maxwellians.* Anderson *et al.* (1996) and Ko *et al.* (1996) concluded that strong tails seem to be incompatible with various coronal and *in situ* observations, but Esser and Edgar (2000) found that the existence of hot halo-like electrons in the corona can provide an explanation for certain *in situ* charge states (see Figure 8). Several independent theoretical studies have also shown that it is possible to produce suprathermal electrons in dense plasmas from the dissipation of high-frequency plasma waves (Roberts and Miller 1998; Ma and Summers 1999; Leubner 2000; Viñas *et al.* 2000), thus providing a resemblance

* In effect, the production of these suprathermal particles is equivalent to the traditional "coronal heating problem," only in this scenario the energization must occur at lower heights where the majority of the particles remain cool (S. Owocki, private communication).

to the AC mechanisms discussed above. The nonintuitive thermodynamic properties of suprathermal plasmas are described by Treumann (1998, 1999, 2001) and Dorelli and Scudder (1999).

4.2. Extended Heating

4.2.1. *Empirical Considerations*

The earliest models of the solar wind assumed that electron heat conduction (Chapman 1954) was sufficiently strong to maintain high temperatures in the extended corona. It is now generally believed that the high-speed solar wind cannot be produced without the existence of gradual energy deposition above the base of the corona (see, e.g., Sturrock and Hartle 1966; Leer *et al.* 1982; Parker 1991; Barnes *et al.* 1995). Indeed, as spacecraft continue to probe the outermost frontiers of the heliosphere (> 50 AU), the measured solar wind temperatures remain significantly higher than expected from pure adiabatic expansion (Zank *et al.* 1999). In the extended corona, the proton heating rate per particle (i.e., Q/n) has been constrained to be approximately $\sim$0.1 eV s^{-1} at 2 $R_\odot$ (this is equivalent to a heating rate per unit mass, Q/ρ, of order $\sim 10^{11}$ cm^2 s^{-3}; see below), which is also of the same order as the heating rate per particle at the coronal base.

The hydrodynamic response of the solar wind plasma to extended heating depends on whether the energy is deposited in the subsonic or supersonic wind (Leer and Holzer 1980; Pneuman 1980). Heating in the subsonic, i.e., nearly hydrostatic, corona raises the density scale height. Although in this case the gas pressure gradient is increased locally, the asymptotic wind flow speed can *decrease* (relative to a subsonic corona without the added heating) because there is less kinetic energy per particle in this denser corona. Heating in the supersonic part of the corona results mainly in a larger asymptotic flow speed because the "supply" of material through the sonic point is already determined. It seems likely that substantial heating is present in both regions.

Prior to discussing the physical processes that have been suggested to be responsible for the extended heat deposition, it will be useful to examine the magnitude of the problem; i.e., what temperatures are *required* in models (with no momentum deposition) to accelerate the high-speed wind? Figure 7 shows the results of integrating equation (6), the two-fluid momentum conservation equation that allows for different electron and proton temperatures and proton anisotropy. The expansion geometry is specified as the Banaszkiewicz *et al.* (1998) polar flux tube and the three independent temperatures (T_e, $T_{\parallel p}$, $T_{\perp p}$) are specified as *ad hoc*—but empirically constrained—functions of radial distance (see § 2.2.2). Ultraviolet spectroscopy suggests that $T_{\perp p}$ exceeds the other two temperatures and is probably responsible for the bulk of the gas pressure in coronal holes (e.g., Kohl *et al.* 1996, 1998).

Seven different parameterizations for $T_{\perp p} \geq T_{\parallel p}$ are plotted in Figure 7. To be able to reach the observed *Ulysses* asymptotic wind speeds of $\sim$750 km s^{-1}, the

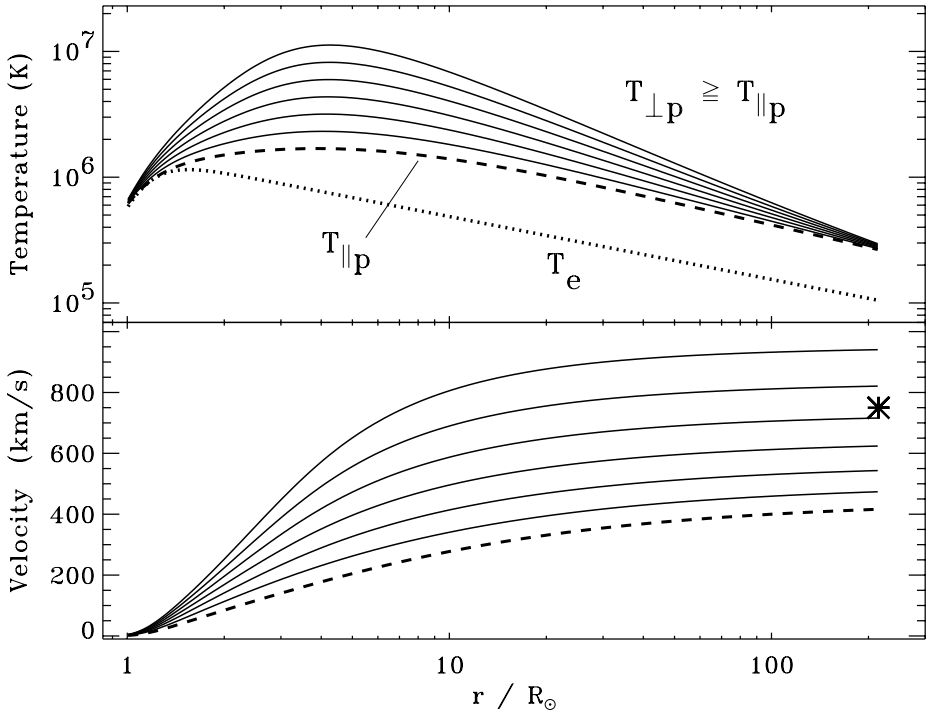

Figure 7. Two-fluid model temperatures (top) and outflow velocities (bottom) used to investigate the impact of anisotropic proton pressure on high-speed wind acceleration. The empirical electron temperature (dotted line) is less than the parallel proton temperature (dashed line), which is less than or equal to the adopted values of the perpendicular proton temperature (solid lines). The velocity curves correspond to the 7 modeled values of $T_{\perp p}$ and the dashed velocity curve is the isotropic case, $T_{\perp p} = T_{\parallel p}$. The asterisk denotes a representative high-latitude fast wind speed at solar minimum.

maximum value for $T_{\perp p}$ in this set of models must be at least 6×10^6 K. It should be noted, however, that there is considerable uncertainty in the assumed radial dependences of the temperatures, and different choices could produce different conclusions (see also Sandbæk *et al.* 1994; Esser *et al.* 1997; Hu *et al.* 1997). The proton temperatures derived from H I Lyα line widths are typically less than 6×10^6 K, although this neutral hydrogen diagnostic ceases to be sensitive to the proton plasma properties above 3–4 $R_\odot$ (Olsen *et al.* 1994; Allen *et al.* 1998, 2000). Below 3 $R_\odot$, the major source of uncertainty is how the observed line widths are partitioned between thermal and wave motions (see equation 1). Ofman and Davila (1999, 2001), Cuseri *et al.* (1999), and Esser *et al.* (1999) have presented models where a significant fraction of the observed H I Lyα width is due to unresolved transverse wave motions. No consensus has been reached, though, on the most reliable way of deconvolving these two components.

In the extended corona, the uncertainties in the determination of $T_{\perp p}$ from H I Lyα line widths are still large enough so that it is not yet possible to know which of the temperature curves in Figure 7 are closest to reality. The question of whether extended heating alone is sufficient to drive the high speed wind, or if momentum deposition is also required (§ 4.3), is still unanswered.

4.2.2. *Physical Processes*

The vast majority of theoretical models of the extended heating of the corona and heliosphere involve the transfer of energy from propagating magnetic fluctuations (waves, shocks, or turbulence) to the particles. This broad-brush consensus arises because the ultimate source of energy must be solar in origin, and thus it must somehow *propagate* out to the distances where the heating occurs (see, e.g., Hollweg 1975, 1978; Barnes 1979; Tu and Marsch 1995). This stands in contrast to the wider range of possibilities for heating the coronal base, where the spatial extent of the emerging loops and other magnetic structures is of the same order as the distance from the photosphere where heat deposition occurs. For the more distant extended corona, however, there are three general questions that need to be answered:

1. How and where are the fluctuations generated?
2. Which linear or nonlinear MHD modes are important?
3. How and where are the fluctuations damped?

Empirical constraints from spectroscopy, radio, and *in situ* measurements typically allow us to work backward, from 3 to 1 on the above list; first determining where the energy deposition occurs, then how it may be consistent with the presence of a specific type of fluctuation, then finally yielding clues about the origin of the fluctuations. The most satisfying *ab initio* theoretical studies proceed, with causality, from 1 to 3 on the above list. Below we discuss how ample cross-fertilization between observers and theorists has led to potential answers to the above questions.

Wave generation encompasses questions 1 and 2 above. The shorthand term "waves" here can be assumed to include the phenomena of shocks, turbulent power spectra, or any other nonlinear by-products of wavelike oscillations in the high-speed wind. The ultimate source of fluctuation energy must come from the Sun, but there is a clear division between theories that propose:

1a. that the waves responsible for extended heating originate at the coronal base and propagate virtually unaltered to where they are damped, and

1b. that the waves responsible for extended heating are generated locally in the corona—near where they are damped—and take their energy either from other waves or from nonequilibrium distributions of particles.

The most recent example of a base-generation scenario (1a) is that small-scale reconnection events in the low corona generate high-frequency (10–10,000 Hz) ion cyclotron waves (Axford and McKenzie 1992, 1997; McKenzie *et al.* 1995; see also related references in § 4.1). Lee and Wu (2000) suggested that base re-

connection events fill the extended corona with fast shocks, rather than waves, that convert some of their energy into particle heating and acceleration.

Local wave generation scenarios (1b) for the extended corona are more numerous, encompassing MHD turbulent cascade, kinetic plasma instabilities, mode conversion driven by reflection or refraction, or some combination of these processes (Kennel and Scarf 1968; Schwartz 1980; Isenberg and Hollweg 1983; Hollweg 1986b; Tu 1988; Voytenko *et al.* 1990; Matthaeus *et al.* 1999; Hu *et al.* 1999; Markovskii 2001). Large-scale MHD instabilities arising from lateral shears (i.e., relative flow between plumes and interplume regions, or corotating interaction regions between fast and slow wind) have also been suggested as possible sources of waves or turbulent fluctuations in the solar wind (e.g., Jokipii and Davis 1969; Roberts *et al.* 1992; Parhi *et al.* 1999). Distinguishing between scenarios 1a and 1b requires knowledge about wave damping (see below) and how heavy ions respond to the presence of waves (§ 5).

The specific wave modes that are responsible for extended heating and solar wind acceleration (see question 2 above) are not known. If the fluctuations are generated locally, the amplitudes of the three low-frequency MHD modes (Alfvén, fast magnetosonic, and slow magnetosonic) could be of comparable magnitude. Higher frequency electrostatic and electromagnetic waves such as Langmuir, hybrid, and Bernstein modes are typically neglected in scenarios of turbulent cascade or direct base generation, though they may be dynamically important if instabilities are dominant (e.g., Viñas *et al.* 2000). Although waves propagating along the open magnetic field lines have long been considered as the most likely, there has been much renewed interest in the ability of oblique and perpendicular-propagating waves to heat the plasma (e.g., Grappin *et al.* 2000; Leamon *et al.* 2000; Marsch and Tu 2001a; Li and Habbal 2001; Markovskii 2001; Hollweg and Markovskii 2002). Nonideal effects, such as the compressibility of Alfvén waves at large obliqueness angles (Harmon 1989) and at large amplitudes (Hollweg 1971a; Spangler 1989; Vasquez and Hollweg 1999) are probably not negligible.

Extended heating is believed to arise mainly from the dissipation of wave energy (question 3 above). Physical dissipation mechanisms for waves fall into two categories: collisional and collisionless. Coulomb collisions can damp waves below about 2–3 $R_\odot$ via viscosity, thermal conductivity, or (Joule/Ohmic) resistivity, but at larger distances from the Sun classical transport theory breaks down (see, e.g., Williams 1997; Li 1999). Whang (1997) rigorously derived the collisional damping rates for low-frequency MHD waves. For Alfvén and fast-mode waves propagating parallel to the magnetic field, proton viscosity is the dominant dissipation channel. For representative conditions in coronal holes at 2 $R_\odot$, the wave damping length is given by

$$\ell \;=\; \frac{2V_A^3}{\omega^2 \nu_p} \;\sim\; 3\,R_\odot \left(\frac{P}{5\,\mathrm{min}}\right)^2 \quad , \tag{9}$$

where V_A is the Alfvén speed, ω is the wave angular frequency, ν_p is the classical proton kinematic viscosity (Braginskii 1965), and P is the wave period. Note that for low-frequency waves the above damping length *exceeds* the range of distances over which the plasma is collisional. Also, this estimate is only a lower limit on ℓ because the appropriate viscosity coefficient for Alfvén wave damping may be smaller than the standard shear term used above (Hollweg 1986a; Montgomery 1992) by a factor of $(\Omega_p \tau_p)^{-1}$ or $(\Omega_p \tau_p)^{-2}$, where the product of the proton Larmor frequency Ω_p and the proton collision time τ_p is much greater than 1 in the extended corona. Thus, the bulk of Alfvén and fast-mode wave energy is not thought to be damped significantly by collisions in the extended corona (although higher frequency waves would have smaller damping lengths). Slow-mode MHD waves propagating along the field act like pure acoustic waves, and their collisional damping is dominated by electron thermal conductivity, with

$$\ell \; = \; \frac{15 c_s^3 n_e}{2\omega^2 \kappa_e} \; \sim \; 10^{-4} \, R_\odot \left(\frac{P}{5 \, \mathrm{min}} \right)^2 \quad , \tag{10}$$

where c_s is the sound speed, κ_e is the parallel electron conductivity, and the linear fluctuations are assumed to be adiabatic (see also Hung and Barnes 1973). Slow-mode waves thus damp extremely rapidly in the corona, and thus can only be a substantial source of heating if they are *generated* nearly as rapidly as they are damped. Acoustic waves also steepen into shocks after traveling only a few tenths of a solar radius (e.g., Cuntz and Suess 2001).

In order to heat the protons and heavy ions at heights above 2–3 $R_\odot$, one must look to collisionless wave dissipation mechanisms. The most attention has been paid to linear resonant damping, where particles can exchange energy with wave fluctuations if they experience nearly constant electric and magnetic fields in their own rest frames. Heating occurs as a net second-order outcome of energy gains and losses for particles interacting with waves of different relative phases. The resonance condition for particle species i encountering waves of frequency ω and parallel wavenumber $k_\parallel$ is

$$\omega - v_{\parallel i} k_\parallel - s \Omega_i \; = \; 0 \quad , \tag{11}$$

where s is an integer that determines the nature of the resonance and Ω_i is the particle's Larmor frequency. The condition $s = 0$ corresponds to classical Landau damping and so-called "transit time magnetic pumping" (see, e.g., Pinsker 2001), and $s \neq 0$ is generally denoted cyclotron or gyroresonant damping. The thermal spread of parallel velocities $v_{\parallel i}$ (characterized by the parallel most-probable speed $w_{\parallel i}$) about the mean flow speed $u_{\parallel i}$ causes the resonance to be broadened in frequency. For a Maxwellian distribution in the parallel direction, the linear damping rates are proportional to the following resonance factor:

$$\exp \left[- \left(\frac{\omega - u_{\parallel i} k_\parallel - s \Omega_i}{w_{\parallel i} k_\parallel} \right)^2 \right] \quad . \tag{12}$$

This simple expression allows the relative strengths of different resonance processes to be estimated. For example, Landau damping of parallel-propagating Alfvén or fast-mode waves is expected to be extremely *unimportant* as a heat source for positive ions in the extended corona because the comoving phase speed $(\omega/k_\parallel) - u_{\parallel i}$ is of order 2000 km s^{-1}, but $w_{\parallel i}$ for protons and heavy ions is not thought to exceed 100–200 km s^{-1}. This results in an extremely small resonance factor of order e^{-100}. Landau damping may be able to heat electrons in the extended corona, however, because their $w_{\parallel i}$ is of the same order as the wave phase speed (see, e.g., Barnes 1968; Habbal and Leer 1982).

Cyclotron damping of left-hand-polarized Alfvén waves (i.e., $s > 0$) has been studied for several decades as a promising mechanism for producing high proton and ion temperatures, strong anisotropies ($T_\perp \gg T_\parallel$), and faster bulk outflow for heavy ions (see, e.g., Toichi 1971; Harvey 1975; Abraham-Shrauner and Feldman 1977; Hollweg and Turner 1978; Dusenbery and Hollweg 1981; Marsch *et al.* 1982a; McKenzie and Marsch 1982; Isenberg and Hollweg 1983; Isenberg 1984; Gomberoff and Elgueta 1991). The first application of proton cyclotron damping to the corona and acceleration region of the wind was by Hollweg (1986b), Hollweg and Johnson (1988), and Isenberg (1990). The spectroscopic observations made by *SOHO* and *Spartan 201* (see § 2.2.2) have led to a resurgence of interest in cyclotron resonance models. McKenzie *et al.* (1995, 1997) and Czechowski *et al.* (1998) summarized the required physical constraints on self-consistent models and demonstrated the necessity of strong perpendicular heating. Tu and Marsch (1997, 2001), Marsch (1998), Li *et al.* (1999), Hu and Habbal (1999), Cranmer *et al.* (1999a), and Marsch and Tu (2001a) studied the energization of positive ions using moment-based (e.g., Maxwellian and bi-Maxwellian) methods. Cranmer *et al.* (1997) and Hollweg (1999a, 1999b, 1999c, 2000b) used a test-particle approach to simulate the averaged response of proton and ion velocity distributions to a known spectrum of resonant waves. Shevchenko *et al.* (1998), Tam and Chang (1999), Galinsky and Shevchenko (2000), Isenberg *et al.* (2000, 2001), Vocks and Marsch (2001), Marsch and Tu (2001b), and Cranmer (2001) have begun the process of examining the kinetic departures from bi-Maxwellian distributions when cyclotron waves are present in the solar wind.

It is instructive to evaluate the proton cyclotron heating rate in the extended corona and determine how large a resonant wave flux is required. Using quasi-linear kinetic theory (e.g., Rowlands *et al.* 1966; Kennel and Engelmann 1966) and assuming bi-Maxwellian velocity distributions,* the perpendicular heating rate for

* Note, however, that the damping of gyroresonant waves produces decidedly non-bi-Maxwellian diffusion of protons in velocity space. Isenberg *et al.* (2000, 2001) and Galinsky and Shevchenko (2000) have explored the properties of the resulting "resonant shell" proton velocity distributions in a purely collisionless corona; see § 5 for further discussion of this effect for minor ions.

protons can be approximated as

$$\frac{Q_{\perp p}}{m_p n_p} = \frac{\partial}{\partial t}\left(\frac{2k_B T_{\perp p}}{m_p}\right) \approx \frac{\langle \delta B^2 \rangle_{\rm res}}{B_0^2} V_A^2 \begin{cases} \Omega_p , & \text{for case E} \\ k_{\rm res}^{-1} |\partial \Omega_p / \partial r| , & \text{for case S} . \end{cases} \quad (13)$$

The resonant magnetic field variance $\langle \delta B^2 \rangle_{\rm res}$ is a wavenumber integral (from $k_\parallel = k_{\rm res} \equiv \Omega_p / V_A$ to $k_\parallel \rightarrow \infty$) of the assumed parallel fluctuation power spectrum, and B_0 is the background field strength. The two cases (E and S) represent two assumptions about how the waves are generated. Case E (for "extended" generation) assumes that a power-law wave spectrum is maintained continuously at the level specified by $\langle \delta B^2 \rangle_{\rm res}$. Case S (for "sweeping") assumes the wave spectrum was generated at the base of the corona and is rapidly damped at $\omega \approx \Omega_p$. The only locally available wave power in case S comes from the secular decrease in Ω_p with increasing radius (see Schwartz *et al.* 1981; Tu and Marsch 1997). Cases E and S correspond to "optically thin" and "optically thick" resonances in the Sobolev radiative transfer analogy developed by Cranmer (2000). Observations of heavy ions provide additional information about which limiting case comes closest to describing the extended corona (see § 5).

At 2 $R_\odot$, the proton inertial length ($k_{\rm res}^{-1}$) is approximately $10^{-6}\ R_\odot$ and the length over which Ω_p changes significantly ($\Omega_p |\partial \Omega_p / \partial r|^{-1}$) is approximately 0.1 $R_\odot$. Thus, to produce the same heating rate, the case S power spectrum must be $\sim 10^5$ times stronger than the case E power spectrum. The resonant magnetic variance $\langle \delta B^2 \rangle_{\rm res}$ is a fraction of the total magnetic variance $\langle \delta B^2 \rangle$, and the latter has been constrained empirically in the corona by both extrapolation inward from *in situ* and radio measurements (see, e.g., Mancuso and Spangler 1999), and by spectral line broadening (Esser *et al.* 1999). The total dimensionless amplitude $\langle \delta B^2 \rangle^{1/2} / B_0$ of Alfvénic fluctuations at 2 $R_\odot$ seems to be of order 0.01 to 0.1, and if the wavenumber spectrum is a power law (i.e., $P_B \propto k_\parallel^{-\eta}$), the resonant magnetic variance can be computed from

$$\langle \delta B^2 \rangle_{\rm res} = \langle \delta B^2 \rangle \left(\frac{k_{\rm res}}{k_{\rm out}}\right)^{1-\eta} , \quad (14)$$

where $k_{\rm out} \approx 10^{-10}$ cm^{-1} is a characteristic "outer scale" wavenumber corresponding to the lowest-frequency waves in the spectrum. For a reasonable choice of $\eta \approx 5/3$, the above empirical constraints imply ranges of proton heating rates (in units of the left-hand side of equation 13) of 10^{13} to 10^{15} cm^2 s^{-3} (for case E) and 10^8 to 10^{10} cm^2 s^{-3} (for case S) at 2 $R_\odot$. Empirical proton temperature gradients (from, e.g., Figures 3 and 7) allow us to estimate the actual heating rate to be of order $\sim 10^{11}$ cm^2 s^{-3} at 2 $R_\odot$, which implies that if case E applies, there appears to be sufficient wave power to heat the protons, but if case S applies, there does not. Note that Tu and Marsch (1997) modeled the proton heating in the extended corona and solar wind with a realistic total $\langle \delta B^2 \rangle$ and $\eta \approx 1$. This choice of η produced a

heating rate of order 10^{11} cm^2 s^{-3} for case S, but most turbulence models do not predict such a low value of η to extend up to $k_{\rm res}$ in wavenumber space.

To resolve the issue of proton heating via wave-particle resonance, it becomes necessary to better understand the *competition* between resonant damping, turbulent cascade, and local wave-growth instabilities in the extended corona. The assumption above of a power-law spectrum that extends to high $k_\parallel$ (and thus to high frequencies for Alfvénic fluctuations) may not be valid. Both numerical simulations of MHD turbulence and analytic descriptions such as "reduced MHD" (RMHD) indicate that the spectral cascade to high wavenumber occurs most rapidly for transverse ($k_\perp$) fluctuations (see, e.g., Montgomery 1982; Shebalin *et al.* 1983; Matthaeus *et al.* 1996; Goldreich and Sridhar 1997; Cho and Vishniac 2000; Bhattacharjee and Ng 2001; Nakayama 2001). Alfvénic fluctuations having large $k_\perp$ and small $k_\parallel$ do not have high frequencies approaching the cyclotron resonances. Observations of *in situ* solar wind fluctuations support the view that high-$k_\perp$ modes dominate (Matthaeus *et al.* 1990; Bieber *et al.* 1996), but there does seem to be evidence for high-$k_\parallel$ modes that dissipate via ion gyroresonance (e.g., Leamon *et al.* 1998). Coronal MHD waves that propagate obliquely to the background field direction can damp by multiple harmonics of the cyclotron resonance, and studies of how these waves heat and accelerate ions as a function of charge and mass are also underway (Li and Habbal 2001; Marsch and Tu 2001a; Hollweg and Isenberg 2001; Hollweg and Markovskii 2002).

Finally, there have been numerous *nonlinear* collisionless damping mechanisms suggested for waves in the solar wind. These processes are probably most important to consider at large heliocentric distances (e.g., $r > 20\,R_\odot$) where the total fluctuation amplitude $\langle \delta B^2 \rangle^{1/2}$ becomes of the same order as B_0 (e.g., Roberts *et al.* 1990). Nonlinear Landau damping, which occurs when particle motions come into resonance with the beat frequency between two populations of waves,

$$\omega_1 - \omega_2 \;=\; (\mathbf{k}_1 - \mathbf{k}_2) \cdot \mathbf{v}_i \quad , \tag{15}$$

has been modeled as a solar wind heat source by Hollweg (1971c), Lee and Völk (1973), and Lacombe (1976). Closely related to this phenomenon are decay and modulational instabilities of large-amplitude MHD waves (e.g., Cohen and Dewar 1974; Hollweg 1994; Vasquez and Hollweg 1999), as well as the potential ability of nonlinear MHD waves to damp at frequencies significantly *lower* than the cyclotron frequency (Chen *et al.* 2001). The very presence of a turbulent cascade is inherently nonlinear, and the ultimate rate of dissipation depends on the supply of energy at the largest spatial scales. Hollweg's (1986b) phenomenological cascade heating rate,

$$Q \;=\; \frac{\rho V_A^3}{L_{\rm corr}} \left(\frac{\langle \delta B^2 \rangle}{B_0^2} \right)^{3/2} \tag{16}$$

thus also seems to qualify as a nonlinear heat source in the extended corona (see also Coleman 1968). Here $\langle \delta B^2 \rangle$ denotes the total wave field, dominated by low

frequencies, and $L_{\rm corr}$ is an outer scale length assumed to be the mean distance between interacting flux tubes. For the empirical proton heating rate given above, we can solve for the required value of $L_{\rm corr}$ for specified wave amplitudes. A factor of three range in $\langle \delta B^2 \rangle^{1/2}/B_0$ yields a factor of $\sim$30 spread in $L_{\rm corr}$. For values of the dimensionless fluctuation amplitude between 0.01 and 0.03, the assumption of representative conditions at 2 $R_\odot$ leads to a realistic range for $L_{\rm corr}$ between solar granule ($\sim$1000 km) and supergranule ($\sim$30,000 km) sizes.

Other aspects of nonlinear wave evolution in the solar wind include phenomena such as steepening and mode coupling. Nonlinear steepening occurs for compressive fluctuations with longitudinal velocity variations, and dissipation is enhanced in the resulting shock trains (e.g, Stein and Schwartz 1972). Even Alfvén waves—traditionally believed not to steepen—exhibit non-negligible degrees of compressibility and parallel velocity oscillations at moderate degrees of nonlinearity, for both small and large angles of propagation to the ambient magnetic field (e.g., Harmon 1989). Numerical simulations that employ the derivative nonlinear Schroedinger equation (DNLS) have produced a rich variety of steepening phenomena that efficiently produce power at high frequency harmonics of an input wave spectrum (see Spangler 1997; Buti *et al.* 1999). Multi-mode coupling (i.e., wave reflection, refraction, and transformation of energy between Alfvén, fast, and slow modes) also should occur for waves in the extended corona. Computational simulations of both *linear* mode coupling (e.g., Poedts *et al.* 1998) and the *nonlinear* production of "daughter" waves from an input "mother" (via, e.g., decay or modulational instabilities; see Vasquez and Hollweg 1999; Del Zanna *et al.* 2001; and references therein) have produced a wide variety of results applicable to the solar wind.

The bottom line of this section is that the source of proton heating in the extended corona (i.e., 2 to 10 $R_\odot$) is still not known. The situation is slightly better in the *in situ* interplanetary medium because the fluctuation spectrum can be measured directly (e.g., Leamon *et al.* 1998, 1999; Stawicki *et al.* 2001), but even there no self-consistent theoretical picture exists. The large number of possible mechanisms must be winnowed further by more detailed measurements of the plasma properties and fluctuations.

4.3. Direct Momentum Deposition

Before proton temperatures in excess of 2×10^6 to 3×10^6 K in the corona were measured, the problem of accelerating the high-speed solar wind was considerably more vexing. The pressure gradient force on an electron conduction dominated plasma with a temperature less than or equal to 10^6 K could only produce an asymptotic flow speed of, at most, 300–400 km s^{-1}. A source of extra momentum on the accelerating wind was justifiably sought, and such a force may still be a necessary component of a fully self-consistent model of the fast wind. Five of the most studied momentum deposition mechanisms are listed below.

1. *Wave pressure.* Just as electromagnetic waves carry momentum and exert pressure on matter, propagating MHD waves also do work on the mean fluid via similar radiation stresses (Bretherton and Garrett 1968; Dewar 1970; Belcher 1971; Alazraki and Couturier 1971; Jacques 1977; Andrews and McIntyre 1978). For linear, dissipationless Alfvén waves in an ionized plasma, the time-averaged acceleration on ion species i was given by Isenberg and Hollweg (1982) and McKenzie (1994) as

$$a_{\rm WP} \;=\; \frac{\partial}{\partial r}\left[\frac{\langle \delta B^2 \rangle}{B_0^2}\left(\frac{\omega^2}{k_\parallel^2} - u_{\parallel i}^2\right)\right] \tag{17}$$

(see previous section for notation). Li *et al.* (1999) showed that the acceleration on protons can be expressed generally as

$$a_{\rm WP} \;=\; -\frac{1}{8\pi\rho\alpha}\frac{\partial}{\partial r}\left(\langle \delta B^2 \rangle\, \alpha^2\right) \;, \qquad \alpha \;=\; 1 + \frac{4\pi n_p k_{\rm B}(T_{\perp p} - T_{\parallel p})}{B_0^2 + \langle \delta B^2 \rangle} \tag{18}$$

with wave dissipation and anisotropic temperature effects included. This "ponderomotive" wave pressure force grows stronger when the waves reach large and nonlinear amplitudes (e.g., Gail *et al.* 1990; Pijpers 1995; Lau and Siregar 1996; Ofman and Davila 1997), but the amplitudes cannot be made arbitrarily large and still be consistent with spectroscopic and *in situ* constraints on the wave power. Wave pressure forces are also modified when the wavelengths are of the same order as the transverse length scales of coronal holes, which then act as "waveguides" (Flå *et al.* 1984; Davila 1985).

2. *Resonant wave damping.* For realistic proton and ion velocity distributions, cyclotron resonance causes a net *diffusion* of particles in velocity space, resulting in both anisotropic heating and bulk acceleration. The energy in resonant Alfvén waves propagating outward along the magnetic field becomes partitioned between heating and acceleration with the following proportionality:

$$\frac{\partial w_{\perp i}^2}{\partial t} \;=\; \left(\frac{2\Omega_i}{k_\parallel}\right)\frac{\partial u_{\parallel i}}{\partial t} \tag{19}$$

(see, e.g., Arunasalam 1976; Wentzel 1977; Hollweg 1999a, 1999b). Although this acceleration may be important in the initial stages of cyclotron-wave energization (i.e., when the velocity distributions are still close to isotropic), it is rapidly overtaken in magnitude by the "mirror acceleration" due to adiabatic pitch-angle focusing in an inhomogeneous field (see Isenberg *et al.* 2000, 2001; Cranmer 2001). Mirror acceleration is included automatically in fluid moment conservation equations that allow for temperature anisotropy; for example, this force dominates the right-hand side of equation (6) when $a_\perp \gg a_\parallel$.

3. *Diamagnetic acceleration.* If a substantial fraction of the solar wind plasma is injected in the form of small-scale loops, or "plasmoids," the lateral displacement

of the ambient magnetic field around these structures will result in a net upward acceleration (Schlüter 1957; Mullan and Ahmad 1982). The additional momentum deposited by this process is given approximately by the effective "buoyancy" pressure gradient

$$a_d = -\frac{3}{2} f_d w_d^2 \frac{\partial}{\partial r}\left(\ln \frac{B_0^2}{8\pi}\right) \quad , \tag{20}$$

where f_d is the ratio of mass flux in the plasmoids to the total wind mass flux and w_d is the most-probable speed in the plasmoids (Pneuman 1983, 1986; Yang and Schunk 1989; Mullan 1990; Tamano 1991). Plasmoid inhomogeneities may arise from reconnection events (Yokoyama and Shibata 1996) and expand to fill a large fraction of the volume of coronal holes (see also Feldman *et al.* 1997). A similar paradigm is emerging for the more stochastic flows from coronal streamers and active regions that are believed to be the primary sources of the slow solar wind (Wang *et al.* 1998b; Wu *et al.* 2000; Einaudi *et al.* 2001).

4. *Cosmic ray pressure.* The dynamics of high-energy (relativistic) protons and ion nuclei can affect the bulk low-energy plasma by scattering with MHD turbulent fluctuations (e.g., Gleeson and Axford 1967; Drury and Völk 1981; Axford *et al.* 1982). In the outer heliosphere, the energy density of the bulk plasma is comparable to the energy density of cosmic rays of extra-heliospheric origin, and the cosmic ray pressure modifies the properties of flows and shocks near the heliopause. Florinski and Jokipii (1997) have argued that cosmic rays of solar origin could transfer substantial amounts of energy flux to the accelerating wind even when the cosmic ray pressure is only a few percent of the total gas pressure. Cosmic rays may also generate Alfvén waves which in turn do work on the mean outflow, as described above (Achterberg 1981).

5. *Gravity damping.* Khabibrakhmanov and Mullan (1994) presented an intriguing and controversial idea: that Alfvén waves (which are dissipationless in the ideal MHD limit in a homogeneous plasma) can damp efficiently in the presence of a gravitational potential. The proposed wave energy loss can be expressed as an effective Joule heating (i.e., $\mathbf{J} \cdot \delta\mathbf{E}_\perp$), where the induced current density $\mathbf{J}$ is proportional to the oscillatory gravitational drift ($\mathbf{g} \times \delta\mathbf{B}_\perp$) and thus $\mathbf{J}$ has a component parallel to the transverse electric field oscillation $\delta\mathbf{E}_\perp$. Cuseri *et al.* (1999) and Khabibrakhmanov and Mullan (1999) concluded that the gravitational damping effect itself probably cannot heat the plasma, but it could either (1) be aided by Coulomb collisions to increase the thermal energy, or (2) provide a source of bulk momentum to the accelerating wind. The existence of gravity damping has been challenged by Hollweg (1997) and McKenzie and Axford (2000), who claimed that the effect is a misinterpretation of the ideal MHD response to transverse field line oscillations. No consensus has been reached on the existence or relative strength of gravity damping as a coronal energization mechanism, but work on the basic process continues (e.g., Khazanov *et al.* 2000).

5. Heavy Ions in the Solar Wind

5.1. General Properties

Heavy ions are valuable to the study of solar wind physics for several reasons. Their kinetic properties, as a function of charge and mass, allow coronal heating and wind acceleration mechanisms to be tested quantitatively. Their elemental and isotopic abundances allow direct connections to be made between features in the chromosphere, corona, and far solar wind. Their ionization fractions are "frozen in" relatively low in the corona, implying that *in situ* measurements can be useful long-distance diagnostics of heating and acceleration processes. Although most ions are "minor" enough to be considered test particles, the properties of the most abundant non-hydrogen species (He^{2+}) can have a major impact on the bulk properties of the solar wind (Bürgi 1992; Hansteen *et al.* 1997), and the next most abundant species (O^{6+}) has been suspected to have non-negligible feedback on the wind as well (Li *et al.* 1997).

The abundances of elements having first ionization potentials (FIP) below about 10 eV are enhanced, relative to those above 10 eV, in the corona and solar wind. This FIP effect is typically a factor of 3 to 4 in the slow solar wind and only of order 1.5 in the fast solar wind (see recent reviews by Raymond 1999; Feldman and Laming 2000). The origin of FIP fractionation is not yet understood completely, but most models involve the loss of rapid collisional coupling in the upper chromosphere, where significant fractions of neutral and singly ionized species coexist (e.g., Geiss 1982; Hénoux 1998; Schwadron *et al.* 1999; McKenzie 2000). The ionization state of the solar wind is determined in the extended corona. Because of the steep decrease in electron density with increasing radius, solar wind ions above a certain "freezing-in radius" encounter virtually no electrons, and thus are not sensitive to ionization and recombination processes in interplanetary space (e.g., Hundhausen *et al.* 1968; Owocki *et al.* 1983; Ko *et al.* 1997).

Ion charge states in the solar wind are determined both by the coronal electron velocity distribution and by relative flow speed differences between species of neighboring ionization state. Figure 8 compares the ionization fractions of five elements, measured by the SWICS instrument on *Ulysses* (see Ko *et al.* 1997), with modeled fractions calculated from empirically derived density and electron temperature models (Esser and Edgar 2000, 2001). Models assuming Maxwellian electron distributions in agreement with the CDS and SUMER constraints discussed in § 2.2.2 (i.e., $T_e \lesssim 800,000$ K) do not agree with the measured charge states. However, models that have a suprathermal "halo" population of electrons similar in character to *in situ* distributions (see § 2.1) succeed in matching the *Ulysses* charge states. The ionization and recombination rates determine where exactly the freezing in occurs, and this location is different for each element (e.g., O ions cease to interact closer to the Sun than Fe ions). The distance between the O and Fe decoupling can be increased if the Fe ions flow more slowly than the O

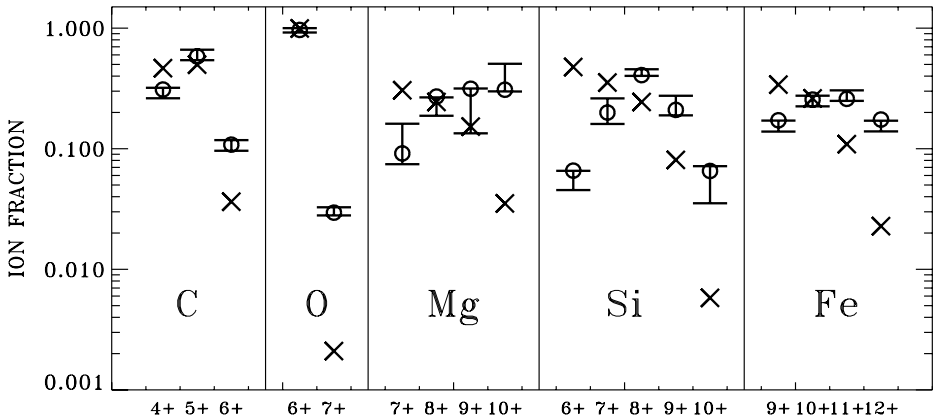

Figure 8. Ionization fractions (i.e., ion number densities relative to total elemental number densities) for C, O, Mg, Si, and Fe at 2 AU. *Ulysses* measurements are denoted by solid vertical lines with horizontal error bars. Modeled charge states are plotted for Maxwellian (crosses) and non-Maxwellian halo (circles) electron distributions.

ions. In order for the five elements in Figure 8 to encounter the electron distribution function that is needed to reproduce the *in situ* ion fractions, the differential flow speeds between the elements must be significant. Since the non-Maxwellian character of the distribution function most likely increases with radial distance from the Sun (rather than decreases), the oxygen ions must flow fastest since they only need a small tail on the distribution; the iron ions, on the other hand, need a larger tail, and must flow more slowly so they can decouple higher up in the corona where the tail is more developed. The model charge states in Figure 8, though, assumed that all ions of the same element flow with the same speed. It was shown, however, by Esser and Leer (1990) that flow speed differences of a factor of 2 to 3 may exist between adjacent O ions. The existence of such strong differential flows would greatly modify the need for a non-Maxwellian electron halo (see also Esser and Edgar 2001; Ko *et al.* 1998).

5.2. Preferential Heating and Acceleration

Heavy ions in the high-speed solar wind undergo preferential energization and a distortion of their velocity distributions away from Maxwellians. To lowest order, this energization manifests itself as: (1) faster outflow compared to the bulk proton-electron plasma, (2) more than mass-proportional heating, and (3) temperature anisotropies that depart strongly from those of protons and electrons. These properties must be reproduced by any successful theoretical model.

Even before a substantial database of ion plasma properties in the corona and solar wind had been accumulated, it was realized that ions cannot be in an idealized thermal equilibrium with the bulk plasma. Ions with temperatures of the same order as the proton and electron temperatures would receive a much *smaller* net outward

acceleration than protons and electrons, as can be seen by estimating the contributions to ion acceleration from the pressure gradient, gravity, and zero-current electrostatic field:

$$\frac{du_i}{dt} \approx -\frac{1}{n_i}\frac{\partial}{\partial r}\left(\frac{n_i k_B T_i}{m_i}\right) - \left(1 - \frac{Z_i}{2A_i}\right)\frac{GM_\odot}{r^2} \tag{21}$$

(see, e.g., Hundhausen 1972). The pressure gradient term is proportional to T_i/m_i, which is smaller than the proton pressure gradient by a factor of $A_i \equiv m_i/m_p$ if $T_i = T_p$. The term proportional to the ion charge-to-mass ratio Z_i/A_i (where Z_i is the net ion charge in units of e) is an approximation to the charge-separation electric field in the limit of a static atmosphere (e.g., Pannekoek 1922; Rosseland 1924). Note that the effective gravitational acceleration is half of the actual gravitational acceleration for protons (i.e., $Z_i/A_i = 1$), but is a *larger* inward acceleration for minor ions ($Z_i/A_i < 1$). Thus, it was expected for many years that heavy ions were accelerated much more slowly than protons and electrons in the extended corona.

Geiss *et al.* (1970) and Alloucherie (1970) investigated the possibility that Coulomb collisional friction could drag out heavy ions and accelerate them to some large fraction of the proton speed. This effect, however, cannot accelerate ions faster than protons (as is observed), and it is limited by the onset of collisional runaway when the drift speeds exceed the local most-probable speeds (e.g., Dreicer 1959; Owocki 1982; Scudder 1996). Ryan and Axford (1975) proposed that the most natural way of accelerating minor ions is to heat them more than the protons and electrons are heated—at least proportionally to their masses (to provide a comparable pressure gradient), or even more than this (to further combat the stronger effective gravity). Hernandez and Marsch (1985) found that collisional friction can heat a minority species and thus modify the asymptotic equilibrium state to give a temperature ratio T_i/T_p that in some cases may be as large as the inverse ratio of mass densities ρ_p/ρ_i.

It is now known (see § 2) that ions are indeed more than mass-proportionally heated, both in the extended corona and in interplanetary space, and thus their rapid acceleration is not surprising. The damping of ion cyclotron resonant waves has been considered for several decades as a likely mechanism in the distant solar wind ($r > 0.3$ AU), and the surprising UVCS observations in the 1990s led to the widespread extension of this idea to the corona. Details concerning this process, including proposed ideas for the origin of these waves, are discussed above (§ 4.2.2). Computing gyroresonant heating and acceleration rates for minor ions is in some ways simpler than for protons. The effective "resonance zones" in the corona (where the factor in equation 12 is non-negligible) are relatively small in radial extent for minor ion resonances with waves of a given frequency (Cranmer 2000). The damping of outward-propagating waves that pass through these zones can be described by an optical-depth-like quantity τ_i, where the ratio of attenuated to initial power is simply $e^{-\tau_i}$. It is straightforward to estimate τ_i in the limit of quasi-linear theory, which demands that the wave damping rate γ_i due to a given

ion species is much smaller than the real resonance frequency Ω_i. In the extended corona,

$$\frac{\gamma_i}{\Omega_i} \approx \left(\frac{m_i n_i}{m_p n_p}\right) \frac{V_A}{2w_{\|i}} \ll 1 \quad \text{(for most minor ions)} , \tag{22}$$

and the optical depth accumulated over the resonance zone is given by

$$\tau_i \equiv \int_{\text{zone}} dr \, \frac{2\gamma_i}{V_{\text{gr}}} \approx \left(\frac{m_i n_i}{m_p n_p}\right) \frac{\Omega_i k_{\text{res}}}{|\partial \Omega_i / \partial r|} , \tag{23}$$

where the group velocity $V_{\text{gr}} \approx V_A$ in the corona (for details, see Cranmer 2000). As described in § 4.2.2, the ratio of the resonance frequency scale height $L_\Omega \equiv \Omega_p |\partial \Omega_p / \partial r|^{-1}$ to the inverse resonant wavenumber k_{res}^{-1} is of order 10^5, so the above relation suggests that ions having $n_i \gtrsim 10^{-6} n_p$ may exhibit $\tau_i \sim 1$ and thus can attenuate resonant waves significantly. This counterintuitive result is a simple consequence of the *slow* secular decrease in Ω_i with radius when compared with the wave attenuation length $\ell_i \sim V_A / \gamma_i$, which itself is large compared to the resonant wavelength $\lambda_{\text{res}} \sim V_A / \Omega_i$; i.e.,

$$\lambda_{\text{res}} \ll \ell_i \ll L_\Omega \lesssim R_\odot . \tag{24}$$

In other words, even the weak quasi-linear damping due to minor ions has *ample room* to dissipate the waves significantly.

The surprisingly strong ability of minor ions to damp cyclotron waves seems to rule out models that propose all of the high-frequency wave power to originate at the base of the corona. Figure 9a illustrates that a wave of a given frequency would first become resonant with low Z_i / A_i ions before becoming resonant with higher Z_i / A_i ions. Cranmer (2000) identified several dozen ion species with Z_i / A_i between 0.1 and 0.2 that have $\tau_i > 1$ in the extended corona. This implies that negligible wave power would remain to energize ions such as O^{5+}, He^{2+}, and protons (see also Liewer *et al.* 1999, 2001). Tu and Marsch (2001) pointed out that ions can be accelerated "out of resonance" by ion cyclotron waves, thus either increasing the effective radius of the resonance zones (see Figure 9b) or decreasing τ_i to negligibly small values. The time required to accelerate ions to this "self-induced transparency" limit depends on the level of resonant wave power that is present in the corona. Cranmer (2001) determined that this effect should be important only if the wave power level is at least 10^3 times the maximum empirically constrained values discussed in § 4.2.2. Thus, the conclusion of Cranmer (2001) was that *realistic* levels of coronal wave power are insufficient to stop the damping of a pure base-generated wave spectrum. If the ion cyclotron resonance mechanism is truly responsible for heating and accelerating high Z_i / A_i ions like O^{5+} and protons, the above implies that some kind of local coronal generation of waves is necessary. This conclusion is still tentative, though, because the kinetic models of Cranmer (2001) did not incorporate the large-scale inhomogeneities of coronal

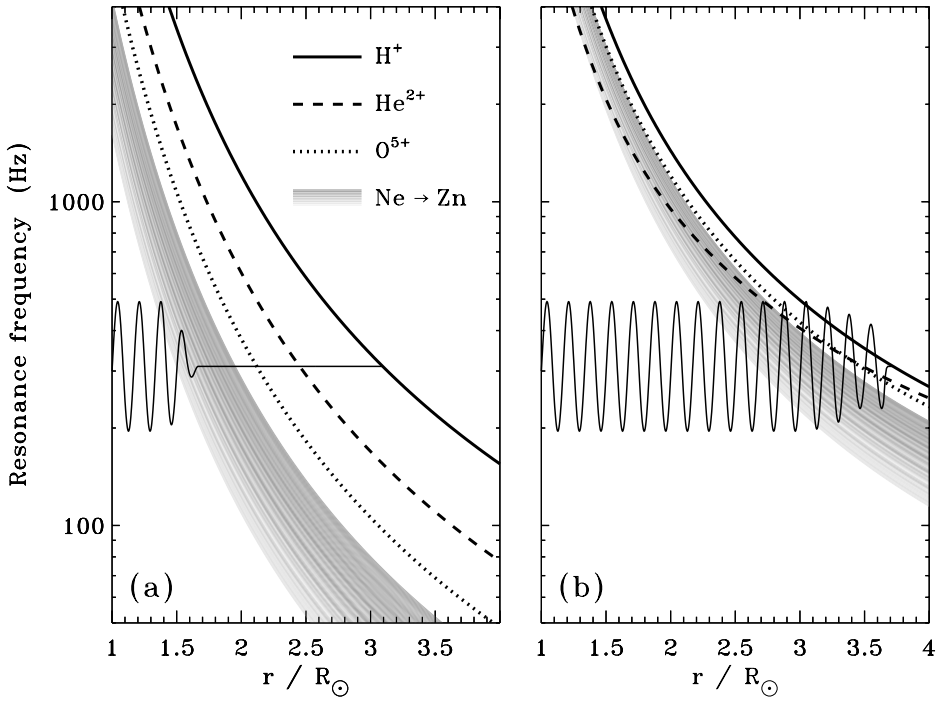

Figure 9. Schematic plot of ion cyclotron resonance frequencies as a function of heliocentric distance in a polar coronal hole. The magnetic field strength is computed from the model of Banaszkiewicz *et al.* (1998). The gray regions indicate the summed damping rate γ due to ions with Z_i/A_i between 0.1 and 0.2. The resonance frequencies are affected by the bulk outflow speeds of the ions, and we plot the limiting cases of: (a) $u_\parallel = 0$, and (b) $u_\parallel$ for protons given by mass flux conservation in the mean coronal hole (see Figure 3) and $u_\parallel$ for minor ions given by the maximum parallel velocity for resonance with Alfvén waves having realistic dispersion (see equation 27 of Cranmer 2001). Panels (a) and (b) represent "optically thick" and "optically thin" damping limits, respectively (see text).

plasma parameters that could affect how ions are accelerated out of resonance (e.g., the magnetic mirror force).

The above analysis seems to indicate that "case S" (pure sweeping of a base-generated wave spectrum) does not apply for minor ions. The illustrative quasi-linear calculation performed in § 4.2.2 for "case E" perpendicular proton heating can be extended straightforwardly to other ions. In fact, the calculation is made considerably simpler for minor ions because the cyclotron resonance is extremely "sharp" in wavenumber space, thus allowing the heating rates to be estimated as proportional to the *local* wave power $P_{\rm res}$ at $k_\parallel = k_{\rm res}$,

$$\frac{\partial w_{\perp i}^2}{\partial t} \approx \frac{\pi \Omega_i^2}{B_0^2} P_{\rm res} V_{\rm ph} \quad , \tag{25}$$

where $V_{\rm ph} \approx V_A (1 - Z_i/A_i)^{1/2}$ is the phase speed at resonance. With a similar assumption of a power-law wave spectrum (with spectral exponent η) as in equations

(13) and (14), we can evaluate $P_{\rm res}$ in terms of the resonant field variance $\langle \delta B^2 \rangle_{\rm res}$, and express the *ratio* of ion to proton perpendicular heating rates as

$$\zeta_i \;=\; \frac{2^{1+\eta}\pi^{1/2}}{5}(1+\eta)\left(\frac{Z_i}{A_i}\right)^{2-\eta}\left(1-\frac{Z_i}{A_i}\right)^{(1+\eta)/2} \tag{26}$$

(see, e.g., Cranmer *et al.* 1999a; Hollweg 1999b, 1999c; Cranmer 2000). A value of $\zeta_i = 1$ would imply that the ion species was heated mass-proportionally with protons, and thus, for example, would lead to $T_{\rm O} = 16T_p$ in the limit of no Coulomb collisions. For O^{5+} ions ($Z_i/A_i = 0.3125$), a reasonable value for $\eta = 5/3$ gives $\zeta_i = 2.5$, which is consistent with the factor of 30 to 60 difference between the UVCS kinetic temperatures of O^{5+} ions and protons (at 2 $R_\odot$) shown in Figure 3. Note that η must be larger than $\sim$1.2 in order for ζ_i to exceed 1 for O^{5+} ions; for $\eta < 1.2$ there is *less* than mass-proportional heating.

The above agreement between the observed and predicted (case E) ion-to-proton heating ratio implies that if there is sufficient wave power to heat the protons in case E, there is also sufficient power to heat O^{5+} ions. However, even though evidence is mounting for ion cyclotron waves being generated rapidly enough to combat minor ion damping (thus validating case E for minor ions), there is no guarantee that either turbulent cascade or local instabilities can generate waves rapidly enough to combat the stronger proton damping (with $\gamma_p \sim \Omega_p$). Thus, case S may be the most appropriate limit for the proton resonances, and in § 4.2.2 we found that this case does not seem efficient enough to provide enough proton heating via the damping of parallel-propagating waves. It may then be reasonable to speculate that some other rapidly damped wave mode (e.g., highly oblique Alfvén or fast-mode waves) could be responsible for proton heating, whereas a relatively low level of parallel-propagating ion cyclotron wave power could be sufficient to heat the minor ions.

The perpendicular heating elaborated in equations (13) and (26) is only one part of the full kinetic picture. Individual ions undergoing cyclotron resonance either gain or lose kinetic energy, depending on the relative phase between the wave and the ion gyromotion, but they *conserve* kinetic energy as measured in the frame moving with the phase speed $V_{\rm ph} = \omega/k_\parallel$ of the waves. The second-order result of these "constrained random walks" is a net diffusion of the velocity distribution along contours of constant wave-frame particle speed, $[v_{\perp i}^2 + (v_{\parallel i} - \omega/k_\parallel)^2]^{1/2}$, and negligible ion motion in directions normal to these contours (Rowlands *et al.* 1966; Kennel and Engelmann 1966; Dusenbery and Hollweg 1981; Galinsky and Shevchenko 2000; Isenberg *et al.* 2000, 2001). This diffusion occurs only for values of $v_{\parallel i}$ that satisfy both the resonance condition (equation 11) and the wave dispersion relation for $\omega(\mathbf{k})$. For positive ions interacting with left-hand polarized Alfvén waves in a low-beta plasma, there can exist one or more resonances for $v_{\parallel i}$ less than a specified $v_{\parallel \rm max}$ and no resonances above $v_{\parallel \rm max}$. Cranmer (2001) provided an analytic fit for $v_{\parallel \rm max}$ as a function of Z_i/A_i, from a numerically computed

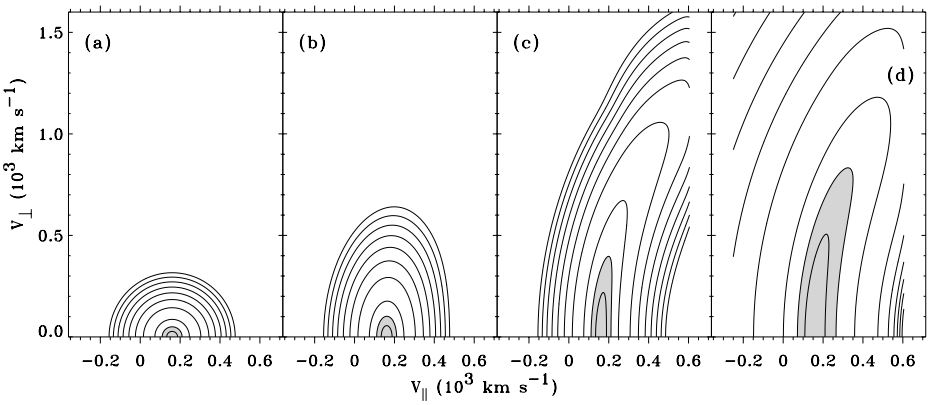

Figure 10. Contour plots of the O^{5+} velocity distribution from the numerical quasi-linear diffusion model of Cranmer (2001), at four times in its evolution: $t = 0$, 100, 2000, and 50,000 seconds. The highest $1/e$ core of the distribution is filled in with gray, and the two enclosed contours intercept (ln $f_{\max} - 0.3$) and (ln $f_{\max} - 1$), where $f_{\max}$ is the maximum value of the distribution. The remaining 8 contours are spread evenly between (ln $f_{\max} - 3$) and (ln $f_{\max} - 40$).

dispersion relation. For most minor ions ($0 < Z_i/A_i < 0.5$), $v_{\parallel\max}$ ranges from the nonresonant inertial-frame phase speed ($u_{\parallel p} + V_A$) as $Z_i/A_i \to 0$ to the bulk wind speed ($u_{\parallel p}$) as $Z_i/A_i \to 0.5$. Thus, ion cyclotron resonance causes an ion velocity distribution $f_i(\mathbf{v})$ to evolve as

$$\frac{\partial f_i}{\partial t} = \begin{cases} \frac{1}{\sin\alpha}\,\frac{\partial}{\partial\alpha}\left(D_{\rm eff}\sin\alpha\,\frac{\partial f_i}{\partial\alpha}\right) & , \quad v_{\parallel i} \le v_{\parallel\max} \\ 0\ , & \quad v_{\parallel i} > v_{\parallel\max} \end{cases} \tag{27}$$

where α is the ion pitch angle measured in a frame moving at $V_{\rm ph}$, i.e., $\tan\alpha = v_{\perp i}/(v_{\parallel i} - V_{\rm ph})$, and $D_{\rm eff}$ is an effective diffusion coefficient proportional to the available resonant wave power.

Figure 10 shows a simulation of resonant diffusion for O^{5+} ions in an otherwise homogeneous plasma at conditions appropriate for $r = 2\,R_\odot$ (Cranmer 2001). Because the phase speed in the corona is dominated by the large Alfvén speed (typically $V_A \approx 1000$–3000 km s^{-1}), the center of the concentric diffusion contours at $v_{\perp i} = 0$ is at a much larger value of $v_{\parallel i}$ than exhibited by most particles in the ion distribution. Thus the initial direction of the diffusion (for small $v_{\parallel i}$ and $v_{\perp i}$) is primarily perpendicular to the mean magnetic field. Diffusion to a zero-gradient state along the curved, constant-energy shells does not occur because of the sharp boundary between resonant and nonresonant parallel velocities (for the model of O^{5+} in Figure 10, this occurs at $v_{\parallel\max} \approx 610$ km s^{-1}). The idealized end-state of fully-diffused shell distributions can only be reached when an equal number of particles are scattered *in both directions* along the shells. The net leakage of particles from the resonant to nonresonant regions of velocity space prevents this from occurring. In reality, of course, other forces not considered here (e.g.,

gravity) should be able to decelerate some ions back into resonance, but not at high values of $v_{\perp i}$ where the magnetic mirror force is dominant (e.g., Isenberg *et al.* 2000, 2001; Isenberg 2001a). In addition, if two populations of resonant waves are present—each with different phase speeds—minor ions can diffuse upwards in $v_{\perp i}$ space along either set of concentric shells, thus resulting in a kind of second-order Fermi acceleration in $v_{\perp i}$ (see Isenberg 2001b; Mitzuta and Hoshino 2001). Finally, the diffusion to strong anisotropies cannot go on indefinitely; eventually the velocity distribution reaches an effective "marginal stability" equilibrium with the waves where no further energy is exchanged (Ofman *et al.* 2001; Gary *et al.* 2001; Cranmer 2001).

There have been several other physical processes, besides ion cyclotron resonance, suggested to preferentially heat and accelerate minor ions in the high-speed solar wind. Lee and Wu (2000) proposed that magnetic reconnection at the coronal base produces fast shocks that propagate through the corona and can accelerate ions. For subcritical collisionless shocks having thicknesses of the same order as the ion inertial length (V_A/Ω_i), ions traversing the shock enter into plasma with a new magnetic field direction before they can fully "deflect," thus converting some of their parallel motion into perpendicular gyromotion (see also Lee *et al.* 1986). This process can increase an ion's perpendicular anisotropy to large values ($T_\perp \gg T_\parallel$) and heat heavy ions more than mass-proportionally compared to protons. However, it is unclear whether shocks of the required strength ($\Delta v \gtrsim 0.3\, V_A$) are numerous enough in the extended corona to encounter the majority of the ions. An alternative idea that also involves shock acceleration was proposed by Whang *et al.* (1990), who found that that heavy ions can be heated nearly mass-proportionally at a standing "coronal slow shock" at 6–10 $R_\odot$. There is, however, no real evidence for the existence of such large-scale, long-lived discontinuity surfaces in coronal holes, as predicted by, e.g., Whang (1986). Finally, mass-proportional ion heating was also suggested by Heinemann (1999) to occur via Fermi acceleration (i.e., multiple nonadiabatic reflections at small-scale wave fronts), but this requires large amplitudes ($\langle \delta B^2 \rangle^{1/2} \sim B_0$) for the Alfvénic fluctuations, and thus may apply only at large distances from the Sun.

6. Summary and Discussion

Considerable progress has been made over the last decade in characterizing the plasma state of the corona and solar wind. As remote-sensing measurements have become possible in the extended acceleration region of the wind, the traditional gap between solar physics (i.e., near-Sun astronomy) and space physics (i.e., interplanetary plasma physics) is being bridged. The fact that the two communities are becoming increasingly aware of the value of each other's data can only lead to an increased understanding of the basic physics. Observations have guided theorists to discard some candidate physical processes and further investigate others (see, e.g.,

Hollweg and Isenberg 2001 for a detailed history of the rise to prominence of the ion cyclotron resonance idea). Nevertheless, a complete understanding of coronal heating and solar wind acceleration must come from successful *ab initio* modeling (i.e., with a minimum of adjustable parameters) that reproduces all observed quantities.

This review paper has focused mainly on observations and theories of the extended corona in large, open-field coronal holes. Even though much has been learned, the *relative contributions* of many likely physical processes are not known. Figure 11 illustrates about a half dozen of these processes within the following general paradigm. It seems likely that the Sun launches a significant population of low-frequency ($f \lesssim 10^{-2}$ Hz) MHD waves, which then are transformed somehow into forms that lead to heating and acceleration of solar wind particles. The processes that give rise to the initial wave spectrum and heat the highly structured coronal base are not portrayed, because in some sense they can be considered to be "decoupled" from the processes important in the collisionless extended corona. This decoupling does *not* imply that unified models of the chromosphere, transition region, corona, and solar wind are unnecessary (see Hammer 1982; Hansteen and Leer 1995; Hackenberg *et al.* 2000). Such models represent, for example, the only way to obtain a self-consistent solar wind mass flux. It seems likely, however, that different energy and momentum deposition processes are dominant in coronal structures with significantly different properties. Following Priest *et al.* (2000), we suggest the following qualitative hierarchy of structures (from high density to low density) that probably exhibit *different* dominant heating mechanisms:

1. active regions and bright points
2. quiet coronal loops
3. open funnels at the coronal base
4. open and closed flux tubes in streamers
5. open flux tubes in coronal hole acceleration regions
6. the high plasma β interplanetary medium.

The plasma in coronal mass ejections (CMEs) obviously should also constitute a separate category, though its place in the above list is unclear.

Improvements in both observations and theory are needed to make further progress in identifying and characterizing the most important heating and acceleration processes in the high-speed wind. One aspect of *in situ* particle experiments at 1 AU that has not been fully explored is the measurement of the full three-dimensional velocity distributions of minor ions. Such measurements, of course, are difficult because of the extremely low number densities of ions, but they would yield valuable constraints on the kinetic physics of the wind. Some solar wind ion distributions have been observed to be non-gyrotropic (i.e., asymmetric about the magnetic field axis; see Astudillo *et al.* 1995), but it remains to be seen if this property is common enough to require consideration in theoretical models (e.g., Kuramitsu and Hada 2000). Missions such as NASA's *Solar Probe* and ESA's *Solar*

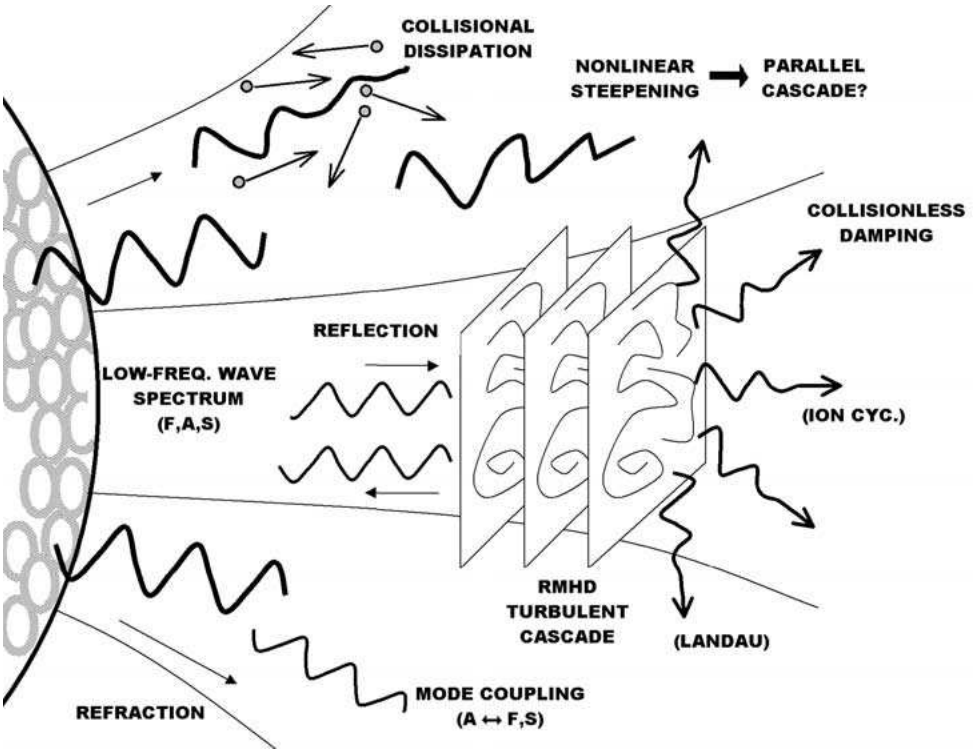

Figure 11. Schematic representation of various physical processes that are believed to be important in heating and accelerating particles in the extended corona. A, F, and S denote Alfvén, fast-mode, and slow-mode MHD waves. This image was inspired in part by Figure 1 of Oughton *et al.* (2001).

Orbiter should extend our direct knowledge of particle and fluctuation properties to much smaller heliocentric distances.

Remote-sensing diagnostics of the accelerating solar wind can also be improved greatly. Next-generation space-based coronagraph spectrometers are being designed with the capability to sample the velocity distributions of dozens of ions in the acceleration region of the high-speed wind in coronal holes. In addition to being sensitive to many more emission lines, such instruments could also detect subtle departures from Gaussian line shapes that signal the presence of specific non-Maxwellian distributions (see, e.g., Cranmer 1998, 2001). Higher spatial and temporal resolution would allow a much more detailed census of mass, momentum, and energy in neighboring flux tubes to be performed. For example, the filamentary nature of coronal holes has been typically interpreted as a two-phase medium—plumes and interplume plasma—but there may be a continuous spectrum of density variations rather than just two separate phases. New diagnostics such as the measurement of the Thomson scattered H I Lyα profile (which probes the line-of-sight electron velocity distribution; see Hughes 1965; Fineschi *et al.* 1998) can put firm constraints on both the "core" electron temperature and the existence of halo-like or

power-law wings with unprecedented confidence limits. Finally, new radio sounding techniques such as the measurement of scintillations in the circularly polarized Stokes parameters (e.g., Macquart and Melrose 2000) may be fruitful in extracting more information about MHD turbulence in the corona and solar wind.

The advances in theory that will lead to a definitive identification and understanding of the dominant physical processes are notoriously difficult to predict. It is becoming increasingly clear, though, that *kinetic models* of the solar wind plasma (§ 3.2) are necessary for a complete treatment of the physics. It is possible that new moment-closure schemes that incorporate kinetic processes will lead to tractable quasi-fluid models (e.g., Chang and Callen 1992; Siregar *et al.* 1998), though these should not be applied to macroscopic solar wind models until the appropriate microscopic physics has been studied in detail. More complete models of the MHD fluctuation spectrum that is ultimately responsible for the kinetic properties of the particles must also be pursued. The dominant physics (of the *combined* system of particles and fluctuations) may become evident only when a number of "competing" physical processes are included together in a solar wind model. Because many of the processes in Figure 11 interact with one another on a multitude of spatial and temporal scales, their true impact on the system may not be made clear until they are studied simultaneously (producing an emergent richness that would not have occurred if each process was studied in isolation).

Many aspects of MHD and plasma physics that are encountered in the study of the corona and solar wind also arise in other contexts. Recent years have seen a healthy increase in cross-fertilization between fields, and progress can only be accelerated by fostering such interdisciplinary work. Related studies of MHD turbulence and ion cyclotron resonance, for example, can be found in relation to the interstellar medium (Rickett 1990; Minter and Spangler 1997), advection-dominated accretion disks around compact objects (Medvedev 2000), fusion plasmas in tokamaks (Pinsker 2001), and new designs for ion rocket systems (Chang Díaz 2001).

Acknowledgements

The author would like to thank the Scientific and Local Organizing Committees of the 2000 UVCS/*SOHO* Science Meeting for planning and executing a successful gathering of theorists and observers. The author acknowledges the significant contributions of Steven Spangler, Ruth Esser, and John Kohl to this paper. The author also thanks Joseph Hollweg, Philip Isenberg, George Field, Adriaan van Ballegooijen, William Matthaeus, Joseph Lemaire, Stan Owocki, Marco Velli, and Ian Axford for many valuable discussions. This work is supported by the National Aeronautics and Space Administration under grant NAG5-11420 to the Smithsonian Astrophysical Observatory, by Agenzia Spaziale Italiana, and by the Swiss contribution to the ESA PRODEX program. *SOHO* is a project of international cooperation between ESA and NASA.

References

Abraham-Shrauner, B., and Feldman, W. C.: 1977, *J. Geophys. Res.* **82**, 618.
Achterberg, A.: 1981, *Astron. Astrophys.* **98**, 195.
Ahmad, I. A., and Withbroe, G. L.: 1977, *Solar Phys.* **53**, 397.
Alazraki, G., and Couturier, P.: 1971, *Astron. Astrophys.* **13**, 380.
Alfvén, H.: 1947, *Mon. Not. Roy. Astron. Soc.* **107**, 211.
Allen, L. A., Habbal, S. R., and Hu, Y. Q.: 1998, *J. Geophys. Res.* **103**, 6551.
Allen, L. A., Habbal, S. R., and Li, X.: 2000, *J. Geophys. Res.* **105**, 23123.
Alloucherie, Y.: 1970, *J. Geophys. Res.* **75**, 6899.
Altschuler, M. D., and Perry, R. M.: 1972, *Solar Phys.* **23**, 410.
Anderson, S. W., Raymond, J. C., and van Ballegooijen, A.: 1996, *Ap. J.* **457**, 939.
Andreev, V. E., Efimov, A. I., Samoznaev, L. N., Chashei, I. V., and Bird, M. K.: 1997, *Solar Phys.* **176**, 387.
Andrews, D. G., and McIntyre, M. E.: 1978, *J. Fluid Mech.* **89**, 609.
Andries, J., Tirry, W. J., and Goossens, M.: 2000, *Ap. J.* **531**, 561.
Andriesse, C. D.: 1979, *Astrophys. Space Sci.* **61**, 205.
Andriesse, C. D.: 2000, *Ap. J.* **539**, 364.
Antonucci, E., Dodero, M. A., and Giordano, S.: 2000, *Solar Phys.* **197**, 115.
Arunasalam, V.: 1976, *Phys. Rev. Letters* **37**, 746.
Aschwanden, M. J., and Acton, L. W.: 2001, *Ap. J.* **550**, 475.
Astudillo, H. F., Marsch, E., Livi, S., and Rosenbauer, H.: 1995, in D. Winterhalter, J. T. Gosling, S. R. Habbal, W. S. Kurth, and M. Neugebauer (eds.), *Solar Wind Eight,* AIP Conf. Proc. 382, AIP Press, Woodbury, New York, 289.
Athay, R. G.: 2002, *Ap. J.* **565**, 630.
Athay, R. G., and White, O. R.: 1978, *Ap. J.* **226**, 1135.
Axford, W. I.: 1968, *J. Geophys. Res.* **73**, 6855.
Axford, W. I.: 1977, in M. A. Shea, D. F. Smart, and S. T. Wu (eds.), *Study of Travelling Interplanetary Phenomena,* D. Reidel, Dordrecht, 145.
Axford, W. I., Leer, E., and McKenzie, J. F.: 1982, *Astron. Astrophys.* **111**, 317.
Axford, W. I., and McKenzie, J. F.: 1992, in E. Marsch and R. Schwenn (eds.), *Solar Wind Seven,* Pergamon, New York, 1.
Axford, W. I., and McKenzie, J. F.: 1997, in J. R. Jokipii, C. P. Sonett, and M. S. Giampapa (eds.), *Cosmic Winds and the Heliosphere,* Univ. of Arizona Press, Tucson, 31.
Axford, W. I., McKenzie, J. F., Sukhorukova, G. V., Banaszkiewicz, M., Czechowski, A., and Ratkiewicz, R.: 1999, *Space Sci. Rev.* **87**, 25.
Axford, W. I., and Newman, R. C.: 1967, *Ap. J.* **147**, 230.
Baker, D. N.: 1998, *Adv. Space Res.* **22** (1), 7.
Balasubramaniam, K. S., Keil, S. L., and Smartt, R. N.: (eds.) 1996, *Solar Drivers of Interplanetary and Terrestrial Disturbances,* ASP Conf. Ser. **95**, Astron. Soc. Pacific, San Francisco.
Banaszkiewicz, M., Axford, W. I., and McKenzie, J. F.: 1998, *Astron. Astrophys.* **337**, 940.
Banerjee, D., Teriaca, L., Doyle, J. G., and Lemaire, P.: 2000, *Solar Phys.* **194**, 43.
Banks, P. M., and Holzer, T. E.: 1968, *J. Geophys. Res.* **73**, 6846.
Barakat, A. R., and Schunk, R. W.: 1982, *Plasma Phys.* **24**, 389.
Barghouthi, I. A., Barakat, A. R., and Persoon, A. M.: 1998, *Astrophys. Space Sci.* **259**, 117.
Barnes, A.: 1968, *Ap. J.* **154**, 751.
Barnes, A.: 1979, in E. Parker, C. Kennel, and L. Lanzerotti (eds.), *Solar System Plasma Physics,* vol. 1, North-Holland, Amsterdam, 249.
Barnes, A.: 1992, *Rev. Geophys.* **30**, 43.
Barnes, A., Gazis, P. R., and Phillips, J. L.: 1995, *Geophys. Res. Letters* **22**, 3309.

Bastian, T. S.: 2001, *Astrophys. Space Sci.* **277**, 107.
Beckers, J. M., and Chipman, E.: 1974, *Solar Phys.* **34**, 151.
Belcher, J. W.: 1971, *Ap. J.* **168**, 509.
Belcher, J. W., and Davis, L., Jr.: 1971, *J. Geophys. Res.* **76**, 3534.
Benz, A. O., and Gold, T.: 1977, *Astron. Astrophys.* **55**, 229.
Bertaux, J. L., Lallement, R., and Quémerais, E.: 1996, *Space Sci. Rev.* **78**, 317.
Bhattacharjee, A., and Ng, C. S.: 2001, *Ap. J.* **548**, 318.
Bieber, J. W., Wanner, W., and Matthaeus, W. H.: 1996, *J. Geophys. Res.* **101**, 2511.
Billings, D. E.: 1966, *A Guide to the Solar Corona,* Academic Press, New York.
Bird, M. K.: 1982, *Space Sci. Rev.* **33**, 99.
Bird, M. K., and Edenhofer, P.: 1990, in R. Schwenn and E. Marsch (eds.), *Physics of the Inner Heliosphere,* vol. 1, Springer-Verlag, Heidelberg, 13.
Braginskii, S. I.: 1965, *Rev. Plasma Phys.* **1**, 205.
Brandt, J. C., and Cassinelli, J. P.: 1966, *Icarus* **5**, 47.
Brandt, J. C., Roosen, R. G., and Harrington, R. S.: 1972, *Ap. J.* **177**, 277.
Bretherton, F. P., and Garrett, C. J. R.: 1968, *Proc. Roy. Soc. A* **302**, 529.
Bromage, B. J. I., Alexander, D., Breen, A., *et al.:* 2000, *Solar Phys.* **193**, 181.
Browning, P. K.: 1991, *Plasma Phys. Control. Fus.* **33**, 539.
Buchlin, E., and Hassler, D. M.: 2000, *Bull. American Astron. Soc.* **32**, 810.
Bürgi, A.: 1992, *J. Geophys. Res.* **97**, 3137.
Buti, B., Galinski, V. L., Shevchenko, V. I., *et al.:* 1999, *Ap. J.* **523**, 849.
Cannon, C. J., and Thomas, R. N.: 1977, *Ap. J.* **211**, 910.
Cargill, P. J.: 1994, in J. L. Burch and J. H. Waite, Jr. (eds.), *Solar System Plasmas in Space and Time,* AGU, Washington, DC, 21.
Chamberlain, J. W.: 1960, *Ap. J.* **131**, 47.
Chamberlain, J. W.: 1961, *Ap. J.* **133**, 675.
Champeaux, S., Gazol, A., Passot, T., and Sulem, P.-L.: 1997, *Ap. J.* **486**, 477.
Chang, Z., and Callen, J. D.: 1992, *Phys. Fluids B* **4**, 1167.
Chang Díaz, F. R.: 2001, in T. K. Mau and J. deGrassie (eds.), *Radio Frequency Power in Plasmas,* AIP Conf. Proc. 595, AIP Press, Melville, New York, 3.
Chapman, S.: 1954, *Ap. J.* **120**, 151.
Chapman, S.: 1957, *Smithsonian Contrib. Astrophys.* **2**, 1.
Chapman, S., and Cowling, T. G.: 1964, *The Mathematical Theory of Nonuniform Gases,* Cambridge Univ. Press, Cambridge.
Chashei, I. V.: 1997, *Astron. Reports* **41**, 85.
Chen, L., Lin, Z., and White, R.: 2001, *Phys. Plasmas* **8**, 4713.
Chew, G. F., Goldberger, M. L., and Low, F. E.: 1956, *Proc. Roy. Soc. London, A* **236**, 112.
Cho, J., and Vishniac, E. T.: 2000, *Ap. J.* **539**, 273.
Cohen, R. H., and Dewar, R. L.: 1974, *J. Geophys. Res.* **79**, 4174.
Coleman, P. J., Jr.: 1968, *Ap. J.* **153**, 371.
Coles, W. A.: 1978, *Space Sci. Rev.* **21**, 411.
Coles, W. A., and Harmon, J. K.: 1989, *Ap. J.* **337**, 1023.
Collier, M. R., Hamilton, D. C., Gloeckler, G., Bochsler, P., and Sheldon, R. B.: 1996, *Geophys. Res. Letters* **23**, 1191.
Cordier, S., and Girard, L.: 1996, *Planet. Space Sci.* **44**, 225.
Corti, G., Poletto, G., Romoli, M., Michels, J., Kohl, J., and Noci, G.: 1997, in *The Corona and Solar Wind Near Minimum Activity,* Fifth SOHO Workshop, ESA SP-404, Noordwijk, 289.
Cowley, C. R.: 1990, *Ap. J.* **348**, 328.
Cranmer, S. R.: 1998, *Ap. J.* **508**, 925.
Cranmer, S. R.: 2000, *Ap. J.* **532**, 1197.

Cranmer, S. R.: 2001, *J. Geophys. Res.,* **106**, 24937.
Cranmer, S. R., Field, G. B., and Kohl, J. L.: 1999a, *Ap. J.* **518**, 937.
Cranmer, S. R., Field, G. B., Noci, G., and Kohl, J. L.: 1997, in *Correlated Phenomena at the Sun, in the Heliosphere, and in Geospace,* 31st ESLAB Symposium, ESA SP-415, Noordwijk, 89.
Cranmer, S. R., Kohl, J. L., Noci, G., *et al.:* 1999b, *Ap. J.* **511,** 481.
Crew, G. B., Chang, T., Retterer, J. M., Peterson, W. K., Gurnett, D. A., and Huff, R. L.: 1990, *J. Geophys. Res.* **95**, 3959.
Cuntz, M., and Suess, S. T.: 2001, *Ap. J. Letters* **549**, L143.
Cuperman, S., Bruma, C., Dryer, M., and Semel, M.: 1995, *Astron. Astrophys.* **299**, 389.
Cuperman, S., Harten, A., and Dryer, M.: 1972, *Ap. J.* **177,** 555.
Cuperman, S., Yatom, H., Dryer, M., and Lewis, D.: 1987, *Ap. J.* **314**, 404.
Curdt, W., and Heinzel, P.: 1998, *Ap. J. Letters* **503**, L95.
Cuseri, I., Mullan, D., Noci, G., and Poletto, G.: 1999, *Ap. J.* **514**, 989.
Czechowski, A., Ratkiewicz, R., McKenzie, J. F., and Axford, W. I.: 1998, *Astron. Astrophys.* **335**, 303.
David, C., Gabriel, A. H., Bely-Dubau, F., Fludra, A., Lemaire, P., and Wilhelm, K.: 1998, *Astron. Astrophys.* **336**, L90.
Davila, J. M.: 1985, *Ap. J.* **291**, 328.
DeForest, C. E., and Gurman, J. B.: 1998, *Ap. J. Letters* **501**, L217.
DeForest, C. E., Hoeksema, J. T., Gurman, J. B., *et al.:* 1997, *Solar Phys.* **175**, 393.
DeForest, C. E., Plunkett, S. P., and Andrews, M. D.: 2001a, *Ap. J.* **546**, 569.
DeForest, C. E., Lamy, P. L., and Llebaria, A.: 2001b, *Ap. J.* **560**, 490.
Del Zanna, L., Velli, M., and Londrillo, P.: 2001, *Astron. Astrophys.* **367**, 705.
Del Zanna, L., von Steiger, R., and Velli, M.: 1998, *Space Sci. Rev.* **85**, 349.
Demars, H. G., and Schunk, R. W.: 1990, *Planet. Space Sci.* **38**, 1091.
Demars, H. G., and Schunk, R. W.: 1991, *Planet. Space Sci.* **39**, 435.
Demars, H. G., and Schunk, R. W.: 1992, *J. Geophys. Res.* **97**, 1581.
Dessler, A. J.: 1967, *Rev. Geophys.* **5**, 1.
Dewar, R. L.: 1970, *Phys. Fluids* **13**, 2710.
Dobrowolny, M., and Moreno, G.: 1977, *Space Sci. Rev.* **20**, 577.
Dobrzycka, D., Raymond, J. C., and Cranmer, S. R.: 2000, *Ap. J.* **538**, 922.
Dobrzycka, D., Cranmer, S. R., Raymond, J. C., Biesecker, D. A., and Gurman, J. B.: 2002, *Ap. J.* **565**, 621.
Domingo, V., Fleck. B., and Poland, A. I.: 1995, *Solar Phys.* **162**, 1.
Dorelli, J. C., and Scudder, J. D.: 1999, *Geophys. Res. Letters* **26**, 3537.
Doschek, G. A., Feldman, U., Laming, J. M., Schühle, U., and Wilhelm, K.: 2001, *Ap. J.* **546**, 559.
Dowdy, J. F., Jr., Rabin, D., and Moore, R. L.: 1986, *Solar Phys.* **105**, 35.
Doyle, J. G., Banerjee, D., and Perez, M. E.: 1998, *Solar Phys.* **181**, 91.
Dreicer, H.: 1959, *Phys. Rev.* **115**, 238.
Drury, L. O'C., and Völk, H. J.: 1981, *Ap. J.* **248**, 344.
Dulk, G. A.: 1985, *Ann. Rev. Astron. Astrophys.* **23**, 169.
Dum, C. T.: 1983, in M. Neugebauer (ed.), *Solar Wind Five,* NASA CP-2280, 369.
Dupree, A. K., Penn, M. J., and Jones, J. P.: 1996, *Ap. J. Letters* **467**, L121.
Dusenbery, P. B., and Hollweg, J. V.: 1981, *J. Geophys. Res.* **86**, 153.
Efimov, A. I., Chashei, I. V., Shishov, V. I., and Bird, M. K.: 1993, *Astron. Letters* **19**, 57.
Einaudi, G., Chibbaro, S., Dahlburg, R. B., and Velli, M.: 2001, *Ap. J.* **547**, 1167.
Erdelyi, R., Doyle, J. G., Perez, M. E., and & Wilhelm, K.: 1998, *Astron. Astrophys.* **337**, 287.
Esser, R.: 1990, *J. Geophys. Res.* **95**, 10261.
Esser, R., and Edgar, R. J.: 2000, *Ap. J. Letters* **532**, L71.
Esser, R., and Edgar, R. J.: 2001, *Ap. J.* **563**, 1055.

Esser, R., Fineschi, S., Dobrzycka, D., Habbal, S. R., Edgar, R. J., Raymond, J. C., Kohl, J. L., and Guhathakurta, M.: 1999, *Ap. J. Letters* **510**, L63.
Esser, R., and Habbal, S. R.: 1997, in J. R. Jokipii, C. P. Sonett, and M. S. Giampapa (eds.), *Cosmic Winds and the Heliosphere,* Univ. of Arizona Press, Tucson, 297.
Esser, R., Habbal, S. R., Coles, W. A., and Hollweg, J. V.: 1997, *J. Geophys. Res.* **102**, 7063.
Esser, R., and Leer, E.: 1990, *J. Geophys. Res.* **95**, 10269.
Esser, R., and Sasselov, D.: 1999, *Ap. J. Letters* **521**, L145.
Fahr, H. J.: 1974, *Space Sci. Rev.* **15**, 483.
Fahr, H. J., Bird, M. K., and Ripken, H. W.: 1977, *Astron. Astrophys.* **58**, 339.
Fahr, H. J., and Shizgal, B.: 1983, *Rev. Geophys. Space Phys.* **21**, 75.
Feldman, U., and Laming, J. M.: 2000, *Physica Scripta* **61**, 222.
Feldman, W. C., Asbridge, J. R., Bame, S. J., and Montgomery, M. D.: 1974, *Rev. Geophys. Space Phys.* **12**, 715.
Feldman, W. C., Asbridge, J. R., Bame, S. J., and Gosling, J. T.: 1976, *J. Geophys. Res.* **81**, 5054.
Feldman, W. C., Gosling, J. T., McComas, D. J., and Phillips, J. L.: 1993, *J. Geophys. Res.* **98**, 5593.
Feldman, W. C., Habbal, S. R., Hoogeveen, G., and Wang, Y.-M.: 1997, *J. Geophys. Res.* **102**, 26905.
Feldman, W. C., and Marsch, E.: 1997, in J. R. Jokipii, C. P. Sonett, and M. S. Giampapa (eds.), *Cosmic Winds and the Heliosphere,* Univ. of Arizona Press, Tucson, 617.
Fineschi, S., Gardner, L. D., Kohl, J. L., Romoli, M., and Noci, G.: 1998, *Proc. S.P.I.E.* **3443**, 67.
Fisher, R. R., and Guhathakurta, M.: 1995, *Ap. J. Letters* **447**, L139.
Fisk, L. A., Schwadron, N. A., and Zurbuchen, T. H.: 1999, *J. Geophys. Res.* **104**, 19765.
Flå, T., Habbal, S. R., Holzer, T. E., and Leer, E.: 1984, *Ap. J.* **280**, 382.
Fleck, B., and Svestka, Z.: (eds.) 1997, *The First Results from SOHO,* Kluwer, Dordrecht.
Florinski, V., and Jokipii, J. R.: 1997, *Geophys. Res. Letters* **24**, 2383.
Gail, H.-P., Ulmschneider, P., and Cuntz, M.: 1990, *Astron. Astrophys.* **234**, 359.
Galeev, A. A., and Sudan, R. N.: (eds.) 1983, *Basic Plasma Physics I,* North Holland, Amsterdam.
Galinsky, V. L., and Shevchenko, V. I.: 2000, *Phys. Rev. Letters* **85**, 90.
Gary, S. P.: 1993, *Theory of Space Plasma Microinstabilities,* Cambridge Univ. Press, Cambridge, UK.
Gary, S. P., Neagu, E., Skoug, R. M., and Goldstein, B. E.: 1999, *J. Geophys. Res.* **104**, 19843.
Gary, S. P., Yin, L., Winske, D., and Ofman, L.: 2001, *J. Geophys. Res.* **106**, 10715.
Geiss, J.: 1982, *Space Sci. Rev.* **33**, 201.
Geiss, J., Hirt, P., and Leutwyler, H.: 1970, *Solar Phys.* **12**, 458.
Giordano, S., Antonucci, E., Benna, C., Romoli, M., Noci, G., Kohl, J. L., Fineschi, S., Michels, J., and Naletto, G.: 1997, in *The Corona and Solar Wind Near Minimum Activity,* Fifth SOHO Workshop, ESA SP-404, Noordwijk, 413.
Giordano, S., Antonucci, E., Noci, G., Romoli, M., and Kohl, J. L.: 2000, *Ap. J. Letters* **531**, L79.
Gleeson, L. J., and Axford, W. I.: 1967, *Ap. J. Letters* **149**, L115.
Gold, T.: 1964, in W. N. Hess (ed.), *AAS-NASA Symposium on the Physics of Solar Flares,* NASA SP-50, Washington, 389.
Goldreich, P., and Sridhar, S.: 1997, *Ap. J.* **485**, 680.
Goldstein, B. E., Neugebauer, M., Phillips, J. L., *et al.:* 1996, *Astron. Astrophys.* **316**, 296.
Goldstein, M. L.: 2001, *Astrophys. Space Sci.* **277**, 349.
Goldstein, M. L., Roberts, D. A., and Matthaeus, W. H.: 1995, *Ann. Rev. Astron. Astrophys.* **33**, 283.
Golub, L., and Pasachoff, J. M.: 1997, *The Solar Corona,* Cambridge Univ. Press, Cambridge, UK.
Gomberoff, L., and Elgueta, R.: 1991, *J. Geophys. Res.* **96**, 9801.
Gombosi, T. I., and Rasmussen, C. E.: 1991, *J. Geophys. Res.* **96**, 7759.
Gombosi, T. I., and Schunk, R. W.: 1988, *Planet. Space Sci.* **36**, 753.
Gómez, D. O.: 1990, *Fundamentals of Cosmic Phys.* **14**, 131.
Gosling, J. T.: 1996, *Ann. Rev. Astron. Astrophys.* **34**, 35.

Grall, R. R., Coles, W. A., Klingelsmith, M. T., Breen, A., Williams, P. J., Markkanen, J., and Esser, R.: 1996, *Nature* **379**, 429.
Grappin, R., Léorat, J., and Buttighoffer, A.: 2000, *Astron. Astrophys.* **362**, 342.
Griffel, D. H., and Davis, L.: 1969, *Planet. Space Sci.* **17**, 1009.
Gringauz, K. I., Bezrukikh, V. V., Ozerov, V. D., and Ribchinsky, R. E.: 1961, *Space Res.* **2**, 539.
Grossmann, W., and Smith, R. A.: 1988, *Ap. J.* **332**, 476.
Groth, C. P. T., De Zeeuw, D. L., Gombosi, T. I., and Powell, K. G.: 1999, *Space Sci. Rev.* **87**, 193.
Guhathakurta, M., and Holzer, T. E.: 1994, *Ap. J.* **426**, 782.
Guo, W. P., and Wu, S. T.: 1998, *Ap. J.* **494**, 419.
Habbal, S. R., Esser, R., Hollweg, J. V., and Isenberg, P. A.: (eds.) 1999, *Solar Wind Nine,* AIP Press, Woodbury, New York.
Habbal, S. R., Holzer, T. E., and Leer, E.: 1979, *Solar Phys.* **64**, 287.
Habbal, S. R., and Leer, E.: 1982, *Ap. J.* **253**, 318.
Hackenberg, P., Marsch, E., and Mann, G.: 2000, *Astron. Astrophys.* **360** 1139.
Hammer, R.: 1982, *Ap. J.* **259**, 767.
Hammond, C. M., Feldman, W. C., Phillips, J. L., Goldstein, B. E., and Balogh, A.: 1995, *J. Geophys. Res.* **100**, 7881.
Hansteen, V. H., and Leer, E.: 1995, *J. Geophys. Res.* **100**, 21577.
Hansteen, V. H., Leer, E., and Holzer, T. E.: 1997, *Ap. J.* **482**, 498.
Harmon, J. K.: 1989, *J. Geophys. Res.* **94**, 15399.
Hartle, R. E., and Barnes, A.: 1970, *J. Geophys. Res.* **75**, 6915.
Hartle, R. E., and Sturrock, P. A.: 1968, *Ap. J.* **151**, 1155.
Harvey, R. W.: 1975, *Phys. Fluids* **18**, 1790.
Hassler, D. M., Dammasch, I. E., Lemaire, P., Brekke, P., Curdt, W., Mason, H. E., Vial, J.-C., and Wilhelm, K.: 1999, *Science* **283**, 810.
Hefti, S., Grünwaldt, H., Ipavich, F. M., *et al.:* 1998, *J. Geophys. Res.* **103**, 29697.
Heinemann, M.: 1999, in S. Habbal, R. Esser, J. Hollweg, and P. Isenberg (eds.), *Solar Wind Nine,* AIP Conf. Proc. 471, AIP Press, Woodbury, New York, 453.
Hénoux, J.-C.: 1998, *Space Sci. Rev.* **85**, 215.
Hernandez, R., and Marsch, E.: 1985, *J. Geophys. Res.* **90**, 11062.
Heyvaerts, J., and Priest, E. R.: 1983, *Astron. Astrophys.* **117** 220.
Heyvaerts, J., and Priest, E. R.: 1992, *Ap. J.* **390**, 297.
Hinton, F. L.: 1983, in A. A. Galeev and R. N. Sudan (eds.), *Basic Plasma Physics I,* North Holland, Amsterdam, 147.
Hollweg, J. V.: 1971a, *J. Geophys. Res.* **76**, 5155.
Hollweg, J. V.: 1971b, *J. Geophys. Res.* **76**, 7491.
Hollweg, J. V.: 1971c, *Phys. Rev. Letters* **27**, 1349.
Hollweg, J. V.: 1973, *Ap. J.* **181**, 547.
Hollweg, J. V.: 1975, *Rev. Geophys. Space Phys.* **13**, 263.
Hollweg, J. V.: 1978, *Rev. Geophys. Space Phys.* **16**, 689.
Hollweg, J. V.: 1986a, *Ap. J.* **306**, 730.
Hollweg, J. V.: 1986b, *J. Geophys. Res.* **91**, 4111.
Hollweg, J. V.: 1994, *J. Geophys. Res.* **99**, 23431.
Hollweg, J. V.: 1987, *Ap. J.* **312**, 880.
Hollweg, J. V.: 1997, *Ap. J.* **488**, 895.
Hollweg, J. V.: 1999a, *J. Geophys. Res.* **104**, 505.
Hollweg, J. V.: 1999b, *J. Geophys. Res.* **104**, 24781.
Hollweg, J. V.: 1999c, *J. Geophys. Res.* **104**, 24793.
Hollweg, J. V.: 2000a, *J. Geophys. Res.* **105**, 7573.
Hollweg, J. V.: 2000b, *J. Geophys. Res.* **105**, 15699.

Hollweg, J. V., Bird, M. K., Volland, H., Edenhofer, P., Stelzried, C. T., and Seidel, B. L.: 1982, *J. Geophys. Res.* **87**, 1.
Hollweg, J. V., and Isenberg, P. A.: 2001, *J. Geophys. Res.,* submitted.
Hollweg, J. V., and Johnson, W.: 1988, *J. Geophys. Res.* **93**, 9547.
Hollweg, J. V., and Markovskii, S. A.: 2002, *J. Geophys. Res.* **107**, in press.
Hollweg, J. V., and Turner, J. M.: 1978, *J. Geophys. Res.* **83**, 97.
Holzer, T. E., and Axford, W. I.: 1970, *Ann. Rev. Astron. Astrophys.* **8**, 31.
Holzer, T. E., Fedder, J. A., and Banks, P. M.: 1971, *J. Geophys. Res.* **76**, 2453.
Holzer, T. E., and Leer, E.: 1980, *J. Geophys. Res.* **85**, 4665.
Holzer, T. E., and Leer, E.: 1997, in *The Corona and Solar Wind Near Minimum Activity,* Fifth SOHO Workshop, ESA SP-404, Noordwijk, 379.
Hood, A. W., Ireland, J., and Priest, E. R.: 1997, *Astron. Astrophys.* **318** 957.
Horbury, T. S.: 1999, in M. Ostrowski and R. Schlickeiser (eds.), *Plasma Turbulence and Energetic Particles in Astrophysics,* Obserwatorium Astronomiczne, Krakow, 115.
Hu, Y.-Q., Esser, R., and Habbal, S. R.: 1997, *J. Geophys. Res.* **102**, 14661.
Hu, Y.-Q., and Habbal, S. R.: 1999, *J. Geophys. Res.* **104**, 17045.
Hu, Y.-Q., Habbal, S. R., and Li, X.: 1999, *J. Geophys. Res.* **104**, 24819.
Huber, M. C. E.: 1981, *Space Sci. Rev.* **29**, 295.
Hufbauer, K.: 1991, *Exploring the Sun: Solar Science since Galileo,* Johns Hopkins Univ. Press, Baltimore.
Hughes, C. J.: 1965, *Ap. J.* **142**, 321.
Hundhausen, A. J.: 1972, *Coronal Expansion and Solar Wind,* Springer-Verlag, Berlin.
Hundhausen, A. J., Gilbert, H. E., and Bame, S. J.: 1968, *Ap. J. Letters* **152**, L3.
Hung, R. J., and Barnes, A.: 1973, *Ap. J.* **180**, 253.
Hyder, C. L., and Lites, B. W.: 1970, *Solar Phys.* **14**, 147.
Ionson, J. A.: 1978, *Ap. J.* **226**, 650.
Ip, W.-H., and Axford, W. I.: 1982, in L. L. Wilkening (ed.), *Comets,* Univ. of Arizona Press, Tucson, 588.
Isenberg, P. A.: 1984, *J. Geophys. Res.* **89**, 6613.
Isenberg, P. A.: 1990, *J. Geophys. Res.* **95**, 6437.
Isenberg, P. A.: 1991, in J. A. Jacobs (ed.), *Geomagnetism,* vol. 4, Academic Press, New York, 1.
Isenberg, P. A.: 2001a, *J. Geophys. Res.* **106**, 29249.
Isenberg, P. A.: 2001b, *Space Sci. Rev.* **95**, 119.
Isenberg, P. A., and Hollweg, J. V.: 1982, *J. Geophys. Res.* **87**, 5023.
Isenberg, P. A., and Hollweg, J. V.: 1983, *J. Geophys. Res.* **88**, 3923.
Isenberg, P. A., Lee, M. A., and Hollweg, J. V.: 2000, *Solar Phys.* **193**, 247.
Isenberg, P. A., Lee, M. A., and Hollweg, J. V.: 2001, *J. Geophys. Res.* **106**, 5649.
Jacques, S. A.: 1977, *Ap. J.* **215**, 942.
Jensen, E.: 1963, *Astrophys. Norvegica* **8**, 99.
Jockers, K.: 1970, *Astron. Astrophys.* **6** 219.
Jokipii, J. R.: 1966, *Ap. J.* **146**, 480.
Jokipii, J. R., and Davis, L., Jr.: 1969, *Ap. J.* **156**, 1101.
Jokipii, J. R., Sonett, C. P., and Giampapa, M. S.: (eds.) 1997, *Cosmic Winds and the Heliosphere,* Univ. of Arizona Press, Tucson.
Jordan, C.: 2000, *Plasma Phys. Control. Fus.* **42**, 415.
Kellogg, P. J.: 2000, *Ap. J.* **528**, 480.
Kellogg, P. J., Gurnett, D. A., Hospodarsky, G. B., and Kurth, W. S.: 2001, *Geophys. Res. Letters* **28**, 87.
Kennel, C. F., and Engelmann, F.: 1966, *Phys. Fluids* **9**, 2377.
Kennel, C. F., and Scarf, F. L.: 1968, *J. Geophys. Res.* **73**, 6149.

Keppens, R., and Goedbloed, J. P.: 1999, *Space Sci. Rev.* **87**, 223.
Khabibrakhmanov, I. K., and Mullan, D. J.: 1994, *Ap. J.* **430**, 814.
Khabibrakhmanov, I. K., and Mullan, D. J.: 1999, in S. Habbal, R. Esser, J. Hollweg, and P. Isenberg (eds.), *Solar Wind Nine,* AIP Conf. Proc. 471, AIP Press, Woodbury, New York, 349.
Khazanov, G. V., Khabibrakhmanov, I. K., and Krivorutsky, E. N.: 2000, *Phys. Plasmas* **7**, 1.
Kinzelin, E., and Hubert, D.: 1992, *J. Geophys. Res.* **97**, 4061.
Klimchuk, J. A., and Cargill, P. J.: 2001, *Ap. J.* **553**, 440.
Ko, Y.-K., Fisk, L. A., Gloeckler, G., and Geiss, J.: 1996, *Geophys. Res. Letters* **23**, 2785.
Ko, Y.-K., Fisk, L. A., Geiss, J., Gloeckler, G., and Guhathakurta, M.: 1997, *Solar Phys.* **171**, 345.
Ko, Y.-K., Geiss, J., and Gloeckler, G.: 1998, *J. Geophys. Res.* **103**, 14539.
Kohl, J. L., Esser, R., Cranmer, S. R., *et al.:* 1999, *Ap. J. Letters* **510**, L59.
Kohl, J. L., Esser, R., Gardner, L. D., *et al.:* 1995, *Solar Phys.* **162**, 313.
Kohl, J. L., Gardner, L. D., Strachan, L., and Hassler, D. M.: 1994, *Space Sci. Rev.* **70**, 253.
Kohl, J. L., Noci, G., Antonucci, E., *et al.:* 1997, *Solar Phys.* **175**, 613.
Kohl, J. L., Noci, G., Antonucci, E., *et al.:* 1998, *Ap. J. Letters* **501**, L127.
Kohl, J. L., Reeves, E. M., and Kirkham, B.: 1978, in K. van der Hucht and G. Vaiana (eds.), *New Instrumentation for Space Astronomy,* Pergamon, New York, 91.
Kohl, J. L., Strachan, L., and Gardner, L. D.: 1996, *Ap. J. Letters* **465**, L141.
Kohl, J. L., and Withbroe, G. L.: 1982, *Ap. J.* **256**, 263.
Kojima, M., and Kakinuma, T.: 1990, *Space Sci. Rev.* **53**, 173.
Kopp, R. A., and Holzer, T. E.: 1976, *Solar Phys.* **49**, 43.
Koutchmy, S.: 1988, *Space Sci. Rev.* **47**, 95.
Koutchmy, S., and Bocchialini, K.: 1998, in *Solar Jets and Coronal Plumes,* ESA SP-421, Noordwijk, 51.
Krall, N. A., and Trivelpiece, A. W.: 1973, *Principles of Plasma Physics,* McGraw Hill, New York.
Krieger, A. S., Timothy, A. F., and Roelof, E. C.: 1973, *Solar Phys.* **29**, 505.
Krucker, S., and Benz, A. O.: 1998, *Ap. J. Letters* **501**, L213.
Krucker, S., and Benz, A. O.: 2000, *Solar Phys.* **191**, 341.
Kudoh, T., and Shibata, K.: 1997, in *The Corona and Solar Wind Near Minimum Activity,* Fifth SOHO Workshop, ESA SP-404, Noordwijk, 477.
Kuperus, M., Ionson, J. A., and Spicer, D. S.: 1981, *Ann. Rev. Astron. Astrophys.* **19**, 7.
Kuramitsu, Y., and Hada, T.: 2000, *Geophys. Res. Letters* **27**, 629.
Lacombe, C.: 1976, *Astron. Astrophys.* **48**, 11.
Lamy, P., Llebaria, A., Koutchmy, S., Reynet, P., Molodensky, M., Howard, R., Schwenn, R., and Simnett, G.: 1997, in *The Corona and Solar Wind Near Minimum Activity,* Fifth SOHO Workshop, ESA SP-404, Noordwijk, 487.
Lau, Y.-T., and Siregar, E.: 1996, *Ap. J.* **465**, 451.
Leamon, R. J., Matthaeus, W. H., Smith, C. W., Zank, G. P., Mullan, D. J., and Oughton, S.: 2000, *Ap. J.* **537**, 1054.
Leamon, R. J., Smith, C. W., Ness, N. F., Matthaeus, W. H., and Wong, H. K.: 1998, *J. Geophys. Res.* **103**, 4775.
Leamon, R. J., Smith, C. W., Ness, N. F., and Wong, H. K.: 1999, *J. Geophys. Res.* **104**, 22331.
Leblanc, F., and Hubert, D.: 1997, *Ap. J.* **483**, 464.
Leblanc, F., Hubert, D., and Blelly, P.-L.: 2000, *Ap. J.* **530**, 478.
Lee, L. C., Lin, Y., and Choe, G. S.: 1996, *Solar Phys.* **163**, 335.
Lee, L. C., and Wu, B. H.: 2000, *Ap. J.,* **535**, 1014.
Lee, L. C., Wu, C. S., and Hu, X. W.: 1986, *Geophys. Res. Letters* **13**, 209.
Lee, M. A., and Völk, H. J.: 1973, *Astrophys. Space Sci.* **24**, 31.
Leer, E., and Axford, W. I.: 1972, *Solar Phys.* **23**, 238.

Leer, E., Hansteen, V. H., and Holzer, T. E.: 1998, in L. Kaper and A. W. Fullerton (eds.), *Cyclical Variability in Stellar Winds,* Springer-Verlag, Berlin, 263.
Leer, E., and Holzer, T. E.: 1980, *J. Geophys. Res.* **85**, 4631.
Leer, E., Holzer, T. E., and Flå, T.: 1982, *Space Sci. Rev.* **33**, 161.
Leer, E., and Marsch, E.: 1999, *Space Sci. Rev.* **87**, 67.
Lemaire, J.: 1972, *Space Res.* **12**, 1414.
Lemaire, J., and Pierrard, V.: 2001, *Astrophys. Space Sci.* **277**, 169.
Lemaire, J., and Scherer, M.: 1971, *J. Geophys. Res.* **76**, 7479.
Lemaire, J., and Scherer, M.: 1973, *Rev. Geophys. Space Phys.* **11**, 427.
Lemons, D. S., and Feldman, W. C.: 1983, *J. Geophys. Res.* **88**, 6881.
Leubner, M. P.: 2000, *Planet. Space Sci.* **48**, 133.
Levine, R. H.: 1974, *Ap. J.* **190**, 457.
Li, J., Jewitt, D., and LaBonte, B.: 2000, *Ap. J. Letters* **539**, L67.
Li, X.: 1999, *J. Geophys. Res.* **104**, 19773.
Li, X., Esser, R., Habbal, S. R., and Hu, Y.-Q.: 1997, *J. Geophys. Res.* **102**, 17419.
Li, X., and Habbal, S. R.: 2001, *J. Geophys. Res.* **106**, 10669.
Li, X., Habbal, S. R., Hollweg, J. V., and Esser, R.: 1999, *J. Geophys. Res.* **104**, 2521.
Li, X., Habbal, S. R., Kohl, J. L., and Noci, G.: 1998, *Ap. J. Letters* **501**, L133.
Lie-Svendsen, Ø., Hansteen, V. H., and Leer, E.: 1997, *J. Geophys. Res.* **102**, 4701.
Lie-Svendsen, Ø., and Leer, E.: 2000, *J. Geophys. Res.* **105**, 35.
Lie-Svendsen, Ø., and Rees, M. H.: 1996, *J. Geophys. Res.* **101**, 2415.
Liewer, P. C., Velli, M., and Goldstein, B. E.: 1999, in S. Habbal, R. Esser, J. Hollweg, and P. Isenberg (eds.), *Solar Wind Nine,* AIP Conf. Proc. 471, AIP Press, Woodbury, New York, 449.
Liewer, P. C., Velli, M., and Goldstein, B. E.: 2001, *J. Geophys. Res.* **106**, 29261.
Lifschitz, A., and Goedbloed, J. P.: 1997, *J. Plasma Phys.* **58**, 61.
Lin, R. P., Larson, D. E., Ergun, R. E., *et al.:* 1997, *Adv. Space Res.* **20** (4–5), 645.
Linker, J. A., Mikić, Z., Biesecker, D. A., *et al.:* 1999, *J. Geophys. Res.* **104**, 9809.
Livi, S., and Marsch, E.: 1987, *J. Geophys. Res.* **92**, 7255.
Longcope, D. W., and Sudan, R. N.: 1992, *Phys. Fluids B* **4**, 2277.
Low, B. C.: 1990, *Ann. Rev. Astron. Astrophys.* **28**, 491.
Ma, C.-Y., and Summers, D.: 1999, *Geophys. Res. Letters* **26**, 1121.
Macquart, J.-P., and Melrose, D. B.: 2000, *Phys. Rev. E* **62**, 4177.
Maksimovic, M., Pierrard, V., and Lemaire, J. F.: 1997, *Astron. Astrophys.* **324**, 725.
Malara, F., Primavera, L., and Veltri, P.: 1996, *Ap. J.* **459**, 347.
Mancuso, S., and Spangler, S. R.: 1999, *Ap. J.* **525**, 195.
Mancuso, S., and Spangler, S. R.: 2000, *Ap. J.* **539**, 480.
Markovskii, S. A.: 2001, *Ap. J.* **557**, 337.
Marsch, E.: 1991, in R. Schwenn and E. Marsch (eds.), *Physics of the Inner Heliosphere,* vol. 2, Springer-Verlag, Heidelberg, 45.
Marsch, E.: 1998, *Nonlin. Proc. Geophys.* **5**, 111.
Marsch, E.: 1999, *Space Sci. Rev.* **87**, 1.
Marsch, E., Goertz, C. K., and Richter, K.: 1982a, *J. Geophys. Res.* **87**, 5030.
Marsch, E., Mühlhäuser, K.-H., Rosenbauer, H., Schwenn, R., and Neubauer, F. M.: 1982b, *J. Geophys. Res.* **87**, 35.
Marsch, E., Mühlhäuser, K.-H., Schwenn, R., Rosenbauer, H., Pilipp, W., and Neubauer, F. M.: 1982c, *J. Geophys. Res.* **87**, 52.
Marsch, E., and Tu, C.-Y.: 2001a, *J. Geophys. Res.* **106**, 227.
Marsch, E., and Tu, C.-Y.: 2001b, *J. Geophys. Res.* **106**, 8357.
Marsden, R. G.: 2001, *Astrophys. Space Sci.* **277**, 337.
Matthaeus, W. H., Ghosh, S., Oughton, S., and Roberts, D. A.: 1996, *J. Geophys. Res.* **101**, 7619.

Matthaeus, W. H., Goldstein, M. L., and Roberts, D. A.: 1990, *J. Geophys. Res.* **95**, 20673.
Matthaeus, W. H., Oughton, S., Pontius, D. H., and Zhou, Y.: 1994, *J. Geophys. Res.* **99**, 19267.
Matthaeus, W. H., Zank, G. P., Oughton, S., Mullan, D. J., and Dmitruk, P.: 1999, *Ap. J. Letters* **523**, L93.
McKenzie, J. F.: 1994, *J. Geophys. Res.* **99**, 4193.
McKenzie, J. F.: 2000, *Solar Phys.* **196**, 329.
McKenzie, J. F., and Axford, W. I.: 2000, *Ap. J.* **537**, 516.
McKenzie, J. F., Axford, W. I., and Banaszkiewicz, M.: 1997, *Geophys. Res. Letters* **24**, 2877.
McKenzie, J. F., Banaszkiewicz, M., and Axford, W. I.: 1995, *Astron. Astrophys.* **303**, L45.
McKenzie, J. F., and Marsch, E.: 1982, *Astrophys. Space Sci.* **81**, 295.
Medvedev, M. V.: 2000, *Ap. J.* **541**, 811.
Meister, C.-V.: 1992, in E. Marsch and R. Schwenn (eds.), *Solar Wind Seven,* Pergamon, New York, 517.
Meyer-Vernet, N.: 1999, *Eur. J. Phys.* **20**, 167.
Meyer-Vernet, N., and Issautier, K.: 1998, *J. Geophys. Res.* **103**, 29705.
Milano, L. J., Gómez, D. O., and Martens, P. C. H.: 1997, *Ap. J.* **490**, 442.
Minter, A. H., and Spangler, S. R.: 1997, *Ap. J.* **485**, 182.
Miralles, M. P., Panasyuk, A. V., Strachan, L., Gardner, L. D., Suleiman, R. M., Smith, P. L., and Kohl, J. L.: 2000, *Bull. American Astron. Soc.* **32**, 815.
Miralles, M. P., Cranmer, S. R., Panasyuk, A. V., Romoli, M., and Kohl, J. L.: 2001a, *Ap. J. Letters* **549**, L257.
Miralles, M. P., Cranmer, S. R., and Kohl, J. L.: 2001b, *Ap. J. Letters* **560**, L193.
Miralles, M. P., Cranmer, S. R., Esser, R., and Kohl, J. L.: 2001c, *Eos Trans. AGU* **82** (47), F1005.
Mitzuta, T., and Hoshino, M.: 2001, *Geophys. Res. Letters* **28**, 3099.
Möbius, E., Gloeckler, G., Goldstein, B., Habbal, S., McNutt, R., Randolph, J., Title, A., and Tsurutani, B.: 2000, *Adv. Space Res.* **25** (9), 1961.
Montgomery, D.: 1982, *Physica Scripta* **T2:1**, 83.
Montgomery, D.: 1992, *J. Geophys. Res.* **97**, 4309.
Montgomery, D. C., and Tidman, D. A.: 1964, *Plasma Kinetic Theory,* McGraw Hill, New York.
Moore, R. L., Hammer, R., Musielak, Z. E., Suess, S. T., and An, C.-H.: 1992, *Ap. J. Letters* **397**, L55.
Moore, R. L., Suess, S. T., Musielak, Z. E., and An, C.-H.: 1991, *Ap. J.* **378**, 347.
Moses, S., and Kennel, C.: 1991, *Adv. Space Res.* **11** (9), 3.
Mullan, D. J.: 1990, *Astron. Astrophys.* **232**, 520.
Mullan, D. J., and Ahmad, I. A.: 1982, *Solar Phys.* **75**, 347.
Mullan, D. J., and Cheng, Q. Q.: 1994, *Ap. J.* **420**, 392.
Mullan, D. J., and Yakovlev, O. I.: 1995, *Irish Astron. J.* **22**, 119.
Munro, R. H., and Jackson, B. V.: 1977, *Ap. J.* **213**, 874.
Nakayama, K.: 2001, *Ap. J.* **556**, 1027.
Narain, U., and Ulmschneider, P.: 1990, *Space Sci. Rev.* **54**, 377.
Narain, U., and Ulmschneider, P.: 1996, *Space Sci. Rev.* **75**, 453.
Narayan, R., and Medvedev, M. V.: 2001, *Ap. J. Letters* **562**, L129.
Ness, N. F., and Burlaga, L. F.: 2001, *J. Geophys. Res.* **106**, 15803.
Neugebauer, M.: 1975, *Space Sci. Rev.* **17**, 221.
Neugebauer, M.: 1982, *Space Sci. Rev.* **33**, 127.
Neugebauer, M.: 1997, *J. Geophys. Res.* **102**, 26887.
Neugebauer, M., Forsyth, R. J., Galvin, A. B., *et al.:* 1998, *J. Geophys. Res.* **103**, 14587.
Newkirk, G., Jr., and Harvey, J.: 1968, *Solar Phys.* **3**, 321.
Nicholson, D. N.: 1983, *Introduction to Plasma Theory,* Wiley, New York.

Nindos, A., Kundu, M. R., White, S. M., Shibasaki, K., and Gopalswamy, N.: 2000, *Ap. J. Suppl.* **130**, 485.
Noble, L. M., and Scarf, F. L.: 1963, *Ap. J.* **138**, 1169.
Noci, G., Kohl, J. L., Antonucci, E., *et al.:* 1997, *Adv. Space Res.* **20** (12), 2219.
Noci, G., Kohl, J. L., and Withbroe, G. L.: 1987, *Ap. J.* **315**, 706.
Noci, G., and Maccari. L.: 1999, *Astron. Astrophys.* **341**, 275.
Nolte, J. T., Krieger, A. S., Timothy, A. F., *et al.:* 1976, *Solar Phys.* **46**, 303.
Ofman, L., and Davila, J. M.: 1997, *Ap. J.* **476**, 357.
Ofman, L., and Davila, J. M.: 1998, *J. Geophys. Res.* **103**, 23677.
Ofman, L., and Davila, J. M.: 1999, in S. Habbal, R. Esser, J. Hollweg, and P. Isenberg (eds.), *Solar Wind Nine,* AIP Conf. Proc. 471, AIP Press, Woodbury, New York, 405.
Ofman, L., and Davila, J. M.: 2001, *Ap. J.* **553**, 935.
Ofman, L., Nakariakov, V. M., and DeForest, C. E.: 1999, *Ap. J.* **514**, 441.
Ofman, L., Nakariakov, V. M., and Sehgal, N.: 2000, *Ap. J.* **533**, 1071.
Ofman, L., Viñas, A., and Gary, S. P.: 2001, *Ap. J. Letters* **547**, L175.
Ogilvie, K. W., Bochsler, P., Geiss, J., and Coplan, M. A.: 1980, *J. Geophys. Res.* **85**, 6069.
Ogilvie, K. W., and Desch, M. D.: 1997, *Adv. Space Res.* **20** (4–5), 559.
Øien, A. H., and Alendal, G.: 1993, *Ap. J.* **412**, 827.
Olsen, E. L., and Leer, E.: 1996a, *Ap. J.* **462**, 982.
Olsen, E. L., and Leer, E.: 1996b, *J. Geophys. Res.* **101**, 15591.
Olsen, E. L., and Leer, E.: 1999, *J. Geophys. Res.* **104**, 9963.
Olsen, E. L., Leer, E., and Holzer, T. E.: 1994, *Ap. J.* **420**, 913.
Osterbrock, D. E.: 1961, *Ap. J.* **134**, 347.
Oughton, S., Matthaeus, W. H., Dmitruk, P., Milano, L. J., Zank, G. P., and Mullan, D. J.: 2001, *Ap. J.* **551**, 565.
Owocki, S. P.: 1982, Ph.D. Dissertation, University of Colorado and the National Center for Atmospheric Research, NCAR/CT-66.
Owocki, S. P., Holzer, T. E., and Hundhausen, A. J.: 1983, *Ap. J.* **275**, 354.
Pannekoek, A.: 1922, *Bull. Astron. Inst. Neth.* **1**, 107.
Pantellini, F., and Landi, S.: 2001, *Astrophys. Space Sci.* **277**, 149.
Parhi, S., and Suess, S. T.: 2000, *Phys. Plasmas* **7**, 2995.
Parhi, S., Suess, S. T., and Sulkanen, M.: 1999, *J. Geophys. Res.* **104**, 14781.
Parker, E. N.: 1958a, *Ap. J.* **128**, 664.
Parker, E. N.: 1958b, *Ap. J.* **128**, 677.
Parker, E. N.: 1958c, *Phys. Rev.* **109**, 1874.
Parker, E. N.: 1963, *Interplanetary Dynamical Processes,* Interscience Publishers, New York.
Parker, E. N.: 1964, *Ap. J.* **139**, 690.
Parker, E. N.: 1965, *Space Sci. Rev.* **4**, 666.
Parker, E. N.: 1981, *Ap. J.* **244**, 644.
Parker, E. N.: 1988, *Ap. J.* **330**, 474.
Parker, E. N.: 1991, *Ap. J.* **372**, 719.
Parker, E. N.: 1994, *Spontaneous Current Sheets in Magnetic Fields,* Oxford Univ. Press, Oxford.
Parker, E. N.: 1997a, *Solar Phys.* **176**, 219.
Parker, E. N.: 1997b, in J. R. Jokipii, C. P. Sonett, and M. S. Giampapa (eds.), *Cosmic Winds and the Heliosphere,* Univ. of Arizona Press, Tucson, 3.
Parker, E. N.: 1999, in S. Habbal, R. Esser, J. Hollweg, and P. Isenberg (eds.), *Solar Wind Nine,* AIP Conf. Proc. 471, AIP Press, Woodbury, New York, 3.
Parker, E. N.: 2001, *J. Geophys. Res.* **106**, 15797.
Patsourakos, S., and Vial, J.-C.: 2000, *Astron. Astrophys.* **359**, L1.

Pätzold, M., Bird, M. K., Volland, H., Levy, G. S., Seidel, B. L., and Stelzried, C. T.: 1987, *Solar Phys.* **109**, 91.
Perkins, F.: 1973, *Ap. J.* **179**, 637.
Peter, H.: 2000, *Astron. Astrophys.* **360**, 761.
Peter, H.: 2001, *Astron. Astrophys.* **374**, 1108.
Peter, H., and Judge, P. G.: 1999, *Ap. J.* **522**, 1148.
Peter, H., and Marsch, E.: 1997, in *The Corona and Solar Wind Near Minimum Activity,* Fifth SOHO Workshop, ESA SP-404, Noordwijk, 591.
Phillips, J. L., Feldman, W. C., Gosling, J. T., and Scime, E. E.: 1995, *Adv. Space Res.* **16** (9), 95.
Phillips, J. L., and Gosling, J. T.: 1990, *J. Geophys. Res.* **95**, 4217.
Pierrard, V., Maksimovic, M., and Lemaire, J.: 1999, *J. Geophys. Res.* **104**, 17021.
Pijpers, F. P.: 1995, *Astron. Astrophys.* **295**, 435.
Pikel'ner, S. P.: 1950, *Izv. Krymsk. Astrofiz. Obs. (Bull. Crimean Astrophys. Obs.)* **5**, 34.
Pinsker, R. I.: 2001, *Phys. Plasmas* **8**, 1219.
Pneuman, G. W.: 1980, *Astron. Astrophys.* **81**, 161.
Pneuman, G. W.: 1983, *Ap. J.* **265**, 468.
Pneuman, G. W.: 1986, *Space Sci. Rev.* **43**, 105.
Pneuman, G. W., and Kopp, R. A.: 1971, *Solar Phys.* **18**, 258.
Poedts, S., Goossens, M., and Kerner, W.: 1990, *Ap. J.* **360**, 279.
Poedts, S., Rogava, A. D., and Mahajan, S. M.: 1998, *Ap. J.* **505**, 369.
Poletto, G., Suess, S. T., Biesecker, D. A., Esser, R., Gloeckler, G., *et al.:* 2002, *J. Geophys. Res.* **107**, in press.
Priest, E. R.: 1994, in J. L. Burch and J. H. Waite, Jr. (eds.), *Solar System Plasmas in Space and Time,* AGU, Washington, DC, 1.
Priest, E. R.: 1996, *Astrophys. Space Sci.* **237**, 49.
Priest, E. R., Foley, C. R., Heyvaerts, J., Arber, T. D., Mackay, D., Culhane, J. L., and Acton, L. W.: 2000, *Ap. J.* **539**, 1002.
Raymond, J. C.: 1999, *Space Sci. Rev.* **87**, 55.
Raymond, J. C., Fineschi, S., Smith, P. L., *et al.:* 1998, *Ap. J.* **508**, 410.
Reginald. N. L., and Davila, J. M.: 2000, *Solar Phys.* **195**, 111.
Reisenfeld, D. B., Gary, S. P., Gosling, J. T., Steinberg, J. T., McComas, D. J., Goldstein, B. E., and Neugebauer, M.: 2001, *J. Geophys. Res.* **106**, 5693.
Reisenfeld, D. B., McComas, D. J., and Steinberg, J. T.: 1999, *Geophys. Res. Letters* **26**, 1805.
Richardson, J. D., Paularena, K. I., and Wang, C.: 1999, in S. Habbal, R. Esser, J. Hollweg, and P. Isenberg (eds.), *Solar Wind Nine,* AIP Conf. Proc. 471, AIP Press, Woodbury, New York, 183.
Rickett, B. J.: 1990, *Ann. Rev. Astron. Astrophys.* **28**, 561.
Roberts, D. A.: 1989, *J. Geophys. Res.* **94**, 6899.
Roberts, D. A., and Goldstein, M. L.: 1998, *Geophys. Res. Letters* **25**, 595.
Roberts, D. A., Goldstein, M. L., and Klein, L. W.: 1990, *J. Geophys. Res.* **95**, 4203.
Roberts, D. A., Goldstein, M. L., and Matthaeus, W. H.: 1992, *J. Geophys. Res.* **97**, 17115.
Roberts, D. A., and Miller, J. A.: 1998, *Geophys. Res. Letters* **25**, 607.
Romoli, M., Benna, C., Cranmer, S. R., *et al.:* 1997, in *The Corona and Solar Wind Near Minimum Activity,* Fifth SOHO Workshop, ESA SP-404, Noordwijk, 633.
Romoli, M., *et al.:* 2002, in preparation.
Rosseland, S.: 1924, *Mon. Not. Roy. Astron. Soc.* **84**, 720.
Rottman, G. J., Orrall, F. Q., and Klimchuk, J. A.: 1982, *Ap. J.* **260**, 326.
Rowlands, J., Shapiro, V. D., and Shevchenko, V. I.: 1966, *Soviet Phys. JETP* **23**, 651.
Ruzmaikin, A., and Berger, M. A.: 1998, *Astron. Astrophys.* **337**, L9.
Ryan, J. M., and Axford, W. I.: 1975, *Z. Geophysik* **41**, 221.
Sakurai, T.: 1985, *Astron. Astrophys.* **152**, 121.

Sakurai, T., and Spangler, S. R.: 1994, *Ap. J.* **434**, 773.
Sandbæk, Ø., Leer, E., and Hansteen, V. H.: 1994, *Ap. J.* **436**, 390.
Schlüter, A.: 1957, in H. C. van de Hulst (ed.), *Radio Astronomy,* IAU Symp. 4, Cambridge U. Press, 356.
Schrijver, C. J.: 1987, in J. L. Linsky and R. E. Stencel (eds.), *Cool Stars, Stellar Systems, and the Sun,* Proc. of the Fifth Cambridge Workshop, Springer-Verlag, Berlin, 135.
Schrijver, C. J., Title, A. M., Harvey, K. L., *et al.:* 1998, *Nature* **394**, 152.
Schunk, R. W.: 1977, *Rev. Geophys. Space Phys.* **15**, 429.
Schwadron, N. A., Fisk, L. A., and Zurbuchen, T. H.: 1999, *Ap. J.* **521**, 859.
Schwartz, S. J.: 1980, *Rev. Geophys. Space Phys.* **18**, 313.
Schwartz, S. J., Feldman, W. C., and Gary, S. P.: 1981, *J. Geophys. Res.* **86**, 541.
Schwartz, S. J., and Marsch, E.: 1983, *J. Geophys. Res.* **88**, 9919.
Schwenn, R., and Marsch, E.: (eds.) 1990, *Physics of the Inner Heliosphere,* vol. 1, Springer-Verlag, Heidelberg.
Scime, E. E., Bame, S. J., Feldman, W. C., Gary, S. P., and Phillips, J. L.: 1994, *J. Geophys. Res.* **99**, 23401.
Scudder, J. D.: 1992a, *Ap. J.* **398**, 299.
Scudder, J. D.: 1992b, *Ap. J.* **398**, 319.
Scudder, J. D.: 1994, *Ap. J.* **427**, 446.
Scudder, J. D.: 1996, *J. Geophys. Res.* **101**, 13461.
Seely, J. F., Feldman, U., Schühle, U., Wilhelm, K., Curdt, W., and Lemaire, P.: 1997, *Ap. J. Letters* **484**, L87.
Sen, H. K.: 1969, *J. Franklin Inst.* **287**, 451.
Shebalin, J. V., Matthaeus, W. H., and Montgomery, D.: 1983, *J. Plasma Phys.* **29**, 525.
Shevchenko, V. I., Galinsky, V. L., Medvedev, M. V., Diamond, P. H., Ride, S. K., and Sagdeev, R.: 1998, *Eos Trans. AGU* **79** (45), F692.
Shibata, K.: 1996, *Adv. Space Res.* **17** (4–5), 9.
Shibata, K.: 1997, in *The Corona and Solar Wind Near Minimum Activity,* Fifth SOHO Workshop, ESA SP-404, Noordwijk, 103.
Shoub, E. C.: 1988, in V. Pizzo, T. Holzer, and D. Sime (eds.), *Proceedings of the Sixth International Solar Wind Conference,* High Altitude Observatory, Boulder, Colorado, 59.
Sibeck, D. G., and Richardson, J. D.: 1997, *J. Geophys. Res.* **102**, 14721.
Simon, G. W., Title, A. M., and Weiss, N. O.: 2001, *Ap. J.* **561**, 427.
Siregar, E., Viñas, A. F., and Goldstein, M. L.: 1998, *Phys. Plasmas* **5**, 333.
Sittler, E. C., Jr., and Guhathakurta, M.: 1999, *Ap. J.* **523**, 812.
Sittler, E. C., Jr., and Guhathakurta, M.: 2002, *Ap. J.* **564**, 1062.
Smith, E. J., and Wolfe, J. H.: 1979, *Space Sci. Rev.* **23**, 217.
Snyder, C. W., and Neugebauer, M.: 1964, *Space Res.* **4**, 89.
Spangler, S. R.: 1989, *Phys. Fluids B* **1**, 1738.
Spangler, S. R.: 1997, in T. Hada and H. Matsumoto (eds.), *Nonlinear Waves and Chaos in Space Plasmas,* Terra Sci. Pub., Tokyo, 171.
Spangler, S. R., and Mancuso, S.: 2000, *Ap. J.* **530**, 491.
Spangler, S. R., Kavars, D. W., Kortenkamp, P. S., Bondi, M., Mantovani, F., and Alef, W.: 2002, *Astron. Astrophys.* **384**, 654.
Spitzer, L., Jr.: 1962, *Physics of Fully Ionized Gases,* 2nd ed., Wiley, New York.
Spitzer, L., Jr., and Härm, R.: 1953, *Phys. Rev.* **89**, 977.
Spruit, H. C., Schüssler, M., and Solanki, S. K.: 1991, in A. Cox, W. Livingston, and M. Matthews (eds.), *Solar Interior and Atmosphere,* Univ. of Arizona Press, Tucson, 890.
Stawicki, O., Gary, S. P., and Li, H.: 2001, *J. Geophys. Res.* **106**, 8273.
Stein, R. F., and Schwartz, R. A.: 1972, *Ap. J.* **177**, 807.

Steinolfson, R. S., Suess, S. T., and Wu, S. T.: 1982, *Ap. J.* **255**, 730.
Stern, D. P.: 1989, *Rev. Geophys.* **27**, 103.
Stewart, G. A., and Bravo, S.: 1997, *J. Geophys. Res.* **102**, 11263.
Stix, T. H.: 1962, *The Theory of Plasma Waves,* McGraw Hill, New York.
Strachan, L., Kohl, J. L., Weiser, H., Withbroe, G. L., and Munro, R. H.: 1993, *Ap. J.* **412**, 410.
Strachan, L., Panasyuk, A. V., Dobrzycka, D., Kohl, J. L., Noci, G., Gibson, S. E., and Biesecker, D. A.: 2000, *J. Geophys. Res.* **105**, 2345.
Sturrock, P. A., and Hartle, R. E.: 1966, *Phys. Rev. Letters* **16**, 628.
Sturrock, P. A., Roald, C. B., and Wolfson, R.: 1999, *Ap. J. Letters* **524**, L75.
Suess, S. T., Wang, A.-H., Wu, S. T., Poletto, G., and McComas, D. J.: 1999, *J. Geophys. Res.* **104**, 4697.
Swings, P.: 1941, *Lick Obs. Bull.* **19** (508), 131.
Tam, S. W. Y., and Chang, T.: 1999, *Geophys. Res. Letters* **26**, 3189.
Tamano, T.: 1991, *Solar Phys.* **134**, 187.
Tarbell, T., Ryutova, M., Covington, J., and Fludra, A.: 1999, *Ap. J. Letters* **514**, L47.
Thieme, K. M., Marsch, E., and Schwenn, R.: 1990, *Ann. Geophys.* **8**, 713.
Timothy, A. F., Krieger, A. S., and Vaiana, G. S.: 1975, *Solar Phys.* **42**, 135.
Toichi, T.: 1971, *Solar Phys.* **18**, 150.
Treumann, R. A.: 1998, *Phys. Rev. E* **57**, 5150.
Treumann, R. A.: 1999, *Physica Scripta* **59**, 19.
Treumann, R. A.: 2001, *Astrophys. Space Sci.* **277**, 81.
Tsinganos, K., and Sauty, C.: 1992, *Astron. Astrophys.* **257**, 790.
Tsurutani, B. T., Goldstein, B. E., Smith, E. J., *et al.:* 1990, *Planet. Space Sci.* **38**, 109.
Tsurutani, B. T., Ho, C. M., Arballo, J. K., *et al.:* 1996, *J. Geophys. Res.* **101**, 11027.
Tu, C.-Y.: 1988, *J. Geophys. Res.* **93**, 7.
Tu, C.-Y., and Marsch, E.: 1995, *Space Sci. Rev.* **73**, 1.
Tu, C.-Y., and Marsch, E.: 1997, *Solar Phys.* **171**, 363.
Tu, C.-Y., and Marsch, E.: 2001, *J. Geophys. Res.* **106**, 8233.
Tu, C.-Y., Marsch, E., Wilhelm, K., and Curdt, W.: 1998, *Ap. J.* **503**, 475.
Uchida, Y., and Kaburaki, O.: 1974, *Solar Phys.* **35**, 451.
Usmanov, A. V., Goldstein, M. L., Besser, B. P., and Fritzer, J. M.: 2000, *J. Geophys. Res.* **105**, 12675.
Uzzo, M., Raymond, J. C., Biesecker, D., Marsden, B., Wood, C., Ko, Y.-K., and Wu, R.: 2001, *Ap. J.* **558**, 403.
Vaiana, G. S., and Rosner, R.: 1978, *Ann. Rev. Astron. Astrophys.* **16**, 393.
van Ballegooijen, A. A.: 1986, *Ap. J.* **311**, 1001.
van de Hulst, H. C.: 1950, *Bull. Astron. Inst. Netherlands* **11**, 135.
van de Hulst, H. C.: 1953, in G. P. Kuiper (ed.), *The Sun,* Univ. of Chicago Press, Chicago, Illinois, 302.
Vasquez, B. J., and Hollweg, J. V.: 1999, *J. Geophys. Res.* **104**, 4681.
Velli, M.: 1999, in T. Passot and P.-L. Sulem (eds.), *Nonlinear MHD Waves and Turbulence,* Lecture Notes in Physics **536**, Springer-Verlag, Berlin, 198.
Velli, M.: 2001, *Astrophys. Space Sci.* **277**, 157.
Viñas, A. F., Wong, H. K., and Klimas, A. J.: 2000, *Ap. J.* **528**, 509.
Vocks, C., and Marsch, E.: 2001, *Geophys. Res. Letters* **28**, 1917.
Völk, H. J.: 1975, *Space Sci. Rev.* **17**, 255.
Voytenko, Y. M., Krishtal, A. N., Kuts, S. V., Malovichko, P. P., and Yukhimuk, A. K.: 1990, *Geomag. Aeronomy* **30**, 766.
Waldmeier, M.: 1957, *Die Sonnenkorona* **2**, Verlag Birkhäuser, Basel.

Walker, A. B. C., Jr., DeForest, C. E., Hoover, R. B., and Barbee, T. W., Jr.: 1993, *Solar Phys.* **148**, 239.
Wang, A.-H., Wu, S. T., Suess, S. T., and Poletto, G.: 1993, *Solar Phys.* **147**, 55.
Wang, Y.-M.: 1994, *Ap. J. Letters* **435**, L153.
Wang, Y.-M., and Sheeley, N. R., Jr.: 1990, *Ap. J.* **355**, 726.
Wang, Y.-M., Sheeley, N. R., Jr., Socker, D. G., *et al.*: 1998a, *Ap. J.* **508**, 899.
Wang, Y.-M., Sheeley, N. R., Jr., Walters, J. H., *et al.*: 1998b, *Ap. J. Letters* **498**, L165.
Weber, E. J., and Davis, L., Jr.: 1967, *Ap. J.* **148**, 217.
Wentzel, D. G.: 1976, *Solar Phys.* **50**, 343.
Wentzel, D. G.: 1977, *J. Geophys. Res.* **82**, 714.
Whang, Y. C.: 1971, *J. Geophys. Res.* **76**, 7503.
Whang, Y. C.: 1972, *Ap. J.* **178**, 221.
Whang, Y. C.: 1986, *Ap. J.* **307**, 838.
Whang, Y. C.: 1997, *Ap. J.* **485**, 389.
Whang, Y. C., and Chang, C. C.: 1965, *J. Geophys. Res.* **70**, 4175.
Whang, Y. C., Liu, C. K., and Chang, C. C.: 1966, *Ap. J.* **145**, 255.
Whang, Y. C., Zhao, X., and Ogilvie, K. W.: 1990, *J. Geophys. Res.* **95**, 18781.
Whealton, J. H., and Woo, S.-B.: 1971, *Phys. Rev. A* **6**, 2319.
White, S. M., and Kundu, M. R.: 1997, *Solar Phys.* **174**, 31.
Wilcox, J. M.: 1968, *Space Sci. Rev.* **8**, 258.
Wilhelm, K., Dammasch, I. E., Marsch, E., and Hassler, D. M.: 2000, *Astron. Astrophys.* **353**, 749.
Wilhelm, K., Marsch, E., Dwivedi, B. N., Hassler, D. M., Lemaire, P., Gabriel, A. H., and Huber, M. C. E.: 1998, *Ap. J.* **500**, 1023.
Williams, L. L.: 1997, *Ap. J.* **481**, 515.
Winterhalter, D., Neugebauer, M., Goldstein, B. E., Smith, E. J., Bame, S. J., and Balogh, A.: 1994, *J. Geophys. Res.* **99**, 23371.
Withbroe, G. L., Kohl, J. L., Weiser, H., and Munro, R. H.: 1982, *Space Sci. Rev.* **33**, 17.
Withbroe, G. L., and Noyes, R. W.: 1977, *Ann. Rev. Astron. Astrophys.* **15**, 363.
Woch, J., Axford, W. I., Mall, U., *et al.: Geophys. Res. Letters* **24**, 2885.
Wolff, C. L., Brandt, J. C., and Southwick, R. G.: 1971, *Ap. J.* **165**, 181.
Woo, R., Armstrong, J. W., and Habbal, S. R.: 2000, *Ap. J. Letters* **538**, L171.
Woo, R., Habbal, S. R., Howard, R. A., and Korendyke, C. M.: 1999, *Ap. J.* **513**, 961.
Wood, B. E., Karovska, M., Cook, J. W., Howard, R. A., and Brueckner, G. E.: 1999, *Ap. J.* **523**, 444.
Wu, S. T., Wang, A.-H., Plunkett, S. P., and Michels, D. J.: 2000, *Ap. J.* **545**, 1101.
Yakovlev, O. I., and Mullan, D. J.: 1996, *Irish Astron. J.* **23**, 7.
Yang, W.-H., and Schunk, R. W.: 1989, *Ap. J.* **343**, 494.
Yokoyama, T., and Shibata, K.: 1996, *Publ. Astron. Soc. Japan* **48**, 353.
Zank, G. P., Matthaeus, W. H., Smith, C. W., and Oughton, S.: 1999, in S. Habbal, R. Esser, J. Hollweg, and P. Isenberg (eds.), *Solar Wind Nine,* AIP Conf. Proc. 471, AIP Press, Woodbury, New York, 523.
Zirker, J. B.: (ed.) 1977, *Coronal Holes and High-speed Wind Streams,* Colorado Assoc. Univ. Press, Boulder.
Zirker, J. B.: 1993, *Solar Phys.* **148**, 43.
Zurbuchen, T. H., Hefti, S., Fisk, L. A., Gloeckler, G., and von Steiger, R.: 1999, *Space Sci. Rev.* **87**, 353.